MODELING HYDRAULIC EFFECTS OF UNSUBMERGED IN-STREAM DEFLECTION STRUCTURES

by

DEVAN JEANETTE FITZPATRICK

(Under the Direction of Brian Bledsoe)

ABSTRACT

A wide range of human activities in river environments requires emplacement of in-stream unsubmerged deflection structures (ISUDS) which include groynes, spur dikes, abutments, and temporary structures such as riprap construction platforms. Improved understanding of the hydraulic and geomorphic effects of ISUDS is essential for minimizing unintended consequences such as channel erosion and habitat alteration. Hydraulic modeling and statistical analyses were conducted to assess effects of ISUDS on channel velocities and shear stresses. Over 50,000 HEC-RAS model simulations were performed using variable contractions, discharges, Manning *n* values, and realistic channel geometries. Practical regressions that predict mean changes in velocity and shear stress due to emplacement of ISUDS were developed. Two-dimensional modeling was also performed to analyze spatial patterns of amplified velocities and shear stresses resulting from ISUDS. These hydraulic modeling results can be used in conjunction with the novel regressions to inform preliminary ISUDS design, environmental management, and regulatory decisions.

INDEX WORDS: Groynes, Spurs, Regression, Velocity, Shear stress, HEC-RAS

MODELING HYDRAULIC EFFECTS OF UNSUBMERGED IN-STREAM DEFLECTION STRUCTURES

by

DEVAN FITZPATRICK

B.S., Oregon State University, 2017

A Thesis Submitted to the Graduate Faculty of The University of Georgia in Partial Fulfillment of the Requirements for the Degree

MASTER OF SCIENCE

ATHENS, GEORGIA

2020

MODELING HYDRAULIC EFFECTS OF UNSUBMERGED IN-STREAM DEFLECTION STRUCTURES

by

DEVAN JEANETTE FITZPATRICK

Major Professor: Brian Bledsoe

Committee: Ernest Tollner
Rhett Jackson

Electronic Version Approved:

Ron Walcott
Interim Dean of the Graduate School
The University of Georgia
August 2020

DEDICATION

I dedicate this thesis to my family and friends for their unwavering commitment and support to my growth and well-being throughout my degree.

ACKNOWLEDGEMENTS

Firstly, I would like to acknowledge my professor, Dr. Brian Bledsoe, for his support and wealth of knowledge. His dedication to his student's well-being and success both in their studies and life is truly honorable. To the rest if my committee, Dr. Ernest Tollner and Dr. Rhett Jackson, thank you for your assistance and valuable insights. My sincerest gratitude to my UGA colleagues Daniel Buhr, William Mattison, Tim Stephens, Gregory Coughlin and William Schroer (Shep) for your ceaseless assistance in conducting field work. A special thank you to Tanner Buggs for his immense help conducting hydraulic modeling and to Rod Lammers for insights on coding and development of the final tool. This thesis would not have been possible without the support of my colleagues, family and friends and I am forever grateful for your encouragement. I was strengthened by my families support throughout this process and am appreciative for my Nana and Papa's encouragement and motivational homemade cookie care packages. Finally, my deepest heart felt thank you to Drew for standing by my side during this process providing endless wit, sarcasm, love, and support.

TABLE OF CONTENTS

LIST OF TABLES

Page

LIST OF FIGURES

Page

CHAPTER 1

INTRODUCTION

1.0 Background and Statement of Problem

Population growth and development have led to extensive interactions between people and freshwater environments. Humans have developed lands and built infrastructure near streams and rivers for numerous utilitarian and non-utilitarian purposes, including agricultural water supply, domestic consumption, industrial production, recreation, spiritual wellbeing, aesthetics, and transportation (Beeson *et al.*, 2001; McCool *et al.*, 2008). This myriad of socioeconomic and cultural benefits provided by aquatic systems has in many instances concentrated large populations near freshwater systems, with the highest population densities near large rivers (Kummu *et al.*, 2011). Population growth near rivers has accelerated construction of infrastructure along river corridors and in river floodplains including housing developments, schools, hospitals, and transportation and energy infrastructure. Development near rivers has led to unintended impacts on infrastructure, human settlements, and river ecosystems.

With respect to the built environment, rivers misbehave: they erode streambanks, they migrate, and they flood, all with repercussions for valley structures and inhabitants. In response, the implementation of in-stream structures has been a common means of controlling river behavior (Radspinner *et al.*, 2010). In-stream structures is a broad term that encompasses temporary and semi-permanent structures including river training structures, diversions, and temporary construction platforms. Flooding, bank erosion and scour has necessitated emplacement of these structures to protect existing infrastructure and resources, build new

infrastructure, maintain navigation channels, and improve degraded river habitats. One subset of in-stream structures commonly used are deflection structures. Deflection structures encompass semi-permanent structures including groynes, abutments, and spur dikes and temporary less commonly recognized structures, such as riprap construction platforms. These structures extend from one bank into the main channel constricting and redirecting flow. Constricting and redirecting flow can protect the adjacent bank, deepen channel thalwegs, and increase flow complexity for habitat improvement. However, constricting channel flow can also lead to local increases in velocity and shear stress causing increased bed scour and potentially erosion on the opposite bank. Substantial bed scour and increased velocities may have implications for scour prone habitats such as mussel beds, and high velocities have the potential to limit movement of some fishes. Increased velocity and shear stress around these structures have implications for structure design, as well as geomorphic and ecological processes.

Due to the widespread implementation and recognition of semi-permanent deflection structures, numerous experimental and modeling studies have been conducted to evaluate the 2-D and 3-D flow fields, local scour patterns and turbulence characteristics around them. Additionally, the extensive use of semi-permanent structures has led to establishment of design guidelines (Brown, 1985; Lagasse *et al.*, 2009) and regression equations to predict maximum velocities (Seed, 1997; Yeo *et al.*, 2005) and scour patterns (Pandey *et al.*, 2018). Previous research on semi-permanent structures is extensive but lacks connection to temporary structures limiting the application of semi-permanent structure study results.

Modeling studies focused on deflection structures are often conducted using 2-D or 3-D platforms. Two-dimensional hydraulic modeling is becoming more common in practice; however, 2-D and 3-D modeling techniques can be costly and time consuming, limiting their

utilization by practitioners. There is a need for studies that develop parsimonious predictive regression models for easy application that limit the need for complex modeling. Although many studies have quantified the 2-D and 3-D hydraulics around deflection structures, there is a general lack of practical and transferable relationships for predicting local average velocity and shear stress for a range of channel sizes, contractions, and flow conditions. Ideally such relationships would only require a few physically-based predictor variables derived from readily available information for ease of application. Practical predictive relationships have a wide range of applications for both temporary and semi-permanent deflection structures related to design, environmental management, and regulatory decision making.

2.0 Objectives

The overall goal of this research is to develop parsimonious models to predict changes in average channel hydraulics due to emplacement of both temporary and semi-permanent in-stream unsubmerged deflection structures (ISUDS) to inform preliminary structure design, environmental management options, and regulatory decision making. This research aims to develop simple regression models that can be commonly applied to avoid the need for complex modeling for preliminary decision making. Research conducted herein is motivated in part by the necessity to understand the hydraulic effects of temporary in-stream riprap construction platforms utilized for bridge construction projects by state departments of transportation (DOT). For DOT's to effectively respond to environmental permitting agency concerns about the potential geomorphic and ecological effects of temporary in-stream construction platforms there is a need for practical predictive relationships that can be utilized to inform preliminary design decisions. Temporary riprap bridge construction platforms closely resemble semi-permanent structures including spur dikes, groynes and abutments and have similar hydraulic effects.

Therefore, this study is generally applicable to ISUDS that include both temporary in-stream structures as well as semi-permanent structures.

The specific objectives of this study are as follows:

1. Evaluate the use of the readily available 1-D Hydrologic Engineering Center's River Analysis System (HEC-RAS) to predict average changes in velocity and shear stress in regions contracted by ISUDS by applying experimental studies obtained from a literature review to corroborate model predictions.
2. Systematically develop and execute 50,000+ hydraulic modeling simulations that adhere to geomorphic scaling properties to represent a wide range of realistic channel sizes, geomorphic settings, channel roughness characteristics, contraction percentages and discharges.
3. Utilize a combination of automated 1-D hydraulic modeling of 50,000+ realizations and analytical techniques to develop practical regression relationships for predicting average changes in velocity and shear stress at the contracted reach impacted by ISUDS as a function of physically-based and readily available variables.
4. Perform field measurements around installed ISUDS to determine changes in velocity magnitudes due to the contraction compared to unobstructed channel conditions. Utilize field results and existing flume studies with installed ISUDS to corroborate predictive relationships.
5. Employ a subset of 2-D HEC-RAS models to provide information about the spatial distributions of velocity and shear stress near ISUDS concentrating on areas of maximum values and near bank regions.

6. Make recommendations for development of a tool that synthesizes study results to inform preliminary design decisions for ISUDS. Results and recommendations from this study are meant to be simple for ease of application for a variety of users including state DOTs.

3.0 Thesis Outline

The focus of this thesis is developing relationships for predicting hydraulic effects of ISUDS including spur dikes, groynes, abutments and riprap construction platforms used for bridge construction. Chapter 2 provides a brief review of pertinent literature focused on: unsubmerged deflection structure types, uses, and hydraulic effects; hydraulic modeling, experimental flume and field studies; and implications for bridge construction practices.

Chapter 3 is presented as a standalone manuscript outlining the use of 1-D HEC-RAS modeling and analytical techniques to predict average changes in velocity and shear stress in the contracted reach effected by unsubmerged deflection structures. This chapter includes presentation of practical regression models for predicting average changes in velocity and shear stress in the contracted reach effected by ISUDS as a function of physically-based variables derived from readily available information. Results from this chapter can be utilized by researchers and practitioners to determine the potential hydraulic and geomorphic effects of ISUDS prior to structure emplacement.

Chapter 4 describes 2-D HEC-RAS modeling analyses and provides information about the spatial distributions of velocity and shear stress near ISUDS concentrating on areas of maximum values and near bank regions. This chapter builds upon the parsimonious regression models described in Chapter 3, presenting a means for spatial interpretation of results.

The overall findings and conclusions of this study are presented in Chapter 5. Appendix A contains supplemental material for hydraulic modeling and regression statistical analysis complementing Chapter 3. Appendix B contains supplemental material for Chapters 3 and 4 providing additional insight into potential errors associated with assuming rectangular channel geometries when utilizing developed regressions for actual channel bathymetries. Finally, Appendix C contains additional selected results from a Qualtrics Survey sent to state DOTs to garner insights about ISUDS implementation across the United States for bridge construction and maintenance.

References

Beeson, P.E., D.N. DeJong, and W. Troesken, 2001. Population Growth in U.S. Counties, 1840–1990. Regional Science and Urban Economics 31:669–699.

Brown, S., 1985. Design of Spur-Type Streambank Stabilization Structures. McLean, Virginia.

Kummu, M., H. de Moel, P.J. Ward, and O. Varis, 2011. How Close Do We Live to Water? A Global An. of Pop. Distance to Freshwater Bodies M. Perc (Editor). PLoS ONE 6:e20578.

Lagasse, P.F., P.E. Clopper, J.E. Pagan-Ortiz, L.W. Zevenbergen, L. a. Arneson, J.D. Schall, and L.G. Girard, 2009. Bridge Scour and Stream Instability Countermeasures: Experience, Selection, and Design Guidance-Third Edition.

McCool, S.F., R.N. Clark, and G.H. Stankey, 2008. Water and People: Challenges at the Interface of Symbolic and Utilitarian Values. http://www.fs.fed.us/pnw/pubs/pnw_gtr729.pdf.

Pandey, M., Z. Ahmad, and P.K. Sharma, 2018. Scour around Impermeable Spur Dikes: A Review. ISH Journal of Hydraulic Engineering 24:25–44.

Radspinner, R.R., P. Diplas, A.F. Lightbody, and F. Sotiropoulos, 2010. River Training and Ecological Enhancement Potential Using In-Stream Structures. Journal of Hydraulic Engineering 136:967–980.

Seed, D.J., 1997. Guidelines on the Geometry of Groynes for River Training.

Yeo, H.-K., J.-G. Kang, and S.-J. Kim, 2005. An Exp. Study on Tip Velocity and Downstream Recirculation Zone of Single Groyne Conditions. KSCE J. of Civil Eng. 9:29–38.

CHAPTER 2

LITERATURE REVIEW AND BACKGROUND

A wide range of human activities requires emplacement of both temporary and semi-permanent structures in streams and rivers. In-stream river training structures can be broadly classified into two categories, sills and deflectors (Radspinner *et al.*, 2010). Sills are structures that generally extend across the entire channel, whereas deflection structures protrude into the channel flow from one bank and do not reach the other side (Shields, 1983). In-stream deflection structures obstruct the channel flow, directing flow away from the adjacent bank and increasing velocity. This study focuses on the use of in-stream unsubmerged deflection structures (ISUDS) including spur dikes, abutments, groynes, and temporary riprap construction platforms. These structures are implemented due to their capacity to reduce bank erosion directly downstream of the structure, facilitate sediment deposition or removal, and alter flow characteristics (Brown, 1985).

1.0 ISUDS Overview

Unsubmerged in-stream deflection structures encompass semi-permanent structures including groynes, spur dikes, and abutments, and temporary, less commonly recognized structures such as riprap construction platforms. These structures exhibit similar hydraulic characteristics. In-stream unsubmerged deflection structures are commonly used to stabilize channels, modify river planform, protect existing infrastructure and resources, improve channel navigation, reduce flood risks, construct bridges, and improve habitat quality. These structures can have significant effects on river hydraulic and geomorphic processes. For example,

constricting channel flow can lead to local increases in velocity and shear stress that may result in increased bed scour and erosion on the opposite bank. Increased velocity can impede movement of aquatic organisms and scour can alter habitats such as mussel beds.

Due to the widespread implementation of ISUDS, spurs, groynes, and abutments are commonly studied. Temporary riprap construction platforms exhibit similar characteristics as the aforementioned well-studied structures but are not commonly recognized in literature. Previous research on semi-permanent structures is extensive but lacks connection to temporary structures, limiting the application of semi-permanent structure study results. There is an absence of recognition of the similarities between temporary riprap construction platforms and other semi-permanent unsubmerged deflection structures. Temporary riprap construction platforms are placed in river channels and used for bridge construction and maintenance projects by state departments of transportation (DOT). Additionally, temporary construction platforms can be used for dam removal (Figure 2.1). The lack of connection between well-studied structures and temporary riprap construction platforms can make it challenging for practitioners to utilize an existing relevant body of literature.

2.0 Hydraulic and Geomorphic Effects of ISUDS

In-stream deflection structures extend from one bank into the main channel, constricting and redirecting flow. They can vary in their contraction ratio, construction material, permeability, tip shape, and bank orientation (Brown, 1985), depending on the desired use. The percent of the channel flow obstructed, the deflection structure permeability, tip shape, and orientation can all impact local velocity and scour patterns (Brown, 1985; Seed, 1997).

2.1 Velocity and Flow Field

Implementation of ISUDS obstructs channel flow, reducing the overall flow area, *A*, for a constant discharge, *Q*. By conservation of mass (Eq. 2.1), it is well-known that constricting flow area for a constant discharge will cause an increase in velocity, *V*. Thus, implementation of ISUDS is expected to increase velocity. The magnitude of the change in velocity, and the general flow field, has been found to depend on the physical characteristics of the in-stream flow structure itself.

Eq 2.1 $Q=VA$

The flow field around ISUDS has been found to be turbulent and three-dimensional, consisting of three general regions: the main flow zone, the mixing zone, and the return flow zone (Figure 2.2; Zhang & Nakagawa, 2008). Highest velocities due to ISUDS have been found to occur near the structure tip (Molinas *et al.*, 1998; Rajaratnam and Nwachukwu, 1983). Velocities in the main flow zone are also accelerated due to the contraction. Eddies develop upstream and downstream of the structure due to the abrupt change in flow area. In the return flow zone, two eddies of different sizes commonly occur with a small eddy near the structure and a larger eddy farther downstream (Zhang and Nakagawa, 2008). The reattachment point is the location downstream of the emplaced structure where the separated flow reattaches to the channel bank (Zhang and Nakagawa, 2008).

The reattachment length has been a common phenomenon discussed in both flume and modeling studies (Karim and Ali, 1999; Oullion and Dartus, 1997; Yazdi *et al.*, 2010). The length has been found to be dependent on the length the emplaced structure projects into the main flow. However, the exact multiplier to the length of the structure has varied between studies. Oullion and Dartus (1997) reported the reattachment length for a structure perpendicular

to the channel flow to be $11.5L_s$ for experimental flume results and $10.7L_S$ for a numerical modeling study, where L_S is the structure protrusion length into the flow. Karim and Ali (1990) reported a reattachment length of $11L_S$ for a modeling study. The reattachment length suggests the approximate downstream length required for flow conditions to begin returning to upstream, unimpacted flow patterns and is useful to determine potential structure impact areas.

2.2 Scour

Total bed scour in a riverine system is comprised of three components: general scour, contraction scour, and local scour (Fischenich and Landers, 1999). General scour removes bed material across the entire width of a channel, while contraction scour and local scour are processes that occur in certain locations. Contraction scour occurs at a channel contraction and local scour occurs where a structure obstructs flow (Fischenich and Landers, 1999). In areas impacted by ISUDS, all three types of bed scour occur. Scour depth at ISUDS depends on fluid and bed sediment characteristics, flow conditions, channel geometry, and the geometry of the emplaced structure (Zhang and Nakagawa, 2008). A horseshoe vortex forms in the scour hole upstream of the structure, and a wake vortices system forms on the downstream side of emplaced structures (Pandey *et al.*, 2018; Zhang and Nakagawa, 2008). These vortex systems are important to scour processes.

Bed scour is a patchy phenomenon and often is hard to predict (Haschenburger, 1999). Velocity and shear stress can be used as proxies for identifying potential locations at risk for scour. Critical shear stress and permissible velocities can provide estimates for sediment entrainment near ISUDS. In addition to bed scour, bank scour may occur at contracted regions impacted by ISUDS due to increased velocities, development of eddies, and realignment of channel flows.

3.0 Experimental and Modeling Studies

3.1 Experimental Studies: Flume and Field

Numerous experimental and modeling studies have been conducted to evaluate mean flow fields, local scour patterns and turbulence characteristics around singular unsubmerged spurs, groynes, and abutments. Early experimental flume studies focused on local mean flow fields, scour depths and bed shear stress distributions around ISUDS (Melville, 1992; Molinas et al., 1998; Rajaratnam & Nwachukwu, 1983b, 1983a). These early studies found increases in velocity and shear stress in the contracted regions with maximum bed shear stress occurring near the tip of the structure (Molinas et al., 1998; Rajaratnam & Nwachukwu, 1983a, 1983b). Several studies sought to improve understanding of 2-D flow features utilizing visual observation and large-scale particle velocimetry (Ettema & Muste, 2004; Koken & Constantinescu, 2008; Yeo et al., 2005). Recent experimental studies have focused not only on mean flow fields, but also on characterizing 3-D turbulence dedicated to understanding scour mechanisms or providing data for verification of numerical modeling results (Dey & Barbhuiya, 2005; Duan, 2009; Duan et al., 2009; Jeon et al., 2018; Zhang et al., 2009). Previous studies have used rectangular flumes and collected 3-D velocity data using acoustic doppler velocimeters (ADV) (Duan et al., 2009; Duan, 2009; Jeon et al., 2018). Duan et al. (2009) presented mean flow fields and 3-D hydraulic characteristics in a stable flat bed, while Duan (2009) presented hydraulic characteristics for both a scoured bed and smooth channel bed. Jeon et al. (2018) evaluated 3-D flow characteristics for two different discharges in the vicinity of ISUDS for a stable bed and provided detailed 3-D ADV data. Experimental flume studies have evaluated the effects of structure length, shape, permeability, and orientation angle on hydraulic characteristics. However, flume studies are generally limited in the number of scenarios that can be evaluated, often necessitating hydraulic

model simulation to further understand outcomes of interacting variables across variable site conditions.

3.2 Hydraulic Modeling Studies

Due to the 3-D nature of flow fields in contracted reaches impacted by ISUDS, numerical modeling studies typically are two- or three-dimensional. Studies utilizing 2-D depth-averaged models have computed velocity (Molls *et al.*, 1995) and, in some cases, bed shear stress distributions in contracted reaches (Ali *et al.*, 2017; Tingsanchali and Maheswaran, 1990). Three-dimensional hydraulic models have been conducted to further evaluate mean-flow fields and bed shear stresses (Karim and Ali, 1999; Oullion and Dartus, 1997), determine effects of permeability and contraction percentages on tip velocities (Ho *et al.*, 2007), evaluate impacts of orientation angle on flow fields (Koken, 2011; Yazdi *et al.*, 2010), and provide detailed insight into turbulence characteristics and scour mechanisms (Koken, 2011; Koken and Constantinescu, 2008; Li *et al.*, 2013; Zhang *et al.*, 2009). Some studies have utilized commercially available software including Flow-3D (Ho *et al.*, 2007; Li *et al.*, 2013) and Fluent (Karim and Ali, 1999; Yazdi *et al.*, 2010). Multi-dimensional hydraulic modeling is becoming more common in practice; however, 2-D and 3-D modeling techniques can be costly and time consuming, limiting their utilization by practitioners.

3.3 Design Guidelines and Predictive Relationships

The extensive research conducted and widespread application of semi-permanent structures has led to establishment of design guidelines (Brown, 1985; Lagasse *et al.*, 2009a) and regression equations to predict maximum velocities (Seed, 1997; Yeo *et al.*, 2005). Though these design guidelines and predictive relationships may be helpful for structural design, they do not

address the cross section-averaged (mean) changes in hydraulics that may be useful to address permitting and regulatory concerns such as for fish passage and physical habitat.

Brown (1985) provided general recommendations for application and design of spur-like structures, addressing permeability, structure length, spacing between multiple structures for bank protection, structure orientation angle relative to the bank, structure height, structure geometry, and maintaining structure contact with the channel bed and bank. This early report outlined recommendations for spur design largely based on bank protection efforts and provides initial insight into potential velocity and scour effects due to structure emplacement. However, this report lacks development of equations that can be applied to quantify potential changes in velocity or shear stress for a range of structure types and contractions.

Seed (1997) used results from a validated 2-D rectangular model to predict relative changes in velocities due to groynes considering structure length, spacing between multiple structures for bank protection, structure orientation angle relative to the bank, and the taper of the groyne. The study focused on predicting three velocities: the maximum depth-averaged velocity in the main channel between groynes, the near-bed velocity near the groyne tip, and the near-bed velocity at the toe of the riverbank. This study is useful for predicting maximum bed velocities; however, it lacks predictive relationships for cross section-averaged changes in velocity and does not attempt to predict shear stress. Yeo et al. (2005) developed relationships to predict depth-averaged velocity at the tip of a single groyne using results from flume studies, expanding upon results by (Seed 1997).

The Federal Highways Administration has synthesized bridge scour and stream stability countermeasures in a series of reports (Lagasse *et al.*, 2009a; b). Volume 2 of this report specifically addressed design guidelines for spur dike structures. The study focused on the use of

spurs for bank protection and improving flow alignment under bridges. The report provided general guidelines to select spur type, permeability, spur orientation angle relative to the bank, and riprap sizing. Similar to the peer-reviewed literature, this report also lacks quantitative predictions for changes in velocity and shear stress.

Molinas et al. (1998) developed regressions to predict the total bed shear stress near abutments based on experimental data for three different contraction percentages (10%, 20%, and 30%). Total bed shear stress was calculated as the sum of shear stress due to the contraction and shear stress due to the emplaced structure. These equations for bed shear stress require the Froude number, making shear stress challenging to predict without having conducted hydraulic modeling or knowing the depth of water at the structure.

3.4 Summary of ISUDS characteristic effects on velocities and shear stress

Numerous ISUDS characteristics including structure length, permeability, geometry, and installation angle relative to the bank have been found to impact velocity and shear stress in regions contracted by ISUDS. Table 2.1 summarizes general conclusions about ISUDS characteristic effects on velocity and bed shear stress for straight rectangular channels assuming constant channel size and discharge.

4.0 Implications for Bridge Construction

In 2019, the Federal Highway Administration reported 617,084 bridges in the United States (U.S.), with 12,518 of those bridges in Georgia (“National Bridge Inventory ASCII Files 2019,” 2019). Thirty-seven percent of U.S. bridges reported in 2019 need repair costing an estimated $164 billion dollars (Bridge Report, 2020). The most recent ASCE Infrastructure Report Card from 2017 gave the U.S.’s bridge infrastructure a C^+ rating, indicating the need for further improvement on bridge infrastructure(Infrastructure Report Card 2017, 2017). Though the

percentage of bridges in poor condition appears to be decreasing in recent years (Status of the Nation's Highways, Bridges and Transit: Conditions and Performance, 2019), it is estimated to take at least 50 years to complete repairs (Bridge Report, 2020). Bridge construction and maintenance are on-going efforts to maintain the nations aging transportation infrastructure.

When constructing or replacing bridges over waterways, DOTs and construction managers have numerous options to choose from for bridge construction access. Temporary riprap construction platforms are commonly implemented on wide, relatively shallow rivers where access is not possible from the bank using a crane. Barges can be used where currents are low and the water is deep enough, while work bridges can be constructed when there is a suitable depth of stable substrate. Determination of structure access is highly project- and site-dependent.

Construction of temporary riprap platforms to conduct bridge construction and maintenance requires ample communication between state DOTs, environmental regulatory agencies, and contractors implementing the projects (Figure 2.3). For bridges crossing waterways, environmental permitting agencies may seek documentation, and in some cases quantification, of the potential effects of temporary construction structures on in-stream velocities, channel bank erosion and bed scour. Bridge construction projects are largely a balance between project feasibility, environmental considerations, and sociological factors. This thesis focuses on developing a suite of predictive regression equations to estimate changes in hydraulics around ISUDS, including temporary riprap construction platforms, that can be incorporated into a communication tool to inform preliminary design decisions. The relationships developed in this thesis can be utilized as an important communication tool between regulatory permitting agencies and state DOTs working to balance project feasibility and environmental considerations during bridge construction projects (Figure 2.3).

References

Ali, M.S., M.M. Hasan, and M. Haque, 2017. Two-Dimensional Simulation of Flows in an Open Channel with Groin-Like Structures by IRIC Nays2DH. Math. Problems in Eng. 2017:1–10.

Bridge Report, 2020. https://www.bridge-salon.jp/report_bridge/archives/eng/7776/20100922.html.

Brown, S., 1985. Design of Spur-Type Streambank Stabilization Structures. McLean, Virginia.

Fischenich, C. and M. Landers, 1999. Computing Scour. Vicksburg, MS. http://oai.dtic.mil/oai/oai?verb=getRecord&metadataPrefix=html&identifier=ADA373783.

Haschenburger, J.K., 1999. A Probability Model of Scour and Fill Depths in Gravel-Bed Channels. Water Resources Research 35:2857–2869.

Ho, J., H.K. Yeo, J. Coonrod, and W.-S. Ahn, 2007. Numerical Modeling Study for Flow Pattern Changes Induced by Single Groyne. Proceedings of the Congress-International Association for Hydraulic Research. http://66.221.229.18/pdfs/tp/wat_env_tp/numerical-modeling-study-for-flow-pattern-changes-induced-by-single-groyne-25-07.pdf.

Infrastructure Report Card 2017, 2017.

Karim, O.A. and K.H.M. Ali, 1999. Simulation of the Flow Pattern Around Spur Dykes Using FLUENTS. Jurnal Kejuruteraan 11:3–19.

Koken, M., 2011. Coherent Structures around Isolated Spur Dikes at Various Approach Flow Angles. Journal of Hydraulic Research 49:736–743.

Koken, M. and G. Constantinescu, 2008. An Investigation of the Flow and Scour Mechanisms around Isolated Spur Dikes in a Shallow Open Channel: 1. Conditions Corresponding to the Initiation of the Erosion and Deposition Process. Water Resources Research 44:1–19.

Lagasse, P.F., P.E. Clopper, J.E. Pagan-Ortiz, L.W. Zevenbergen, L. a. Arneson, J.D. Schall, and L.G. Girard, 2009a. Bridge Scour and Stream Instability Countermeasures: Experience, Selection, and Design Guidance-Third Edition.

Lagasse, P.F., P.E. Clopper, J.E. Pagan-Ortiz, L.W. Zevenbergen, L. a. Arneson, J.D. Schall, and L.G. Girard, 2009b. Bridge Scour and Stream Instability Countermeasures: Experience, Selection, and Design Guidance-Third Edition.

Li, G., L. Lang, and J. Ning, 2013. 3D Numerical Simulation of Flow and Local Scour around a Spur Dike. IAHR World Congress.

Molinas, A., K. Kheireldin, and B. Wu, 1998. Shear Stress around Vertical Wall Abutments. Journal of Hydraulic Engineering 124:822–830.

Molls, T., M. Hanif Chaudhry, and K. Wasey Khan, 1995. Numerical Simulation of Two-Dimensional Flow near a Spur-Dike. Advances in Water Resources 18:227–236.

National Bridge Inventory ASCII Files 2019, 2019. https://www.fhwa.dot.gov/bridge/nbi/ascii2019.cfm.

Oullion, S. and D. Dartus, 1997. Three-Dimesnional Computation of Flow Around Groyne. Journal of Hydraulic Engineering 123:962–970.

Pandey, M., Z. Ahmad, and P.K. Sharma, 2018. Scour around Impermeable Spur Dikes: A Review. ISH Journal of Hydraulic Engineering 24:25–44.

Radspinner, R.R., P. Diplas, A.F. Lightbody, and F. Sotiropoulos, 2010. River Training and Ecological Enhancement Potential Using In-Stream Structures. Journal of Hydraulic Engineering 136:967–980.

Rajaratnam, N. and B.A. Nwachukwu, 1983. Flow Near Groin-Like Structures. Journal of Hydraulic Engineering 109:463–480.

Seed, D.J., 1997. Guidelines on the Geometry of Groynes for River Training.

Shields, F., 1983. Design of Habitat Structures for Open Channels. Journal of Water Resources Planning and Managment 109:331–344.

Status of the Nation's Highways, Bridges and Transit: Conditions and Performance, 2019.

Tingsanchali, T. and S. Maheswaran, 1990. 2-D Depth-Averaged Flow Computation Near Groyne. 116:71–86.

Yazdi, J., H. Sarkardeh, H.M. Azamathulla, and A.A. Ghani, 2010. 3D Simulation of Flow around a Single Spur Dike with Free-Surface Flow. International Journal of River Basin Management 8:55–62.

Yeo, H.-K., J.-G. Kang, and S.-J. Kim, 2005. An Exp.Study on Tip Velocity and Downstream Recirculation Zone of Single Groyne Conditions. KSCE J. of Civil Eng. 9:29–38.

Zhang, H. and H. Nakagawa, 2008. Scour around Spur Dyke: Recent Advances and Future Researches. Annuals of Disas. Prev. Res. Inst., Kyoto Univ., Kyoto Univ:633–652.

Zhang, H., H. Nakagawa, K. Kawaike, and Baba Yasuyuki, 2009. Experiment and Simulation of Turbulent Flow in Local Scour around a Spur Dyke. International Journal of Sediment Research 24:33–45.

Tables

Table 2.1. ISUDS effects on velocities and bed shear stress in river channels.

Characteristic	Shear Stress	Velocity	Study Examples
Length	Direct relationship	Direct relationship	Molinas et al., 1998 Yazdi et al., 2010
Permeability	Inverse relationship with shear and tip depth. Scour occurs at all openings in permeable ISUDS	Inverse relationship	Yeo et al., 2005 Ho et al., 2007 e.g., Zhang & Nakagawa, 2008
Installation Angle	Structures at 90° to flow have the highest shear stresses compared to structures orientated upstream or downstream	Structures at 90° have the highest velocities in straight channels	Yazdi et al., 2010 Melville, 1992

Figures

Figure 2.1. Temporary riprap construction structures implemented for bridge construction (a) and dam removal (b).

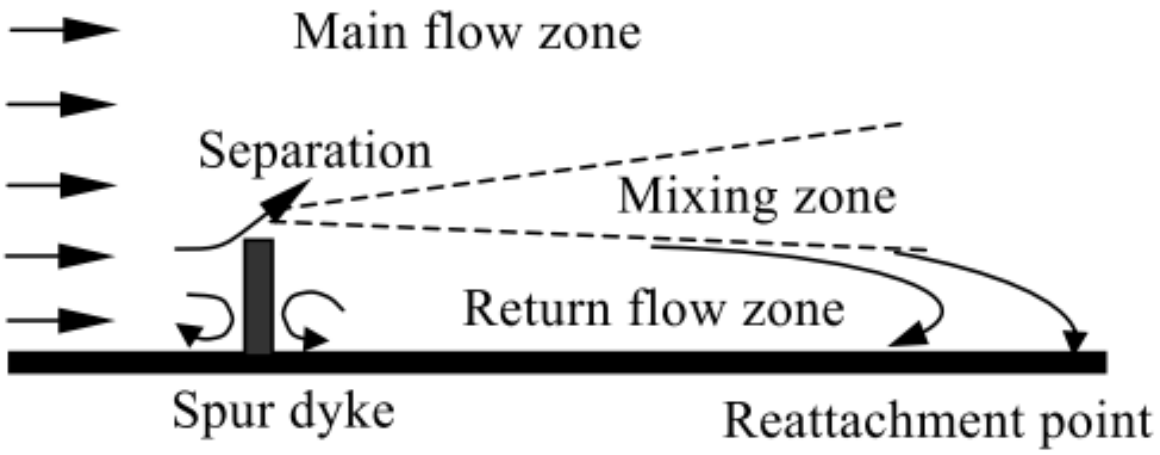

Figure 2.2. Main flow zones near an ISUDS as represented by Zhang et al. (2008).

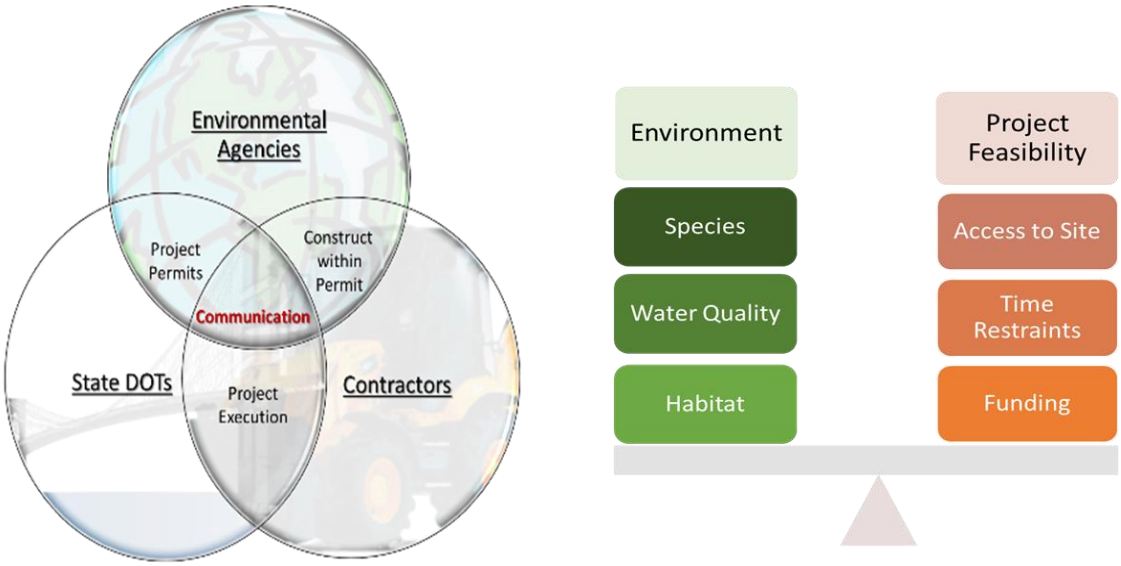

Figure 2.3. Representation of bridge construction project key actors and two components of bridge construction that need to be balanced for project success. Key actors in bridge construction include state DOTs, environmental permitting agencies, and contractors.

CHAPTER 3

PREDICTING EFFECTS OF IN-STREAM UNSUBMERGED DEFLECTION STRUCTURES ON CHANNEL HYDRAULICS

---

[1] Fitzpatrick, D., Stephens, T., and B. Bledsoe. To be submitted to *Journal of American Water Resources Association* or *River Research and Applications*.

Abstract

In-stream unsubmerged deflection structures (ISUDS) encompass semi-permanent structures including groynes, spur dikes, and abutments, and temporary structures such as riprap construction platforms. This study utilized a combination of analytical approaches, 1-D automated hydraulic modeling and regression analysis to assess changes in mean hydraulics resulting from ISUDS. An ensemble of 50,000 HEC-RAS simulations was generated using variable Manning's *n* values, contraction percentages, discharges, and realistic channel geometries that adhere to geomorphic scaling properties. Practical relationships to predict mean changes in velocity and shear stress due to emplacement of ISUDS were developed based on the modeling results to inform preliminary structure design, environmental management, and regulatory decisions. Changes in velocity and shear stress estimated with HEC-RAS for a wide range of conditions are well represented by easily applied regression models based on a channel contraction area ratio for contraction percentages $\leq$ 50% and Froude numbers < 0.8. The new regression relationships for velocity change are reasonably supported by results from a field study and previously conducted flume studies.

1.0 Introduction

A wide range of human activities requires emplacement of both temporary and semi-permanent structures in streams and rivers. Unsubmerged deflection structures are used for a variety of purposes and include groynes, spur dikes, abutments, and temporary structures such as riprap construction platforms. These structures exhibit similar hydraulic characteristics and can be generally classified as in-stream unsubmerged deflection structures (ISUDS), extending from one bank constricting and redirecting channel flow (Figure 3.1). ISUDS are commonly used to stabilize channels, modify river planform, protect existing infrastructure, and resources, improve

channel navigation, reduce flood risks, construct bridges, and improve habitat quality. These structures can have significant effects on river hydraulic and geomorphic processes. For example, constricting channel flow can lead to local increases in velocity and shear stress that may result in increased bed scour and erosion on the opposite bank. Increased velocities can impede movement of aquatic organisms and scour can alter habitats such as mussel beds. Given the widespread implementation of these structures (Radspinner *et al.*, 2010), there is a pressing need for easily applied tools that can be used to predict potential hydraulic and geomorphic effects prior to ISUDS emplacement. In this study, I develop practical relationships for predicting changes in cross section averaged (mean) channel hydraulics resulting from emplacement of temporary and semi-permanent ISUDS to inform preliminary structure design, environmental management, and regulatory decision making.

There is a substantial body of previous research on ISUDS; however, the applicability of this research to temporary structures with similar characteristics such as riprap construction platforms placed in rivers for bridge construction and maintenance by state departments of transportation (DOT) is not well recognized. This disconnect between the literature on semi-permanent ISUDS and implementation of temporary in-stream structures by DOTs and other entities that build infrastructure in river environments presents an opportunity for bridging a gap between research and practice.

Numerous experimental and modeling studies have been conducted to evaluate mean-flow fields, local scour patterns and turbulence characteristics around singular unsubmerged spurs, groynes, and abutments. Early experimental flume studies focused on local mean flow fields, scour depths and bed shear stress distributions around ISUDS (Melville, 1992; Molinas *et al.*, 1998; Rajaratnam and Nwachukwu, 1983a; b). These early studies found increases in velocity

and shear stress in the contracted regions with maximum bed shear stress occurring near the tip of the structure (Molinas *et al.*, 1998; Rajaratnam and Nwachukwu, 1983a; b). Several studies sought to improve understanding of 2-D flow features utilizing visual observation and large scale particle velocimetry (Ettema and Muste, 2004; Koken and Constantinescu, 2008; Yeo *et al.*, 2005). Recent experimental studies have focused not only on mean flow fields, but also on characterizing 3-D turbulence dedicated to understanding scour mechanisms or providing data for verification of numerical modeling results (Dey and Barbhuiya, 2005; Duan, 2009; Duan *et al.*, 2009; Jeon *et al.*, 2018; Zhang *et al.*, 2009). Previous studies have used rectangular flumes and collected 3-D velocity data using acoustic doppler velocimeters (ADV) (Duan et al., 2009; Duan, 2009; Jeon et al., 2018). Duan et al. (2009) presented mean flow fields and 3-D hydraulic characteristics in a stable flat bed, while Duan (2009) presented hydraulic characteristics for both a scoured bed and smooth channel bed. Jeon et al. (2018) evaluated 3-D flow characteristics for two different discharges in the vicinity of ISUDS for a stable bed and provided detailed 3-D ADV data. Experimental flume studies have evaluated the effects of structure length, shape, permeability, and orientation angle on hydraulic characteristics. However, flume studies are generally limited in the number of scenarios that can be evaluated, often necessitating hydraulic model simulation to further understand outcomes of interacting variables across variable site conditions.

Due to the 3-D nature of flow fields in contracted reaches influenced by ISUDS, numerical modeling studies typically are multi-dimensional. Multi-dimensional hydraulic modeling is becoming more common in practice; however, 2-D and 3-D modeling techniques can be costly and time consuming, limiting their potential to generate large batches of data sets to develop regressions covering an extensive range of channel characteristics, discharges and ISUDS

contraction percentages. Studies utilizing 2-D depth averaged models have computed velocity (Molls *et al.*, 1995) and bed shear stress distributions in contracted reaches (Ali *et al.*, 2017; Tingsanchali and Maheswaran, 1990). Three-dimensional hydraulic models have been used to evaluate mean flow fields and bed shear stresses (Karim and Ali, 1999; Oullion and Dartus, 1997), determine effects of permeability and contraction percentages on tip velocities (Ho *et al.*, 2007), evaluate impacts of orientation angle on flow fields (Koken, 2011; Yazdi *et al.*, 2010) and provide detailed insight into turbulence characteristics and scour mechanisms (Koken, 2011; Koken and Constantinescu, 2008; Li *et al.*, 2013; Zhang *et al.*, 2009). Some studies have utilized computational fluid dynamics software including FLOW-3D (Ho *et al.*, 2007; Li *et al.*, 2013) and Ansys Fluent (Karim and Ali, 1999; Yazdi *et al.*, 2010). Previous multi-dimensional modeling studies have generally focused on two to four contraction percentages, and a limited number of structure angles and discharges (e.g. Ho et al., 2007; Koken, 2011; Yazdi et al., 2010) representing a small subset of the conditions encountered in practice across diverse river settings. Combining previous data sets from multi-dimensional models to develop generalized predictive relationships is substantially limited by data availability and few combinations of channel characteristics, structure lengths, and discharges.

Extensive research and widespread application of semi-permanent structures has led to development of design guidelines (Brown, 1985; Lagasse *et al.*, 2009) and regression equations to predict maximum velocities (Seed, 1997; Yeo *et al.*, 2005) and scour patterns (Pandey *et al.*, 2018; Zhang and Nakagawa, 2008). These design guidelines and predictive relationships may be helpful for structural design; however, they do not consider mean changes in hydraulics that may be useful in addressing permitting and regulatory concerns such as fish passage and physical habitat. There is a need for parsimonious predictive tools that reduce the need for complex

modeling in practice. Although many studies have quantified the 2-D and 3-D hydraulics around deflection structures, there is a general lack of practical and transferable relationships for predicting effects on local mean velocity and shear stress for a range of channel sizes, contractions, and flow conditions. Ideally such relationships would only require a few physically-based predictor variables derived from readily available information for ease of application.

1.1 Study Objectives

The overall goal of this research is to develop parsimonious models to predict changes in mean velocity and bed shear stress due to emplacement of both temporary and semi-permanent ISUDS to inform preliminary structure design, environmental management, and regulatory decision making. This research aims to develop straightforward and efficient tools that can be applied to ISUDS for planning, preliminary design, and decision making when more complex modeling is infeasible.

The specific objectives of this study are:

1. Evaluate the use of 1-D analysis using the widely available Hydrologic Engineering Center - River Analysis System (HEC-RAS) to predict mean changes in velocity and shear stress in regions contracted by ISUDS by comparing model predictions with previous experimental studies.

2. Systematically develop and execute >50,000 hydraulic model simulations that adhere to geomorphic scaling properties to represent a wide range of realistic channel sizes, geomorphic settings, channel roughness characteristics, contraction percentages, and discharges.

3. Utilize automated 1-D hydraulic modeling of 50,000+ simulations in combination with analytical techniques to develop practical regression relationships for predicting mean changes in velocity and shear stress at the contracted ISUDS section as a function of physical variables that can be derived from readily available information.

4. Perform field measurements of velocity changes at ISUDS and combine these observations with existing flume studies to test the new predictive relationships.

2.0 Methods Overview

A combination of analytical approaches, 1-D hydraulic modeling and regression analysis was used to assess the effects of ISUDS on mean hydraulics (Figure 3.2). An analytical approach informed independent variable selection for regression models. One-dimensional hydraulic modeling was performed in HEC-RAS to develop an extensive data set spanning a wide range of channel conditions and geometries to develop predictive regressions for altered shear stress and velocity in ISUDS contraction regions. Field and flume data were used to assess the performance of the developed regression models.

3.0 Analytical Approach

An analytical approach based on conservation of mass and the Manning equation was used to characterize hydraulic changes around ISUDS in rectangular channels and to identify potential independent variables for predictive regression models (Figure 3.2). Continuity under steady flow requires that cross-sectional area, A, discharge, Q, and velocity, V are related according to Eq. 3.1. To determine the relative change in mean V due to structure emplacement Eq. 3.2 can be rearranged to solve for the ratio of the velocity with the structure in place, V_s, to the initial velocity, V_i (Eq. 3.3). Relative changes in V become a simple function of unobstructed flow area, A_i, and flow area with the structure in place, A_s.

Eq 3.1. $Q = VA$

Eq 3.2. $V_i A_i = V_s A_s$

Eq 3.3. $A_i/A_s = V_s/V_i$

When predicting V_s, Eq. 3.3 can be rearranged given that V_i for a given Q is known (Eq. 3.4). In practice the V_i for a given Q can be obtained through direct measurement, hydraulic modeling, or through estimation using the Manning equation. Here I use the Manning equation to develop Eq. 3.5 where *R, S, n* and $\emptyset$ are the hydraulic radius, bed slope, Manning's roughness and a units conversion factor (1.49 for English, and 1 for S.I.), respectively (Chow, 1959), recognizing that hydraulic modeling and field measurements are often infeasible. This is especially true when conducting large numbers of studies at different sites across multiple discharges. The flow area with the structure in place, A_s, can be re-written as A_i subtracted from the structure area, A_{st}.

Eq 3.4. $V_s = V_i * [A_i/A_s]$

Eq 3.5. $V_s = \left[\left(\frac{\emptyset}{n}\right) * R^{\frac{2}{3}} * S^{\frac{1}{2}}\right] * [A_i/(A_i - A_{st})]$

The second term of Eq. 3.5 is the ratio of the unobstructed channel area to the flow area with the structure in place. Since the unobstructed channel area is the flow area with the structure in place added to the structure area, the second term of Eq. 3.5 can be re-written as the structure area divided by the flow area with the structure in place, A_{st}, plus one (Eq. 3.6). The structure area divided by the flow area with the structure in place (*aaratio*) has been identified as a critical empirical variable by other studies to predict tip velocities (Seed, 1997; Yeo *et al.*, 2005), maximum depth-averaged channel velocities and near bank bed velocities around ISUDS (Seed,

1997). To complete the analytical solution, the *R* can be replaced with initial water depth, $D_{i,}$ assuming a large width to depth ratio (Eq.3.7). The structure and flow areas can be expanded into their core variable forms (Eq. 3.7) where W_c and L_s are the channel unobstructed width and the length of the structure projecting into the channel flow.

Eq 3.6. $V_s = \left[\left(\frac{\emptyset}{n}\right) * R^{\frac{2}{3}} * S^{\frac{1}{2}}\right] * \left[\left(\frac{A_{st}}{A_i - A_{st}}\right) + 1\right]$

Eq 3.7. $V_s = \left[\left(\frac{\emptyset}{n}\right) * D_i^{\frac{2}{3}} * S^{\frac{1}{2}}\right] * \left[\left(\frac{(L_s * D_s)}{(W_c * D_i) - (L_s * D_s)}\right) + 1\right]$

Noting that shear stress (τ) is proportional to V^2, it follows that parameters identified by the analytical solution for *V* should also serve as useful predictive variables for τ. To use the analytical solution directly to determine $V_{s,}$ the depth of water interacting with the structure, $D_{s,}$ and the depth of water before structure emplacement, $D_{i,}$ must be known. Use of the analytical solution is limited; determining D_s and D_i requires field measurements, hydraulic modeling, or introduction of additional equations. However, under conditions where the flow is not choked, these depths are assumed to be relatively similar resulting in the *aaratio* being largely dependent on the contracted width (Eq. 3.8). Here I focus on developing an *aaratio* for rectangular channels; however, this ratio can be defined for other simplified geometries or calculated directly if the bathymetry of a channel and the dimensions of an obstruction are known.

Eq 3.8. $V_s = \left[\left(\frac{\emptyset}{n}\right) * D_i^{\frac{2}{3}} * S^{\frac{1}{2}}\right] * \left[\left(\frac{(L_s)}{(W_c) - (L_s)}\right) + 1\right]$

4.0 Hydraulic Modeling

Hydraulic modeling was conducted using the United States Army Corps of Engineers (USACE) 1-D Hydrologic Engineering Center River Analysis System (HEC-RAS) Version 5.0.3

(Brunner, 2016a). Hydraulic modeling was performed as a complement to the analytical solution because HEC-RAS includes eddy losses in the form of contraction and expansion coefficients and ineffective flow areas (Brunner, 2016b) that can occur downstream and upstream of ISUDS. Although previous studies have shown that the flow field around ISUDS is complex in nature, 1-D modeling in HEC-RAS was chosen to allow thousands of model simulations representing a full array of geomorphic settings and ISUDS contractions to be performed. Running the full array of conditions in 2-D is largely infeasible given the significantly greater time and computational demands associated with running 50,000 simulations in 2-D. Additionally, accurate calibration of some 2-D modeling coefficients for a large array of conditions is impractical, leading to potential increased errors. HEC-RAS has been used extensively to model bridge hydraulics and abutments. Hydraulic characteristics around spurs, and groynes are similar to abutments (Molinas *et al.*, 1998; Zhang and Nakagawa, 2008) suggesting 1-D HEC-RAS models can estimate mean velocities around ISUDS with reasonable accuracy. Additionally, HEC-RAS can be controlled autonomously through Visual Basic for Applications (VBA) utilizing the HECRAS Controller (Goodell, 2014), allowing for large numbers of model simulations to be completed in batch mode.

In the present study, I compared 1-D HEC-RAS model results to two previously conducted flume studies (Duan *et al.*, 2009; Jeon *et al.*, 2018) to confirm the capability of 1-D HEC-RAS to accurately determine mean velocities around ISUDS before additional modeling was performed in batch mode. Jeon et al. (2018) flume data from supplemental materials and Duan et al. (2009) relative changes in mean velocity data due to an in-stream structure were used to corroborate HEC-RAS model prediction capabilities around ISUDS. To develop a large data set for developing predictive regressions, I performed 50,000 hydraulic modeling simulations by

automating 1-D HEC-RAS using VBA, where hydraulic modeling ensembles were systematically developed to represent a range of rectangular channel geometries, contraction percentages, roughness scenarios, and discharges.

4.1 Determination of Hydraulic Modeling Ensemble Parameter Ranges

This study sought to improve understanding of the hydraulic influence of common ISUDS types, as well as temporary structures built in rivers for infrastructure construction. Accordingly, parameter ranges for hydraulic modeling were defined using plausible ranges of channel geometries suitable for emplacement of temporary construction platforms and typical platform sizes. Such structures tend to be implemented on wide, relatively shallow rivers where access from the bank using a crane and floating barge are infeasible.

Channel geometric characteristics of interest for HEC-RAS modeling included average channel depth, top width, and bed slope. Structure characteristics included length, installation angle, width, and the percent of the channel constricted (contraction %). Ranges of plausible channel and structure characteristics were defined using plans for seven Georgia Department of Transportation (GDOT) bridge construction projects that implemented temporary riprap construction platforms (Table 3.1) and survey data received from 26 additional state DOTs. Survey results were used to supplement information provided by GDOT to garner insights about temporary structure implementation across the US including structure and channel characteristics (Appendix C). Survey results indicated a contraction % range of 10% -70% with a typical maximum of 50%. Synthesizing results from the survey and example projects I developed realistic model ensemble ranges for channel geometries and contraction percentages (Table 3.2). All model simulations were conducted with structures placed perpendicular to the flow and banks.

4.2 Generation of Channel Geometries

Rectangular channel geometries that adhere to geomorphic scaling properties were developed using downstream hydraulic geometry relationships (Parker *et al.*, 2007) and *R* scripts to automate development of realistic combinations of bed slope, width and depth based on vector inputs of bankfull discharge (Q_b). The resulting channel geometries were filtered to include only geometries within the defined modeling ensemble ranges (Table 3.2) with some exceptions for depth, due to the desire to include geometries developed at smaller discharges. One-hundred channel geometries were randomly selected for 1-D modeling from the remaining 200 geometries. Width to depth ratios and dimensionless specific stream powers (Church, 2006) for selected channels were realistic and ranged between 17 - 35 and 0.03 - 0.2 respectively.

4.3 Modeling Procedure

One-dimensional hydraulic modeling in HEC-RAS was automated with VBA and the HECRAS Controller (Goodell, 2014). The developed VBA code consists of one main module that runs HEC-RAS, records results, and calls four-sub-scripts that alter channel geometry, contraction %, Manning *n* values, and the steady flow file containing scaled discharges and a normal depth downstream boundary condition (Figure 3.3). ISUDS were modeled as blocked obstructions. For each new structure contraction %, the code automatically adjusts the length of ineffective flow areas and the number of cross sections with increased contraction and expansion coefficients. Ineffective flow areas and contraction and expansion coefficients were set based on standard guidelines for abutments (Table 3.2, Brunner, 2016a).

Channel geometries were created by altering individual pairs of station and elevation data via the VBA code which reads input data defining a channel width, depth, and slope from the set of 100 realistic channel geometries (Section 4.2). The length of the model (0.5 miles), and the

number and spacing of cross sections remained constant for all simulations. For a given geometry, the code: 1) set the length of an emplaced structure based on a contraction percentage, 2) set a Manning *n* value, 3) ran the simulation for 10 scaled discharges, 4) recorded velocities, water depths, and shear stresses for each discharge at all cross sections, and 5) continued steps 1-6 for all possible combinations of parameters (Table 3.2). Fifty thousand HEC-RAS model simulations were conducted using 100 channel geometries, 50 combinations of contraction percentages and Manning *n* values, across 10 discharges scaled to channel size as a percentage of the bankfull discharge utilized to generate the channel geometry (Table 3.2).

5.0 Regression Analysis

Multiple regression analysis (MRA) was used to derive predictive regressions to determine relative changes and absolute values of velocity, V_s, and shear stress, τ_s, due to emplacement of ISUDS in simulated river channels. Analysis was conducted in the statistical programs *R* Version 3.5.1 and JMP Pro 14.1 (R Core Team, 2019; SAS Institute Inc., 2018). Evaluation of regression options focused on development of easily applied relationships requiring physically-based predictor variables derived from readily available information (Table 3.3). The Froude number (*Fr*) in the contracted region influenced by an ISUDS may be challenging for a user to estimate since D_s must be known; several alternative representations of the *Fr* were tested in this analysis (Table 3.3).

I initially concentrated on predicting relative changes in *V* and τ calculated as the value with the structure in place divided by the initial value without the structure in place (0% contraction) at the cross section with the emplaced structure. The regressions developed for relative changes were expanded to predict V_s and τ_s in the contracted region impacted by ISUDS by multiplying by the initial value without the structure in place. This approach is conducive to practical

applications, providing the option to utilize a known V_i or τ_i, or allowing for estimation of initial values. Final selected models for predicting relative changes in *V* were corroborated using existing flume data and results from the field study.

5.1 Relative Changes in Velocity and Shear Stress Regressions

I strived to develop parsimonious regression models for predicting relative changes in *V* and τ resulting from ISUDS. Variables with collinearity issues with the *aaratio* (Pearson *r* values over 0.6) were eliminated from best subsets analysis first because previous studies have shown that the *aaratio* is an essential variable for accurately predicting changes in *V* due to emplacement of ISUDS (Seed, 1997; Yeo *et al.*, 2005). I reduced the variable pool to eight by further examining collinearity among the remaining independent variables. The remaining predictor variables (Table 3.3) were employed in the 'leaps' package in R to perform an exhaustive search for the best subset of predictor variables (Lumley, 2020). The regsubsets() function was used to identify the best linear model for a given number of predictor variables. Linear models were evaluated based on their complexity, adjusted R^2 ($adjR^2$) values and overall model accuracy based on root-mean-square error (RMSE). Sensitivity to the input independent variables was evaluated throughout the model selection process by exchanging selected input variables with other similar variables that were originally excluded due to collinearity.

In addition to linear equations, power functions using the best predictors of relative change in *V* were developed using both parametric and non-parametric approaches. Quadratic equations were also evaluated for τ since $\tau \propto V^2$. All regressions were developed using a randomly selected training data set consisting of 80% of the available data from the HEC-RAS simulations. The

remaining 20%, was utilized for cross-validation to ensure models were not over-fit and to test overall regression performance.

Since $adjR^2$ values cannot be used to compare linear and non-linear regressions, models were selected based on RMSE. Model accuracy and bias in predicting relative changes in V at all contraction percentages was also considered and evaluated in cross-validation using percent error between predicted and actual values from HEC-RAS simulations for each contraction %. Percent errors were evaluated using a One-way ANOVA to test for significant differences between mean percent errors by contraction % groups (p-value=0.05). The interquartile ranges (IQR) and the One-way ANOVA results of the percent errors were used to assess model accuracy and bias at all contraction percentages and provide insight into the residual variability of regression predictions.

Contraction percentages over 50% had significantly larger errors for all candidate models and were removed from analysis to improve accuracy, as even temporary contractions exceeding 50% are rarely encountered in construction practice. Froude numbers in the contracted cross section were limited to <0.8 to ensure models were developed for subcritical flow conditions.

5.2 Absolute Velocities and Shear Stress Regressions

Absolute V and τ regressions were developed using the top predictive model for relative change in V and τ based on cross-validation. Relative changes were then multiplied by various estimates of initial values without structures in place. One set of regressions to predict V_s and τ_s used initial values estimated using either the Manning equation or the shear stress equation, respectively. These equations require known values of R and therefore D_i. They also represent estimates that could be obtained from hydraulic models such as HEC-RAS. Additional

regressions were tested where water depth was estimated using variables that may be more easily obtained (*Q*, *S*, *n* etc…).

Three models for predicting V_s were tested. The first two models expanded upon the regression developed for relative changes in *V*. The first model calculated the V_i using the Manning equation assuming the D_i is known, and the second model replaced depth in the Manning equation with a proxy for depth based on at-a-station hydraulic geometry (Knighton, 1998; $D \alpha Q^{0.4}$). The third model mimicked the analytical solution (Eq. 3.7) developing a power function to predict V_s using the Manning equation to calculate the V_i. However, *R* was replaced by depth assuming wide geometry and $\frac{Q}{W_C}$ was used as a proxy for depth (Eq. 3.9). Two models for predicting τ_s were tested. The first model utilized τ_i obtained from the shear stress equation with a known *R*. The second model used substituted D_i for *R* and estimated D_i using a proxy for depth derived from the Manning equation ($D_i = \left[\frac{(Q*n)}{(W_C*S^{0.5}*\emptyset}\right]^{3/5}$).

The regressions were evaluated on their ability to accurately predict absolute values based on the percent errors of predictions. The outlined approach allowed me to predict relative changes based on model accuracy and test the models to predict absolute values using the remaining test data. The goal of predicting absolute values was to determine usable regressions for preliminary analysis of emplacing ISUDS and to understand the regression limitations, especially when estimating depths. Other methods to predict V_s and τ_s likely exist with other variations of depth approximations.

Eq 3.9. $V_s = X * \left[\left(\frac{\emptyset}{n}\right)^a * Q^b * {W_c}^C * S^d\right] * [aaratio + 1]^e$

where *a*, *b*, *c*, *d*, *e* are fitted exponents and *X* is a fitted coefficient.

6.0 Field Work

Field work for this project aimed to estimate changes in mean *V* magnitudes in the contracted region of an installed ISUDS compared to unobstructed channel conditions to test the regression models. Field work was conducted near Lyerly, Georgia at a bridge replacement project on the Chattooga River that implemented temporary riprap construction platforms. Velocity measurements were taken using a Teledyne StreamPro ADCP set up on a tethered pully system (Figure 3.4c) for two different structure configurations (Table 3.4). The first temporary access structure configuration consisted of one platform extending into the channel from the left bank (looking downstream). The second configuration consisted of two structures, one on each bank (Figure 3.4b). The structures impacted the channel width at cross sections 2 and 3 (Figure 3.4a).

Stationary moving bed tests were conducted at each cross section for a minimum of five minutes to ensure measurement accuracy (Mueller and Wagner, 2009). No moving beds were detected. A minimum of four transects were completed at each cross section to provide an average *Q* value. Additional transects were collected if one *Q* varied by > 5% from the mean of all the discharges (Mueller and Wagner, 2009). Transects with discharges varying over 10% of the average *Q* for all transects at a given cross were removed during data analysis. Between site Visits 3 and 4 discharges varied greatly, a large tree washed into the study site, and bridge pier locations and shape varied due to ongoing construction. Due to the differences in relative magnitudes of discharges and the cross section changes, I grouped site Visits 1 and 2 and site Visits 3 and 4 for analysis of relative changes in *V*.

7.0 Results

Practical relationships for predicting mean relative changes and absolute values of *V* and τ resulting from emplacement of ISUDS in rectangular channels are presented in Table 3.5.

Relative changes in mean V and τ determined from 1-D HEC-RAS modeling results were well represented by easily applied regressions developed with one variable, for contraction percentages $\leq$ 50% and Fr <0.8. Regression analysis results indicated the main variable affecting change in V and τ between an unaltered channel and a channel with an ISUDS was a contraction area ratio (*aaratio*). Percent errors between flume studies and regression models of relative change in V ranged from -9% - 17%. Absolute velocity and shear stress in the contracted region impacted by ISUDS can be estimated by rearranging the relative regression models, multiplying by an initial value. Initial values can be known values from field data or hydraulic modeling studies or can be estimated. Models of V_s and τ_s that require input estimates of velocity and shear stress in the absence of ISUDS resulted in median absolute prediction errors of 1-5% with errors in the 90th and 10th percentiles <15% for τ_s and <10% for V_s.

7.1 1-D HEC-RAS Models of Previous Flume Studies

Differences in velocities at ISUDS contracted regions between previous physical modeling studies and HEC-RAS simulations ranged from -5.2% - 17%. Differences in predicted upstream mean velocities ranged from -2.4% - 1. 5% (Appendix A, Table A1). HEC-RAS predicted values were generally more accurate for the Jeon et al. (2018) flume experiments compared to the Duan et al. (2009) flume experiment. The HEC-RAS simulations appeared to adequately predict velocity in contracted regions impacted by ISUDS modeled as obstructions with ineffective flow areas and coefficients of contractions mimicking abutment modeling techniques. Therefore, this technique should provide adequate results for development of predictive relationships for V.

7.2 Predictive Models for Velocity

7.2.1 Effects of ISUDS on Relative Velocities

The *aaratio* was the best predictor of relative changes in *V*, explaining >99% of variability in the linear models (Appendix A, Table A2). This result agrees well with the analytical solution and linear models suggested by Seed et al. (1997) and Yeo et al. (2005). A linear model with *aaratio* as the only variable has a RMSE of 0.027. Relative changes always exceeded unity and for contraction percentages ranging from 10-50% the linear model with *aaratio* only predicted relative changes in *V* from 1.12 - 2.03 with mean errors of 1.3 - 2.4%. The linear *aaratio* model underpredicted *V* for larger *Fr* and overpredicted for smaller *Fr* (Appendix A, Figure A2). Addition of the *Fr*, the second-best predictor variable, to the linear solution improved the RMSE to 0.0205 ($adjR^2$ = 0.995). Addition of the *Fr* provided the largest change in $adjR^2$ compared to addition of other independent variables (Appendix A, Figure A1(b)). A linear model containing all 8 independent variables slightly improved the RMSE to 0.0154 ($adjR^2$ = 0.997; Appendix A, Figure A1(b), Table A2).

Cross validation of the linear *aaratio* model indicated systematic overprediction errors that increased with contraction percentage (Figure 3.5a). The model including *aaratio* and *Fr* slightly underpredicted relative change in *V* (Figure 3.5b). This model had larger IQRs for 10% and 20% contractions compared to the univariate model; however, IQRs were smaller for all other contraction percentages when *Fr* was included. The univariate model with *aaratio* was biased in mean prediction errors across contraction percentages (p<0.001); however, mean percent prediction errors between contraction percentages were not statistically different for the two variable linear model including *Fr* (p=0.055).

Easily applied representations of the *Fr* were tested in linear regressions because predicting *Fr* at the contraction can be challenging. Including alternative representations of *Fr* derived from at-a-station hydraulic geometry and the Darcy-Weisbach equation improved the RMSE from 0.0273 for the *aaratio* model to 0.0217 and 0.0221, respectively (Appendix A Table A2). Though the RMSE was slightly smaller for the hydraulic geometry representation of *Fr*, the residuals for the Darcy-Weisbach were less biased. Power functions using *aaratio* and *Fr* were also tested but did not improve model accuracy.

Adding additional variables, including the *Fr* did marginally improve overall model accuracy (max RMSE decrease of 0.0119); however, the univariate *aaratio* model (Eq. 3.10) was taken to be the best model to predict relative changes in *V* due to its parsimony, and the exclusion of the need to estimate *Fr* which could introduce extraneous error and complexity.

Eq 3.10. V_s/V_i=1.0377*$(aaratio)$+1.0017

The univariate *aaratio* model was physically intuitive and agreed well with data from previous experimental studies and my field measurements (Figure 3.6). The *aaratio* model predicted lower relative changes in *V* compared to the Yeo et al. (2005) and Seed et al. (1997) models for predicting *V* increases at the tip of an ISUDS at 60% depth and the maximum depth averaged main channel *V*, respectively. Differences between flume studies (Duan *et al.*, 2009; Jeon *et al.*, 2018; Molinas *et al.*, 1998) and the *aaratio* model from this study ranged from - 9% - 17%. The *aaratio* model most accurately predicted relative *V* from Molinas et al. (1998) followed by Jeon et al. (2018). The *aaratio* model over predicted relative *V* for two of the field data points and the Duan et al. (2009) study.

7.2.2 ISUDS Effects on Absolute Velocities in the Contracted Region

Both the model using the Manning equation to predict initial values of *V* with a known *R* (Eq. 3.11) and the power function model using $\frac{Q}{W_c}$ as a proxy for relative depth (Eq. 3.12) reasonably predicted the V_s in the region contracted by ISUDS (Figure 3.7). Cross validation indicated that the model using the Manning equation with a known *R* to predict V_s generally over predicted V_s whereas the power function generally underpredicted V_s (Figure 3.7a). Prediction accuracies of linear versus power function models varied among contraction ratios with the IQR of errors increasing for higher contraction percentages for the linear model but decreasing for the power function. Mean errors between contraction percentages were statistically different for both the linear model ($p<0.001$) and the power function ($p<0.001$). Both models were biased, with more accurate and less variable predictions for higher or lower contraction percentages when predicting V_s. However, both models are still valuable options to use to predict V_s with 90th and 10th percentile absolute values of error <10%. Equation 3.11 was developed using English units resulting in units of ft/s. Equation 3.12 is dimensionally homogeneous and can be used with English or SI units resulting in V_s in ft/s or m/s respectively.

Eq. 3.11 $V_s = 0.8 * \left[\left(\frac{1.49}{n}\right)^{0.7} * S^{0.348} * {W_C}^{-0.4} * Q^{0.412}\right] * \left[\left((aaratio) + 1\right)^{1.097}\right]$

Eq. 3.12 V_s=$[1.0377 * (aaratio) + 1.0017\ ] * \left[\left(\frac{\emptyset}{n}\right) * R^{\frac{2}{3}} * S^{\frac{1}{2}}\right]$

7.3 *Predictive Models for Shear Stress*

7.3.1 Effects of ISUDS on Relative Change in Shear Stress

The univariate *aaratio* quadratic model was the best predictor of relative changes in τ (RMSE = 0.117; Appendix A, Table A3). A univariate *aaratio* linear model also reasonably

predicted relative changes in τ (R^2 = 0.975, RMSE = 0.15; Appendix A, Table A3), however was biased in its prediction errors across contraction percentages. Addition of the *Fr*, the second-best predictor variable, to the linear solution resulted in an $adjR^2$ and RMSE of 0.988 and 0.104, respectively.

Cross validation revealed that the median errors in relative τ change for the linear univariate model were highly variable across contraction percentages (underprediction for the 10% and 50% contraction percentages versus overprediction for all other contractions, Figure 3.8a). The quadratic model slightly overpredicted the median IQR of errors increasing with contraction % (Figure 3.8b). Differences in mean errors between contraction ratios were significant for the linear univariate model (p<0.001), but not for the quadratic model (p=0.3955).

The univariate quadratic model based on *aaratio* (Eq. 3.13) was selected based on parsimony, and the exclusion of the need to estimate *Fr* which introduces complexity and the potential for error propagation, and unbiased errors across contraction percentages. However, the variability in prediction errors increases with increasing contraction percentages.

Eq. 3.13 $\frac{\tau_s}{\tau_i} = 1.066 * (aaratio)^2 + 2.13 * (aaratio)$+0.987

7.3.2 ISUDS Effects on Absolute Shear Stresses in the Contracted Region

Both the model using (Eq. 3.14) a known *R* and the model using the Manning equation with $R = D_i$ (Eq. 3.15) reasonably predicted the τ_s in the ISUDS contraction region. Both models overpredicted τ_s with median errors consistently positive (Figure 3.9). Error IQRs increased with contraction ratio and were smaller for the model using the Manning approach compared to the model with a known *R* except at 10% contraction. Median errors increased with contraction ratio

for the model utilizing the Manning approach, but decreased and approached zero for the model using a known *R*. Mean errors were significantly different between contraction percentages for the model with a known *R* (p<0.001) but were not for the model using a depth estimate (p=0.3955). Variability in τ_s prediction errors increased with contraction ratio. Both models were found to be valuable options for predicting τ_s with 90th and 10th percentile absolute values of error not exceeding 15%. Equations 3.14 and 3.15 are dimensionally homogeneous and can be used with English or SI units resulting in τ_s in lbf/ft^2 or Pascals respectively.

Eq. 3.14 $\tau_s = [1.066 * (aaratio)^2 + 2.13 * (aaratio) + 0.987] * \gamma * R * S$

Eq. 3.15 $\tau_s = [1.066 * (aaratio)^2 + 2.13 * (aaratio) + 0.987] * \gamma * (\frac{(Q*n)}{(W_C*S^{0.5}*\emptyset)})^{3/5} * S$

8.0 Discussion

Our study found that 1-D HEC-RAS simulations adequately predicted mean velocity in contracted regions affected by perpendicular ISUDS modeled as obstructions with ineffective flow areas and coefficients of contractions mimicking abutment modeling techniques. Comparisons with previous experimental studies were limited to small scale rectangular flumes with contraction percentages of 33%. Given the paucity of detailed field observations around ISUDS, additional studies across diverse contraction percentages may prove valuable for further testing of 1-D model fidelity to actual ISUDS effects. The HEC-RAS simulations for 33% contractions appeared to adequately predict velocity in contracted regions. Therefore, this technique should have provided adequate results for development of the predictive relationships for *V*.

Practical relationships for predicting mean relative changes and absolute values of *V* and τ due to emplacement of ISUDS in rectangular channels were developed (Table 3.5). These

models can be utilized for diverse applications including structure design to reduce potential bed and bank erosion, as a communication tool about potential effects of emplacement of ISUDS, and for identification of entrainable grain sizes due to changes in hydraulics. Models developed here were based on rectangular channels and vertical-wall rectangular structures constructed perpendicular to the flow. Application of these models to actual channel bathymetries may yield higher percent errors if careful consideration is not taken when estimating depth or calculating *aaratios* (Appendix B). Appendix B of this thesis provides additional insight into using developed equations for actual channel bathymetries.

Relative changes in mean *V* and τ estimated by HEC-RAS simulations were found to be well represented by easily applied regressions based on *aaratio*, and in some instances *Fr*. These results were consistent with models previously developed by Seed et al. (1997) and Yeo et al. (2005) who also identified *aaratio* as the primary variable controlling relative changes in *V*. The selected model for predicting relative changes in *V* agreed well with data from previous experimental studies and field work conducted during this study at an ISUDS emplaced as a temporary bridge construction platform (Figure 3.6). As expected, the developed model predicted lower relative changes in mean *V* at a cross section compared to Yeo et al. (2005) and Seed et al. (1997) models because their models predict *V* changes at the tip of an emplaced structure.

The relative *V* model developed in this study corresponds most closely with the data from Molinas et al. (1998) who presented relative velocities for different contractions as the maximum depth averaged velocities in the contracted region divided by the upstream *V* around abutments. Because they presented maximum depth averaged velocities in the contracted region, I expected to slightly underpredict relative velocities presented by this study. The model from the present

study slightly underpredicted velocities for two out of three of the contractions examined by Molinas et al. (1998). The Jeon et al. (2018) dataset provided detailed data that I would expect to best represent 1-D HEC-RAS velocities since 1-D HEC-RAS predicts cross section depth averaged downstream components of *V*. The model underpredicted the relative mean streamwise components of *V* in the contracted region of a spur dike for two different discharges using the Jeon et al. (2018) dataset. The percent difference between the model and the Jeon et al. (2018) data set was relatively small being $\leq$ 9%. The model over predicted relative velocities for the Duan et al. (2009) study which presented relative *V* as the mean streamwise component of *V* at the contracted section divided by the approaching upstream *V*. The relative change in *V* regression appears physically reasonable with respect to other developed equations for maximum relative velocities (Seed, 1997; Yeo *et al.*, 2005) and how it is bracketed by the best available flume data. Percent errors between all flume studies (Duan *et al.*, 2009; Jeon *et al.*, 2018; Molinas *et al.*, 1998) indicated the model did not over predict or under predict consistently for a range of contraction percentages and discharges suggesting the model is valuable in predicting relative changes in velocities around a variety of ISUDS.

Comparison of the relative change in *V* model to field data collected in this study indicated the model overpredicted change in *V* for two observed data points and underpredicted relative *V* for the remaining two data points. The two underpredicted relative velocities corresponded with the relative velocities calculated at the two cross sections affected by the ISUDS using the first and second field days with high flows relative to the following two site visits with relative changes in *V* that were overpredicted by the developed regression. It is possible that the differences between the two sets of field days may be partially attributed to differences in ADCP accuracy at different flow conditions. During low flow conditions it was challenging to keep the

ADCP boat speed below half the water speed. During high flow conditions the ADCP tended to get caught in eddies and not maintain an orientation perpendicular to the flow. Field data collected during this study may have been impacted by changing channel bathymetries and bed structures (logs) due to large flows between sampling events. Contractions may have been somewhat altered by ongoing construction such as changes in bridge pier shape and locations that could have affected results.

There is a need for detailed field studies in the contracted regions of ISUDS (Duan *et al.*, 2009). This study provided valuable field data estimates on relative changes in mean velocities due to structure emplacement but should be supplemented with data from sites with less influence from construction and flood events. Additionally, there is a need for field studies focused on 3-D flow patterns that can be used for model testing for irregular channels to expand upon existing rectangular flume studies (Dey and Barbhuiya, 2005; Duan, 2009; Duan *et al.*, 2009; Jeon *et al.*, 2018; Zhang *et al.*, 2009).

The selected model to predict relative changes in τ was found to be best represented by a quadratic equation with the *aaratio* as the only variable. This result makes physical sense because $\tau \propto V^2$. The shear stress models were not corroborated with flume or field data. Other studies have presented predictive models to quantify τ amplification in contracted regions impacted by ISUDS (Molinas et al., 1998), while others have developed predictive relationships for scour depths and patterns (eg. Pandey et al., 2018; Zhang & Nakagawa, 2008). However, these models typically require a form of *Fr* and flow depth which may not be readily obtainable. Scour is a patchy phenomenon and difficult to predict (Haschenburger, 1999), nevertheless easily-applied models to predict relative changes in V and τ could prove useful in certain

situations to estimate potential scour impacts due to various ISUDS contraction percentages. Future studies should investigate corroboration of shear stress equations presented here.

Absolute V and τ models were developed by expanding on relative regression models, with the goal of outlining several easily applied physically-based regressions and providing insight into those regression limitations especially when estimating depths. Depth either with or without a structure in the channel can be a limiting factor impacting the ability of academics and practitioners to predict velocities in channels using simply the Manning or shear stress equation if modeling or field data are not available. Absolute V and τ models were presented here with the opportunity to develop predictions based on estimates for depth or based on known values of depth and hydraulic radius. I recognize other methods to predict V_s and τ_s exist (Molinas *et al.*, 1998; Seed, 1997; Yeo *et al.*, 2005) and that there may be other ways to estimate depth than those evaluated here. However, these models were presented as options for practitioner and academic use along with a transparent presentation of variability in model estimates and errors. Relative change models can additionally be used to predict absolute values by multiplying by the initial value. This may reduce error in predictions if measured or modeled initial values are known for the discharge of interest.

Regression models for V_s and τ_s have reasonable accuracy with median absolute prediction errors of 1 - 5% with errors in the 90th and 10th percentiles <15% for τ_s and <10% for V_s. These models along with the relative regression models can be used as tools by practitioners and academics. Using the developed models can save time and money by reducing the need for hydraulic modeling. The models can be used to simplify assessment of potential hydraulic and geomorphic effects of emplacement of ISUDS under numerous conditions. One application of

these models is for understanding the effects of temporary construction access structures implemented in river channels for bridge construction, replacement, and maintenance. Thirty-seven percent of U.S. bridges reported in 2019 need repair costing an estimated $164 billion dollars; the repair process is anticipated to take at least 50 years (Bridge Report, 2020). Application of these models may help improve communication between DOTs and regulating agencies and reduce the time and money needed to preform assessments for permitting of bridge construction projects.

Regression analysis indicated that *Fr* may improve model predictions for both *V* and τ. This finding aligns with previous studies where *Fr* plays an important role in models predicting scour depths (eg. Pandey et al., 2018; Zhang & Nakagawa, 2008) and shear stresses around ISUDS (Molinas *et al.*, 1998). Froude number has also been identified as a key factor in flume studies evaluating relative *V* changes near ISUDS tips (Yeo *et al.*, 2005). Though addition of *Fr* was found to increase model accuracy, I excluded *Fr* based on this study's goal of developing easily-applied, parsimonious models to predict *V* and τ changes. Alternative approximations of *Fr* were examined and were found to also increase model accuracy, albeit at the cost of model complexity and potential error propagation via *Fr* estimation. Future work to evaluate the accuracy and error associated with use of *Fr* approximations is recommended.

Most previous studies on the hydraulic effects of ISUDS have focused on 2-D and 3-D hydraulic models and developing predictive relationships with variables that are sometimes not readily available. This study developed a suite of parsimonious models that can be used to inform preliminary structure design, environmental management options, and regulatory decision making. Additionally, this study outlined the analytical approach defining the importance of the area ratio (*aaratio*). Previous studies suggested the importance of the ratio but did not clearly

present an analytical foundation (Seed, 1997; Yeo *et al.*, 2005). Models presented here can be applied to typically recognized semi-permanent structures including spurs, groynes and abutments and less commonly recognized temporary structures such as riprap construction platforms.

9.0 Conclusions

I developed practical, physically-based relationships to predict mean relative changes and absolute values of V and τ due to emplacement of ISUDS. These models can be easily applied to both semi-permanent in-stream structures, as well as temporary structures such as those used for constructing transportation infrastructure in river environments. Relative changes in mean V and τ estimated with >50,000 HEC-RAS model simulations were well represented by easily applied regressions developed with one variable representing contraction area ratio, with applicability to contraction percentages ≤50% and Froude numbers <0.8. All chosen models were cross validated and had reasonable accuracy. Percent errors between flume studies and regression models of relative change in V ranged from -9% - 17%. Models of V_s and τ_s that require input estimates of velocity and shear stress in the absence of ISUDS resulted in median absolute prediction errors of 1-5% with errors in the 90th and 10th percentiles <15% for τ_s and <10% for V_s. Addition of Fr to models with only the area ratio was found to improve model accuracy for both V and τ predictions. However, determination of the Fr without hydraulic modeling or field work can be challenging, limiting the use of models containing the Fr. Froude number approximations using hydraulic geometry and flow resistance equations were found to also improve model accuracy. These approximations were still excluded from the final model suggestions due to the need for

further study on potential errors due to approximation and added model complexity with limited increases in accuracy.

Regression equations to predict V_s or τ_s with a structure in place requires knowledge of the initial values without the structure in place. Velocity or shear stress for the natural channel condition at the discharge of interest may be determined using hydraulic modeling, field measurements, or can be estimated using the Manning or shear stress equations requiring a known hydraulic radius and therefore water depth. If available, stage-discharge relationships, or hydraulic geometry can be used to determine approximate flow depth for discharges of interest and used to predict initial values. The suite of models presented in this study include models to estimate initial values with known *R* and depth or estimated values for depth using easily obtainable variables.

This study outlined the analytical approach defining the importance of the area ratio in predicting changes in velocity due emplacement of ISUDS. I found that one-dimension HEC-RAS adequately predicts velocities in contracted regions impacted by ISUDS modeled as obstructions with ineffective flow areas and coefficients of contractions and expansions mimicking abutment modeling techniques. Automation of HEC-RAS using VBA and the HECRAS Controller provides valuable opportunities to conduct hydraulic modeling for a range of channel geometries and conditions. This technique does not appear to be commonly utilized and can be an important tool for both academics and practitioners.

The suite of models developed here have a large range of applicability for temporary and semi-permanent ISUDS including groynes, spur dikes, abutments, and temporary construction features to inform preliminary structure design, environmental management options, and

regulatory decision making. The developed relationships were designed to be user-friendly and provide estimates of mean changes in hydraulics due to emplacement of ISUDS that can be used as a planning and communication tool. Accurate prediction of V_i, and τ_i, and the *aaratio* is vital as the quality of available input data determines model accuracy.

References

Ali, M.S., M.M. Hasan, and M. Haque, 2017. Two-Dimensional Simulation of Flows in an Open Channel with Groin-Like Structures by IRIC Nays2DH. Mathematical Problems in Engineering 2017:1–10.

Bridge Report, 2020. https://www.bridge-salon.jp/report_bridge/archives/eng/7776/20100922.html.

Brown, S., 1985. Design of Spur-Type Streambank Stabilization Structures. McLean, Virginia.

Brunner, G.W., 2016a. HEC-RAS River Analysis System User's Manual. Davis, California. https://www.hec.usace.army.mil/software/hec-ras/documentation/HEC-RAS 5.0 Users Manual.pdf.

Brunner, G.W., 2016b. HEC-RAS River Analysis System Hydraulic Reference Manual Version 5.0. Davis, California.

Chow, V. Te, 1959. Open-Channel Hydraulics. McGraw Hill Book Company, Inc.

Church, M., 2006. Bed Material Transport and the Moephology of Alluvial River Channels. Annual Review of Earth and Planetary Sciences 34:325–354.

Dey, S. and A.K. Barbhuiya, 2005. Flow Field at a Vertical-Wall Abutment. Journal of Hydraulic Engineering 131:1126–1135.

Duan, J.G., 2009. Mean Flow and Turbulence around a Laboratory Spur Dike. Journal of

Hydraulic Engineering 135:803–811.

Duan, J.G., L. He, X. Fu, and Q. Wang, 2009. Mean Flow and Turbulence around Experimental Spur Dike. Advances in Water Resources 32:1717–1725.

Ettema, R. and M. Muste, 2004. Scale Effects in Flume Experiments on Flow around a Spur Dike in Flatbed Channel. Journal of Hydraulic Engineering 130:635–646.

Goodell, C., 2014. Breaking the HEC-RAS Code: A User's Guide to Automating HEC-RAS. Portland, OR.

Haschenburger, J.K., 1999. A Probability Model of Scour and Fill Depths in Gravel-Bed Channels. Water Resources Research 35:2857–2869.

Ho, J., H.K. Yeo, J. Coonrod, and W.-S. Ahn, 2007. Numerical Modeling Study for Flow Pattern Changes Induced by Single Groyne. Proceedings of the Congress-International Association for Hydraulic Research. http://66.221.229.18/pdfs/tp/wat_env_tp/numerical-modeling-study-for-flow-pattern-changes-induced-by-single-groyne-25-07.pdf.

Jeon, J., J.Y. Lee, and S. Kang, 2018. Experimental Investigation of Three-Dimensional Flow Structure and Turbulent Flow Mechanisms Around a Nonsubmerged Spur Dike With a Low Length-to-Depth Ratio. Water Resources Research 54:3530–3556.

Karim, O.A. and K.H.M. Ali, 1999. Simulation of the Flow Pattern Around Spur Dykes Using FLUENTS. Jurnal Kejuruteraan 11:3–19.

Knighton, D., 1998. Fluvial Forms & Processes. Oxford University Press Inc., New York, NY.

Koken, M., 2011. Coherent Structures around Isolated Spur Dikes at Various Approach Flow Angles. Journal of Hydraulic Research 49:736–743.

Koken, M. and G. Constantinescu, 2008. An Investigation of the Flow and Scour Mechanisms around Isolated Spur Dikes in a Shallow Open Channel: 1. Conditions Corresponding to the Initiation of the Erosion and Deposition Process. Water Resources Research 44:1–19.

Lagasse, P.F., P.E. Clopper, J.E. Pagan-Ortiz, L.W. Zevenbergen, L. a. Arneson, J.D. Schall, and L.G. Girard, 2009. Bridge Scour and Stream Instability Countermeasures: Experience, Selection, and Design Guidance-Third Edition.

Li, G., L. Lang, and J. Ning, 2013. 3D Numerical Simulation of Flow and Local Scour around a Spur Dike. IAHR World Congress.

Lumley, T., 2020. Package “Leaps”: Regression Subset Selection. https://cran.r-project.org/package=leaps.

Melville, B.W., 1992. Local Scour at Bridge Abutments. Journal of Hydraulic Engineering 118:615–631.

Molinas, A., K. Kheireldin, and B. Wu, 1998. Shear Stress around Vertical Wall Abutments. Journal of Hydraulic Engineering 124:822–830.

Molls, T., M. Hanif Chaudhry, and K. Wasey Khan, 1995. Numerical Simulation of Two-Dimensional Flow near a Spur-Dike. Advances in Water Resources 18:227–236.

Mueller, D.S. and C.R. Wagner, 2009. Measuring Discharge with Acoustic Doppler Current Profilers from a Moving Boat. U. S. Geological Survey Techniques and Methods 3-A22. Reston, Virginia, p. 72.

Oullion, S. and D. Dartus, 1997. Three-Dimesnional Computation of Flow Around Groyne. Journal of Hydraulic Engineering 123:962–970.

Pandey, M., Z. Ahmad, and P.K. Sharma, 2018. Scour around Impermeable Spur Dikes: A Review. ISH Journal of Hydraulic Engineering 24:25–44.

Parker, G., P.R. Wilcock, C. Paola, W.E. Dietrich, and J. Pitlick, 2007. Physical Basis for Quasi-Universal Relations Describing Bankfull Hydraulic Geometry of Single-Thread Gravel Bed Rivers. Journal of Geophysical Research 112:F04005.

R Core Team, 2019. R: A Language and Environment for Statistical Computing.

Radspinner, R.R., P. Diplas, A.F. Lightbody, and F. Sotiropoulos, 2010. River Training and Ecological Enhancement Potential Using In-Stream Structures. Journal of Hydraulic Engineering 136:967–980.

Rajaratnam, N. and B.A. Nwachukwu, 1983a. Erosion near Groyne-like Structures. Journal of Hydraulic Research 21:227–287.

Rajaratnam, N. and B.A. Nwachukwu, 1983b. Flow Near Groin-Like Structures. Journal of Hydraulic Engineering 109:463–480.

SAS Institute Inc., 2018. JMP 14 Basic Analysis.

Seed, D.J., 1997. Guidelines on the Geometry of Groynes for River Training.

Tingsanchali, T. and S. Maheswaran, 1990. 2-D Depth-Averaged Flow Computation Near Groyne. 116:71–86.

Yazdi, J., H. Sarkardeh, H.M. Azamathulla, and A.A. Ghani, 2010. 3D Simulation of Flow around a Single Spur Dike with Free-Surface Flow. International Journal of River Basin Management 8:55–62.

Yeo, H.-K., J.-G. Kang, and S.-J. Kim, 2005. An Experimental Study on Tip Velocity and

Downstream Recirculation Zone of Single Groyne Conditions. KSCE Journal of Civil Engineering 9:29–38.

Zhang, H. and H. Nakagawa, 2008. Scour around Spur Dyke: Recent Advances and Future Researches. Annuals of Disas. Prev. Res. Inst., Kyoto Univ., Kyoto Univ:633–652.

Zhang, H., H. Nakagawa, K. Kawaike, and Baba Yasuyuki, 2009. Experiment and Simulation of Turbulent Flow in Local Scour around a Spur Dyke. International Journal of Sediment Research 24:33–45.

Tables

Table 3.1. Channel and temporary structure characteristics of example projects with temporary structures.

Channel characteristics of example projects with temporary structures			
Parameter	**Symbol**	**Max**	**Min**
Bed Slope	S	0.1%	0.03%
Channel Width (ft)	W_c	332	133
Channel Depth(ft)	D_c	22.5	10
Temporary structure characteristics based on state DOT construction projects			
Parameter	**Symbol**	**Max**	**Min**
Platform Width (ft)	W_s	139	24
Platform Length (ft)	L_s	104	69
Percent Contraction	NA	67%	31%
Angle from Bank	$\angle$	130°	90°
Time in the water (months)	t	24	1

Table 3.2. Summary of model ensemble ranges, parameter ranges and features.

Model Ensemble Ranges			
Parameter	**Symbol**	**Max**	**Min**
Bed Slope	S	2.00%	0.001%
Channel Width (ft)	W_c	664	33
Channel Depth (ft)	D_c	46	3
Percent Contraction	*NA*	80%	10%
Angle from Bank	$\angle$	90°	90°
Model Parameter Ranges			
Parameter	**Description**	**Range**	**Modeling Values**
Contraction Percentage	Percentage of channel width the ISUDS constrict	0%-80%	0%, 10%,20%,30%, 33%, 40%, 50%, 60%, 70%, 80%
Manning's *n*	Representation of channel roughness	0.02-0.04	0.02, 0.025, 0.03, 0.035, 0.04
Discharge, *Q*	Volume of water in channel	0.1*Q_b - Q_b	0.1Q_b, 0.2Q_b, 0.3Q_b, 0.4Q_b, 0.5Q_b, 0.6Q_b, 0.7Q_b, 0.8Q_b, 0.9Q_b, Q_b
Model Features			
Specification	**Description**	**Value**	**Notes**
Ineffective Flow Areas	Areas with minimal downstream flow contribution	1:1 or 2:1	1:1 upstream of structure 2:1 downstream of structure
Contraction coefficients	Account for energy losses due to expansion of flow	0.1 or 0.3	0.1 for cross section unaffected by structure 0.3 for cross sections affected by structure
Expansion coefficients	Account for energy losses due to contraction of flow	0.3 or 0.5	0.3 for cross section unaffected by structure 0.5 for cross sections affected by structure
Downstream Boundary Condition	Downstream boundary condition was set at normal depth	NA	Set to bed slope
Cross Sections	The user defined sections used to represent channel bathymetry	82	Spacing of cross sections was decreased in the vicinity of the ISUDS

Table 3.3. Independent variables used in regression analyses.

Independent Variables			
Independent Variable	**Description**	**Equation**	**Basis for Inclusion**
$\boldsymbol{D_i}$	Initial water depth, before structure emplacement	NA	Analytical solution
$\boldsymbol{D_s}$	Water depth at structure tip	NA	Analytical solution
aaratio*	Area ratio: structure area/flow area	$\frac{(L_s * D_s)}{(W_c * D_i) - (L_s * D_s)}$	Analytical solution
Contraction percentage	Structure length/ channel width	$\left(\frac{L_s}{W_c}\right) * 100$	Constricted flow area
Ls	ISUDS length into stream	NA	Analytical solution
n*	Manning's roughness	NA	Analytical solution
1.49/n	Inverse of Manning's Roughness	NA	Analytical solution
Q*	Discharge	NA	Forcing variable
R	Hydraulic radius	Area/ Wetter perimeter	Analytical solution
S*	Bed Slope	NA	Analytical solution
W_c*	Channel Width	NA	Analytical solution
W_c / D_c*	Width to depth ratio of channel	$\frac{W_c}{D_c}$	Geomorphology
W_{cadj} / D_c	Width to depth ratio adjusted for constriction	$\frac{W_c - L_s}{D_c}$	Geomorphology
xs*	Number of cross sections (*xs*) with ineffective flow areas	NA	Potential modeling effect
Alternative Representations of *Fr*			
Approach *Fr* _ND	Approach Froude # with Normal Depth (*ND*) replacing flow depth	$\frac{Q}{(W_c) * ND^{3/2} * g^{1/2}}$	Obtaining flow depth may be infeasible, *ND* can be estimated
Fr* _at structure	Froude number	$\frac{Q}{(W_c - L_s) * {D_s}^{3/2} * g^{1/2}}$	Influences flow behavior
***Fr* _hydraulic geometry at structure**	*Fr* with depth replaced with $Q^{0.4}$ based on at a station hydraulic geometry	$\frac{Q^{0.4}}{(W_c - L_s) * g^{1/2}}$	Flow depth at the structure may be less obtainable than an estimate of *Q*

Fr #_ND at structure	Froude # with Normal Depth replacing flow depth	$\frac{\mathrm{Q}}{(\mathrm{W}_c - \mathrm{L}_s) * ND^{3/2} * \mathrm{g}^{1/2}}$	Obtaining flow depth may be infeasible, *ND* can be estimated
s/n^2	Proportionality derived from Darcy-Weisbach and Manning relations	$\frac{S}{n^2}$	Influences flow behavior

***Denotes variables used in the 'leaps' package in R for linear regression analysis*

Table 3.4. Collected field data at Lyerly, GA bridge replacement site.

Visit #	Field Visit Type	Avg. Measured Discharge for All XS (cfs)	% Contraction from Temporary Structure
1	Pre- bridge construction	367	0%
2	Structure configuration 1	558	XS 2=16%
			XS 3=18%
3	Structure configuration 2	199	XS 2= 11%
			XS 3= 21%
4	Post-bridge construction	159	0%

Table 3.5. Models for predicting relative changes and absolute values of velocity and shear stress resulting from ISUDs.

Model Type	Model Form	Model
Relative Change in Velocity *	Linear	$\frac{V_s}{V_i} = 1.0377 * (aaratio) + 1.0017$
Absolute Velocity: Velocity at ISUDS	Power Function	$V_s = 0.8 * \left[\left(\frac{1.49}{n}\right)^{0.7} * S^{0.348} * \mathrm{W}_c{}^{-0.4} * Q^{0.412}\right] * \left[\left((aaratio) + 1\right)^{1.097}\right]$
Absolute Velocity: Velocity at ISUDS	Linear: Manning's Eq. predict V_i	V_s=[$1.0377 * (aaratio) + 1.0017$]*$\left[\left(\frac{\emptyset}{n}\right) * R^{\frac{2}{3}} * S^{\frac{1}{2}}\right]$
Relative Change in Shear Stress*	Quadratic	$\frac{\tau_s}{\tau_i} = 1.066 * (aaratio)^2 + 2.13 * (aaratio)$+0.987
Absolute Shear Stress	Quadratic: Manning's estimated D_i	$\tau_s = [1.066 * (aaratio)^2 + 2.13 * (aaratio) + 0.987] * \gamma * \frac{(Q * n)}{(\mathrm{W}_c * S^{0.5} * \emptyset)}^{3/5} * S$
aaratio*		**Full form**: $\frac{(L_s * D_s)}{(\mathrm{W}_c * D_i) - (L_s * D_s)}$ **Simplified form**: $\frac{(\mathrm{L}_s)}{(\mathrm{W}_c) - (L_s)}$

**The relative change equations can be rearranged to solve for absolute values if initial values without a structure are known from field data or modeling studies.*

*** Absolute models provide a means of calculating mean values at a structure without the need for depth data.*

****aaratio can be estimated assuming initial depths and depths with the structure in place are similar, resulting in a ratio of the structure length to the flow area.*

Figures

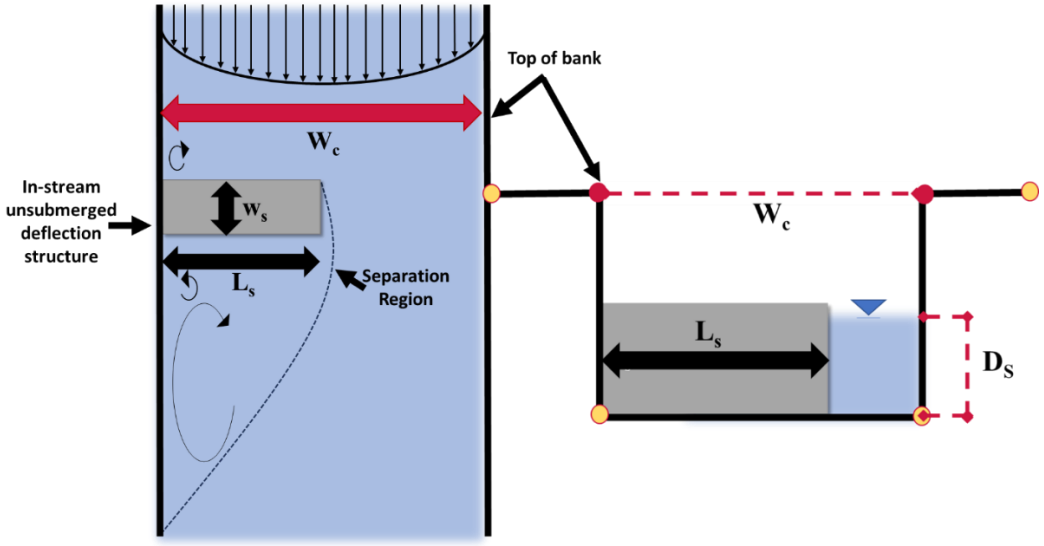

Figure 3.1. Profile and plan view of typical in-stream unsubmerged deflection structure where W_c, L_s, and D_s are the channel width, structure length, and height of the structure in contact with water, respectively.

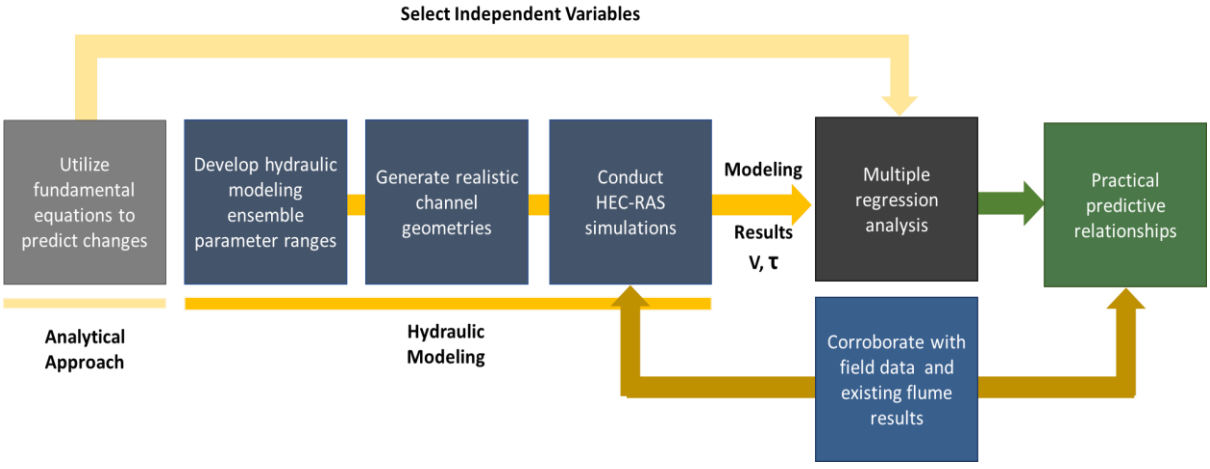

Figure 3.2. Overview of the study methodology that includes an analytical approach, hydraulic modeling, multiple regression analysis and corroboration of modeling results and predictive regression equations using existing flume studies and collected field data.

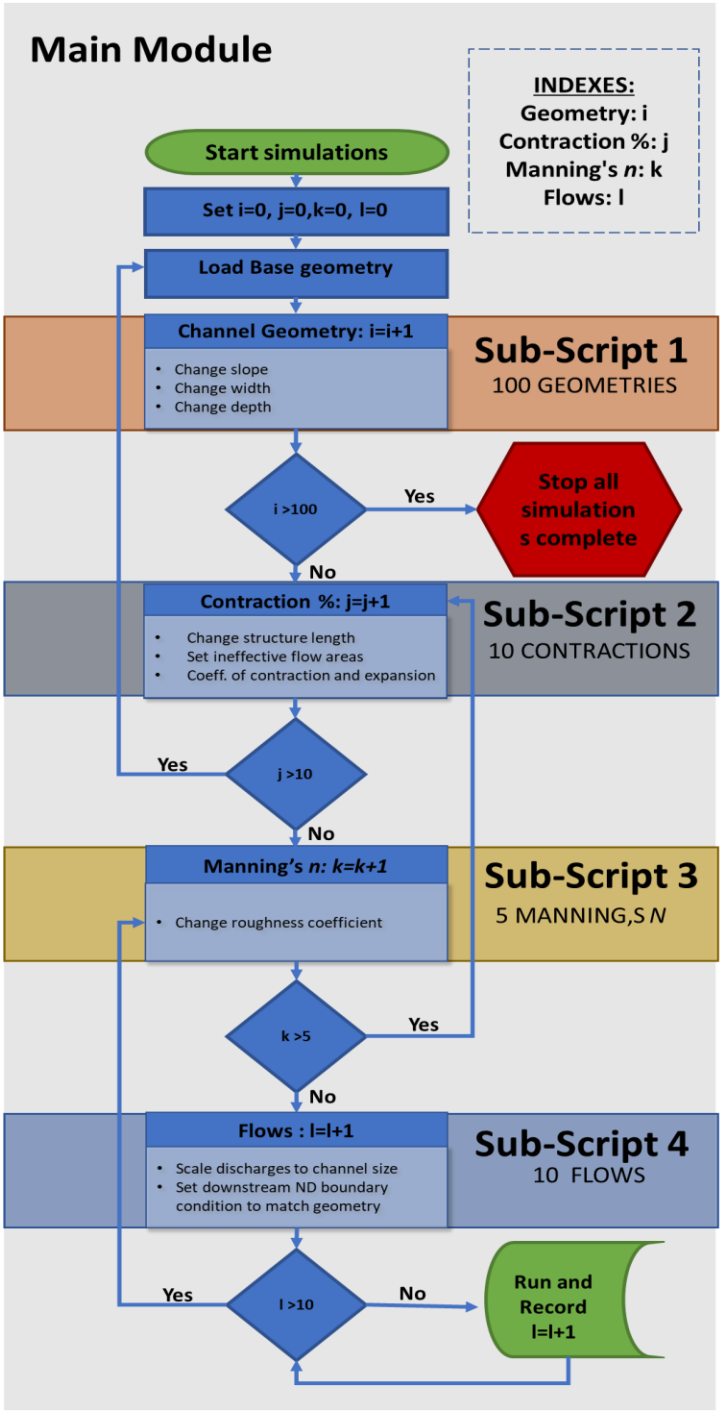

Figure 3.3. Flow diagram of the VBA code that includes a main module that runs HEC-RAS, records results and calls sub-modules that alter the channel geometry, contraction percentage, Manning *n* values, and the steady flow file.

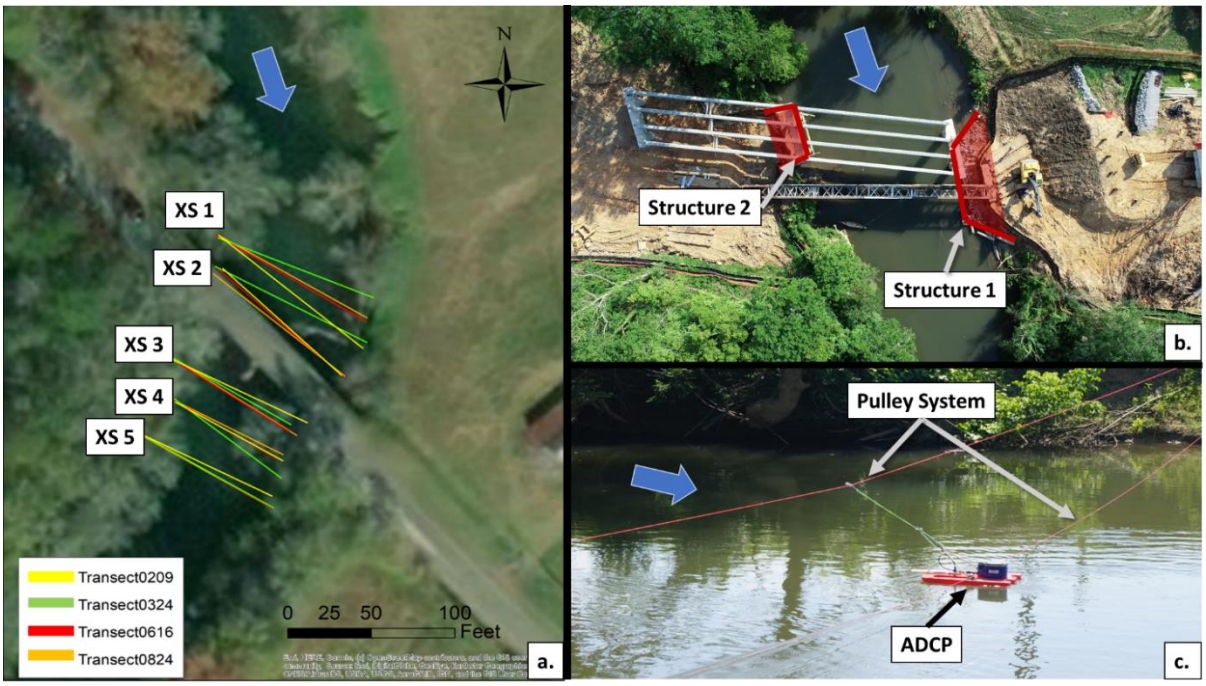

Figure 3.4. Field methods overview where blue arrows represent flow direction. Location of cross sections for all site visits (a). Locations of cross sections on the left bank varied between site visits based on flow heights and changes in bank safety. Temporary riprap structure placement for 6/16/2019 (b). ADCP pulley system set up for one cross section (c).

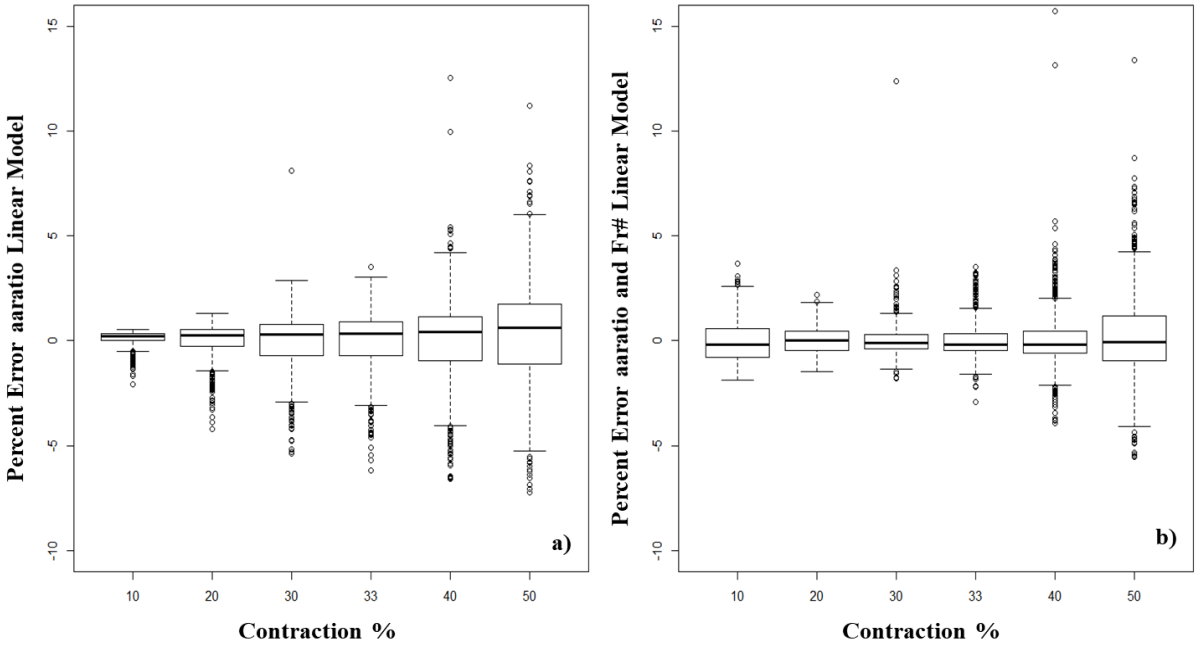

Figure 3.5. Cross-validation results for (a) univariate model based on *aaratio*, and (b) a two variable linear model containing *aaratio* and *Fr*.

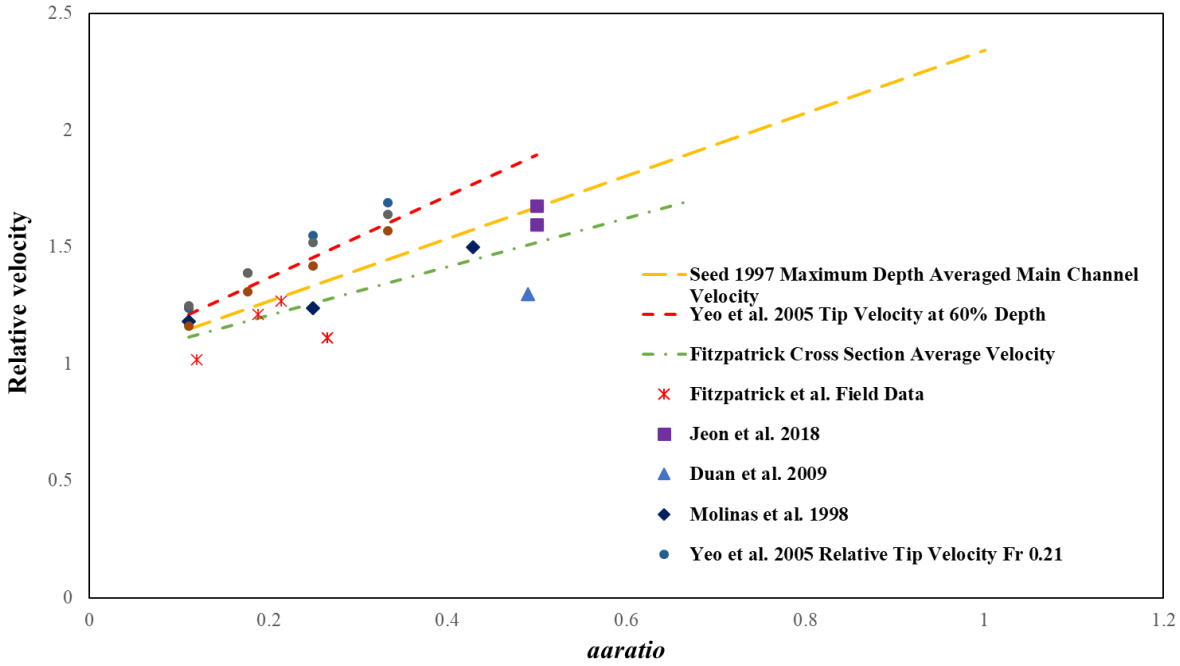

Figure 3.6. Comparison of ISUDS effects on velocity based on a univariate *aaratio* model developed in this study versus previous experiments and field data collected for this study.

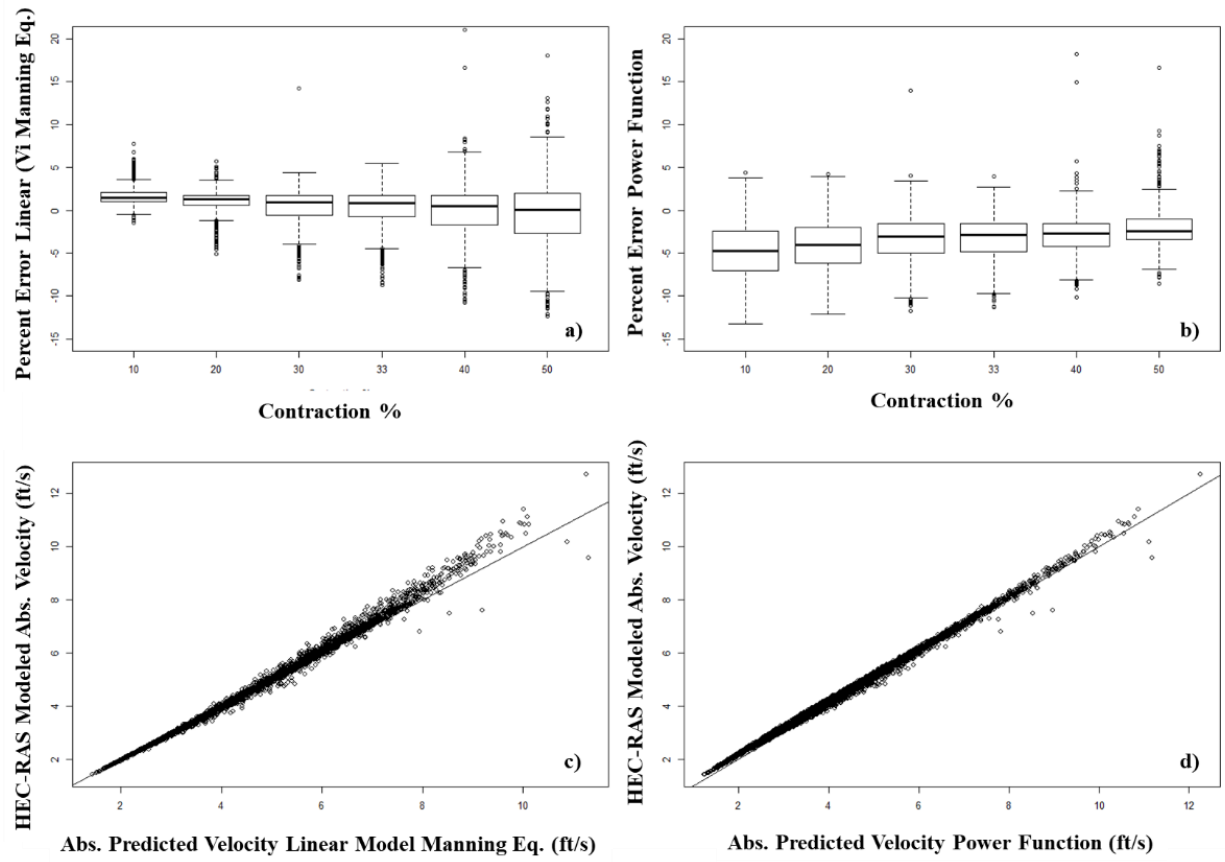

Figure 3.7. Percent errors in prediction of V_s using (a) the linear model utilizing the Manning equation with a known R to predict V_i, and (b) the power function model. The linear model tends to underpredict V_s in a contracted region impacted by an ISUDS (c), and the power function tends to overpredict the V_s (d).

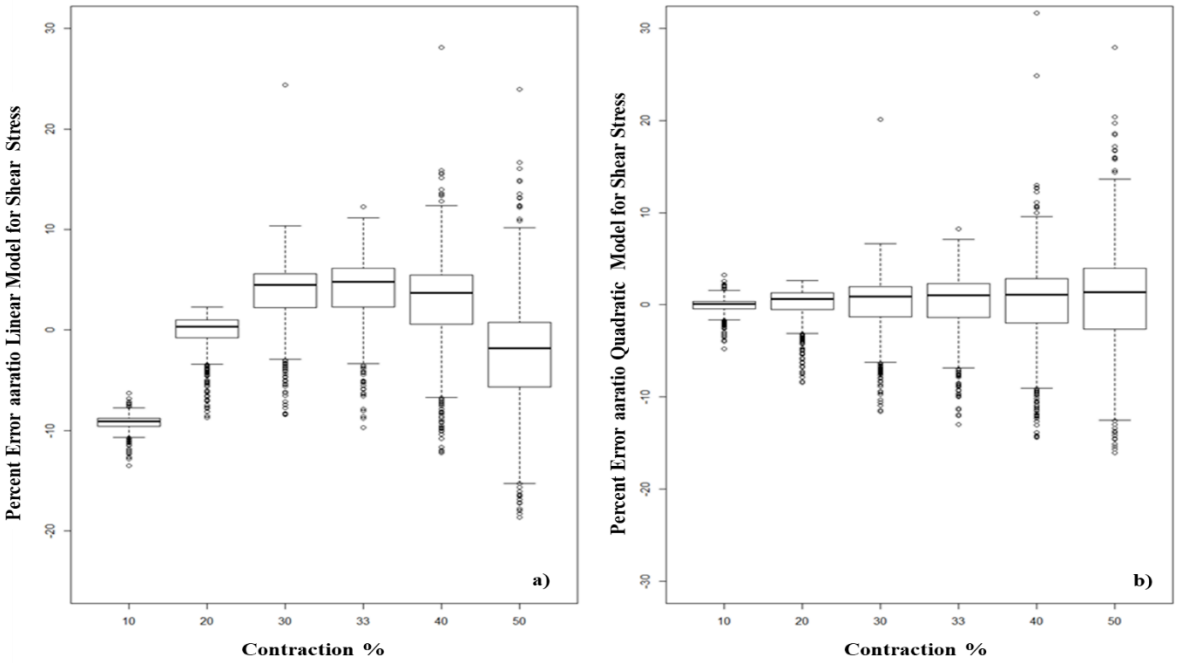

Figure 3.8. Cross-validation results for a (a) linear and (b) quadratic univariate model for predicting relative changes in shear stress based on *aaratio*.

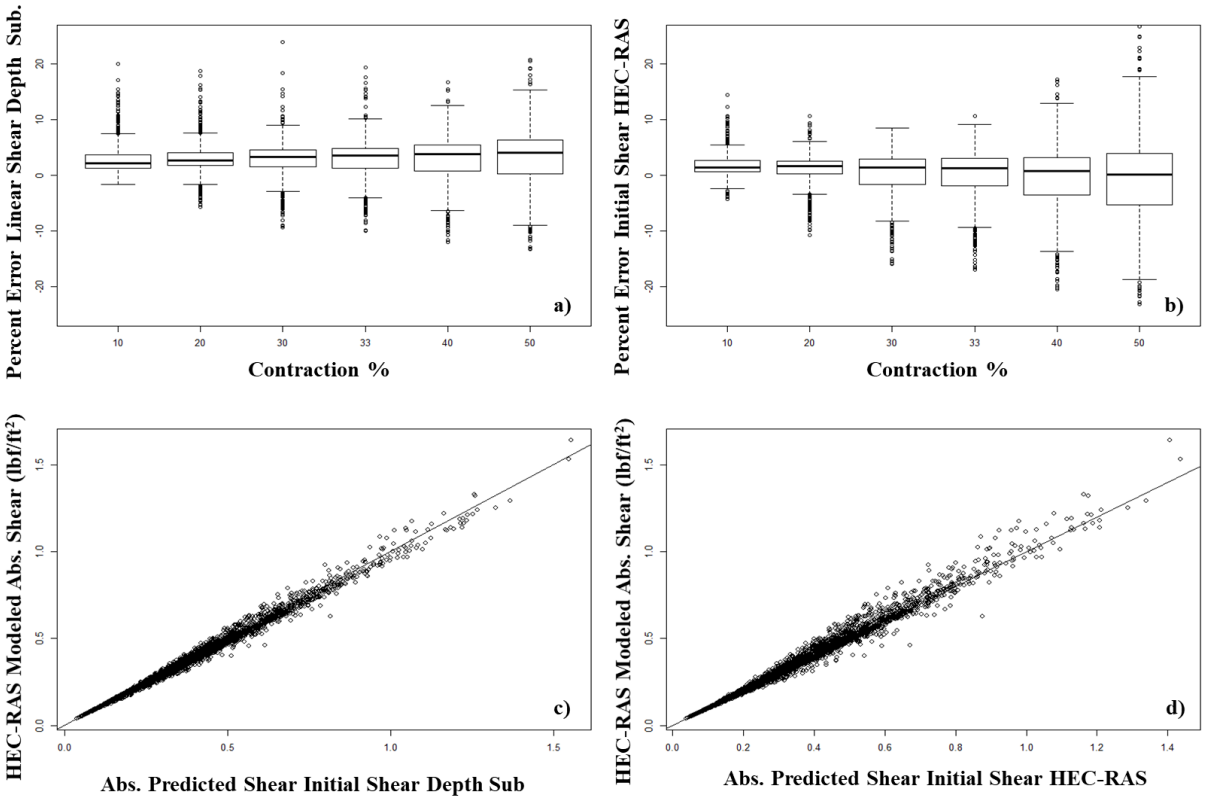

Figure 3.9. Percent errors in prediction of τ_s using the model replacing *R* in the shear stress equation with D_i and estimating D_i using the Manning equation to predict τ_i (a,c) and the model utilizing the shear stress equation with a known *R* to predict τ_i (b,d). Both models on average over predict τ_s with median percent errors consistently above zero.

CHAPTER 4

EFFECTS OF IN-STREAM UNSUBMERGED DEFLECTION STRUCTURES ON SPATIAL PATTERNS OF VELOCITY AND SHEAR STRESS

1.0 Introduction

Emplacement of both temporary and semi-permanent transverse structures in streams and rivers can have significant effects on hydraulic and geomorphic processes. Unsubmerged deflection structures encompass both semi-permanent structures including groynes, spur dikes, abutments, and temporary structures such as riprap construction platforms. These structures exhibit similar hydraulic characteristics and will be referred to as in-stream unsubmerged deflection structures (ISUDS) throughout this chapter. In-stream unsubmerged deflection structures constrict channel flow and can lead to local increases in velocity (V) and shear stress (τ), potentially causing increased bed scour and erosion of the opposing bank. Quantification of V and τ, and identification of high V and τ regions are important for understanding potential hydraulic and geomorphic impacts of ISUDS emplacement. In this study, I evaluate spatial distributions of V and τ due to emplacement of ISUDS to identify locations at highest risk for increased bed or bank erosion due to changes in channel hydraulics. Knowledge of spatial distributions of V and τ can complement predictive relationships quantifying changes in hydraulics (Chapter 3; Seed, 1997; Yeo et al., 2005) to inform preliminary structure design, environmental management options, and regulatory decisions.

Many experimental and modeling studies have evaluated flow fields and τ in regions contracted by ISUDS. The extensive literature serves as a valuable resource for identifying general locations most at risk for bed and bank scour; however, previous studies generally have not evaluated how structure or channel size control the spatial extent of structure influence. Early experimental studies found increases in *V* and τ in regions contracted by transverse structures, with maximum bed shear stress occurring near the tip of the structure (Molinas *et al.*, 1998; Oullion and Dartus, 1997; Rajaratnam and Nwachukwu, 1983a; b). Rajaratnam & Nwachukwu (1983a) found that groynes cause flow disturbance both upstream and downstream. The flow field around ISUDS is turbulent and three dimensional, consisting of three general regions: the main flow zone, the mixing zone and the return flow zone (Figure 4.1; Zhang & Nakagawa, 2008). Velocities in the main flow zone are increased due to the contraction and eddies develop upstream and downstream of the structure due to the abrupt change in flow area. In the return flow zone, two eddies of different sizes commonly occur with a small eddy near the structure and a larger eddy farther downstream (Zhang and Nakagawa, 2008). The main flow zone is an area at high risk for increased bed and bank erosion due to contraction of the flow. Whereas the area directly downstream of the structure is typically subjected to lower shear stresses leading to a depositional environment (Oullion and Dartus, 1997).

Previous studies have identified numerous ISUDS characteristics including structure length, permeability, geometry, and installation angle relative to the bank that affect magnitudes and spatial distributions of *V* and τ in regions contracted by ISUDS (Table 4.1). These studies are useful starting points for identifying general trends in potential hydraulic and geomorphic effects of ISUDS emplacement; however, their applicability is generally limited to a small subset of

channel sizes, structure widths and discharges without explicit consideration of the spatial extent of ISUDS influence.

Extensive application of ISUDS has led to establishment of design guidelines (Brown, 1985; Lagasse et al., 2009) and equations to predict maximum velocities (Seed, 1997; Yeo et al., 2005) scour depths (Pandey et al., 2018; Zhang & Nakagawa, 2008) and shear stresses (Molinas *et al.*, 1998) in regions contracted by ISUDS. Design guidelines typically focus on general recommendations for emplacement of structures including addressing structure length, spacing between multiple structures for bank protection, installation angle and the geometry of the structure (Brown, 1985; Lagasse *et al.*, 2009); however, they typically do not attempt to identify regions most at risk for increased bed and bank erosion based on channel size, discharge and contraction percentage. Predictive relationships to quantify velocity (Seed, 1997; Yeo *et al.*, 2005) and shear stress (Molinas *et al.*, 1998) have focused on one value for a given location and do not identify spatial patterns within a larger affected region. Seed (1997) used results from a validated 2-D numerical model of a rectangular channel to predict relative changes in V due to groynes of varied structure length, spacing between multiple structures for bank protection, structure orientation angle relative to the bank, and groyne taper. The study focused on predicting three V in areas potentially at risk for large changes in hydraulics: the maximum-depth averaged V in the main channel between groynes, the near-bed V near a groyne tip, and the near-bed V at the toe of the riverbank. Yeo et al. (2005) expanded on these results by developing relationships to predict depth averaged V at the tip of a single groyne using results from flume studies. Though several studies have led to general guidelines for design and placement of ISUDS in river channels, most lack identification of high-risk regions within a river reach containing ISUDS where V and τ are most amplified due to changing hydraulics. Areas with

large increases in V and τ compared to unobstructed channel conditions are at higher risk for erosion and impaired organism movement.

The goal of this chapter is to evaluate altered spatial distributions of V and τ in river reaches containing ISUDS and discuss how the spatial distributions are affected by changes in discharge, channel geometry, and structure characteristics. The specific objectives are to:

1. develop a set of 2-D HEC-RAS simulations that describe the spatial distributions of V and τ in a river reach containing an ISUDS for a range of channel dimensions and contraction percentages with emphasis on locations of maxima and near bank regions; and
2. describe how the modeling results can be used with predictive relationships for V and τ (Chapter 3) to identify potential locations at highest risk for increased bed and bank erosion due to structure emplacement.

2.0 Methods

Two-dimensional hydraulic modeling was conducted using the United States Army Corps of Engineers (USACE) Hydrologic Engineering Center River Analysis System (HEC-RAS) Version 5.0.7 (Brunner, 2016a). A total of 42 HEC-RAS models were created representing three channel widths, seven structure contraction percentages, and two streamwise structure widths (20ft and 50ft). The length of the model (0.5 miles), and Manning roughness value (0.035) remained constant for all simulations. The three channel sizes were selected to represent a narrow, medium, and wide channel to evaluate the effect of channel width on erosion potential on the bank opposite the emplaced structure, with emphasis on the moderate and narrow widths. The narrow and wide channel were selected from the 100 channel geometries developed in

Chapter 3. Straight, rectangular channel geometries that adhere to the geomorphic scaling properties of natural channels were developed in Chapter 3 using dimensionless downstream hydraulic geometry relationships (Parker *et al.*, 2007). The medium channel was developed based on average channel dimensions for the Chattooga River near Lyerly, GA where field work was conducted for Chapter 3 at a bridge maintenance site utilizing ISUDS. The narrow, medium and wide channels had widths of 60.4 ft, 114.03 ft and 519.17 ft respectively. Analysis focused on the narrow and medium channel widths due to the limited use of ISUDS in very wide channels. Each channel geometry was run for six structure lengths and two structure widths with contraction percentages of 0%, 10%, 20%, 30%, 33%, 40% and 50%. The simulations with a 0% contraction (no structure) served as a baseline for V and τ in the channel under unobstructed conditions. All model ensembles were conducted for three discharges scaled to channel size (Table 4.2).

Mesh sizes were decreased within the ISUDS contraction zone to improve computation accuracy in the focal area of interest (Table 4.2, Figure 4.2). HEC-RAS has the capability to run 2-D computations using either the Saint-Venant (Full Momentum Method) or Diffusion Wave Equations. The Full Momentum Method was chosen for its superior representation of changes in forces resulting from abrupt contractions such as ISUDS, and the inclusion of an additional turbulence term (Brunner, 2016b). Computation intervals and mesh sizes were set to keep Courant numbers below two for model stability and accuracy; Courant numbers as high as three can still produce accurate results for the Full Momentum Method (Brunner, 2016a).

Eddy viscosity coefficients used to provide turbulence closure were calibrated using the Jeon et al. (2018) Case 1 flume data from their supplemental materials. Given this study's focus on regions of amplified erosion potential, the eddy viscosity coefficient was calibrated using the

reattachment length and locations of relatively large increases in velocity as opposed to velocity values and water surface elevations. Based on this calibration, eddy viscosity coefficients were held constant at 0.25 for all model simulations. This value is typical for straight channels with smooth surfaces and on the upper limits of the "little transverse mixing" intensity range suggested in the HEC-RAS 2-D manual (Brunner, 2016b). Abrupt contractions likely lead to increased transverse mixing; however, a value of 0.25 appears reasonable being on the upper end of the straight channel range and is a precautionary approach that brackets higher estimates of V and erosion potential. A sensitivity analysis on eddy viscosity indicated smaller eddy viscosity coefficients lead to larger V and flow reattachment lengths and thus larger areas of amplified V and τ. Modeled mean V at the structure tip in Jeon et al. (2018) Case 1 was underestimated by 0.16 ft/s, a difference that may be partially attributable to grid resolution and scale effects in simulating the 2.95 ft wide flume.

All models were assessed for changes in spatial distributions of V and τ relative to the unobstructed channel condition. Regions with relative changes in V and τ of 1.1, 1.3, 1.5 and 2.0 times the unobstructed channel condition were compared across discharges, contraction percentages, obstruction widths and channel sizes to draw conclusions about general effects of ISUDS in diverse river settings. The analysis concentrated on areas of maxima and near bank regions to identify locations in the reach with highest potential risk for increased bed scour and bank erosion.

3.0 Results

Hydraulic modeling results indicated that higher discharges and higher contraction percentages lead to larger maximum values of absolute V and τ, as well as longer downstream

distances with V and τ exceeding unobstructed channel conditions by more than 10% (Figure 4.3 a and b). These changes in the length of downstream effects did not increase linearly with structure length (Figure 4.3 c and d). For all channel widths, contraction percentages and discharge combinations explored increases in V of 1.1, 1.3, 1.5 and 2.0 times the unobstructed channel condition extended a maximum length of approximately $9L_S$, $5L_S$, $3.5L_S$ and $1.8L_S$, respectively, from the downstream edge of the structure, where L_S is the structure protrusion length into the channel. Higher discharge and larger contraction percentages led to longer distances downstream impacted by increased V and τ. Channels with a 50% contraction had velocities up to 1.9, 2.1 and 2.5 times the unobstructed channel V for the narrow, medium, and wide channel, respectively. Shear stresses were up to 3.2, 4.6 and 4.4 times the unobstructed channel shear stress (τ_i) for the narrow, medium, and wide channel. Contractions above 30% increased V on the opposite bank by 1.1 - 1.3 times the unobstructed channel condition for all channel sizes and modeled discharges. Increases in structure streamwise width did not systematically increase the length downstream of the impacted regions as no consistent relationship was observed between structure streamwise width and increases in V and τ. General observed trends for changes in discharge, contraction percentage and structure widths were consistent across the three channel widths. At relatively higher discharges and higher contraction percentages some flow conditions became supercritical in the contracted regions.

3.1 Effect of discharge

Increasing relative discharge generally led to an increase in the length of channel with V and τ at least 1.1 times higher than the initial unobstructed channel condition for a constant channel width, structure width, and contraction percentage (Figure 4.4). Increases in discharge also

generally led to an increase in downstream recirculation length. Increasing the discharge while holding contraction percentage constant increased the absolute maximum V and τ for all channel sizes. The location of the maximum was pushed downstream farther away from the structure tip for larger discharges; for smaller discharges the maximum V and τ occurred directly at the structure tip. Due to the increase in impacted streamwise length, larger discharges led to larger areas on the opposite bank impacted by increased V and τ. Regions with relative τ of 1.1, 1.3, 1.5 and 2.0 times the unobstructed channel condition were larger than relative V regions generally extending farther downstream and across the channel.

Areas directly behind the structure had low V and τ with minimal risk for bank erosion and bed scour. Oullion and Dartus (1997) found that areas directly behind ISUDS have low risk for scour and may serve as depositional environments for scoured material of a specific grain size. This finding was consistent with the use of ISUDS, such as groynes and spur dikes, to protect banks directly behind the structure.

3.2 Effect of contraction %

Increasing the percent contraction while holding other parameters constant generally led to an increase in streamwise length of channel with amplified V and τ (Figure 4.5). Additionally, V and τ maxima increased, consistent with previous experimental and modeling studies examining a narrower range of conditions (Molinas *et al.*, 1998; Seed, 1997; Yeo *et al.*, 2005). Maximum depth averaged V in the narrow and medium channel widths at a 10% contraction ranged from 1.1 - 1.3 times the initial velocity (V_i) for all discharges. Maximum depth averaged V in the narrow and medium channel widths at a 50% contraction were higher relative to the 10%

contraction and ranged from 1.7 - 2.2 times the V_i. Maximum depth averaged τ in the narrow and medium channel widths at a 10% contraction ranged from 1.2 - 1.6 times the initial shear stress (τ_i) for all discharges. Maximum depth averaged τ in the narrow and medium channel widths at a 50% contraction were higher relative to the 10% contraction and ranged from 2.4 - 4.6 times the τ_i.

Higher contractions pushed the region of increased V and τ towards the opposite bank, increasing potential risk for bank erosion. Even for relatively large rivers, contractions of 30% can lead to increases of at least 1.1 times the V_i on the opposite bank and 1.5 times the τ_i. For 50% contractions, results indicated that velocities at least 30% larger than the unobstructed condition reach the opposite bank for all discharges and channel sizes.

3.3 Effect of structure width

Increasing the streamwise structure width did not appear to substantially increase the length of regions with amplified V and τ (Figure 4.3; Figure 4.6). No consistent relationship was observed between the streamwise length required to return to unobstructed channel conditions and structure streamwise width.

3.4 Comparison of results to predictive relationships

Maximum relative changes in V (the ratio between the maximum velocity with the structure in place and the unobstructed channel condition) for the medium and narrow channels were plotted for simulations with subcritical flow and compared to predictive relationships from Chapter 3 of this thesis and previous studies (Seed, 1997; Yeo et al., 2005) using an area ratio (*aaratio*) as the independent variable (Figure 4.7). Seed (1997) predicted the maximum-depth

averaged *V* in the main channel between groynes, and Yeo et al. (2005) developed relationships to predict depth averaged *V* at the tip of a single groyne using results from conducted flume studies. I predicted cross section average *V* using 1-D hydraulic modeling in HEC-RAS (Chapter 3). HEC-RAS 2-D predictions of maximum *V* using a constant eddy viscosity coefficient in ISUDS contractions varied substantially for a given *aaratio* (Figure 4.7). Most of the HEC-RAS 2-D predictions for maximum velocity plotted above the relationship presented in Chapter 3 for cross section average *V* as expected.

4.0 Discussion

This study found that increases in contraction percentage and discharge led to larger maximum values of absolute *V* and τ in addition to longer downstream distances with increased *V* and τ relative to unobstructed channel conditions. To minimize risk of potential bed scour and erosion on the opposite bank, contraction designs should be informed by these results with careful consideration of the potential for large runoff events during the expected lifetime of the structure. For semi-permanent structures including groynes and spur dikes that are commonly used for bank protection, designers must consider balancing bank protection behind the implemented structure and increases in bed scour and τ on the opposite bank. Risk of erosion on the opposite bank will depend on bank characteristics such as bank angle, presence of vegetation and material cohesion. For temporary structures such as bridge construction access platforms, in-water working windows may serve as a valuable time frame reference for determining the probability of larger storm events. At relatively high discharges and contraction percentages, some hydraulic model simulations became supercritical in the contracted regions. Supercritical

flow conditions may lead to hydraulic jumps and high velocities that may impede movement of aquatic organisms.

Two-dimensional modeling results indicated that higher contractions push the increased V and τ regions towards the opposite bank, potentially increasing the risk of bank erosion. Contractions of 30% can lead to 10% increases in V and 50% increases in τ on the opposite bank. Previous guidance on installing spurs in narrow river channels (<250ft wide) suggest flow constriction may cause erosion on the bank opposite of the structure but, in some cases, may be purposely used to shift the channel location (Lagasse *et al.,* 2009). For temporary structures and structures not intended to shift the channel location, stability and erodibility of the opposite bank should be carefully evaluated to determine potential risk for contraction percentages ≥30%. Modeling results also indicated that the length downstream impacted by velocities of at least 1.1 times the V_i was not linearly related to structure length. Longer structures contributed to relatively smaller changes in distance impacted downstream compared to shorter structures. This finding should be further evaluated.

Calibration of the eddy viscosity coefficient for a range of channel contraction percentages and discharges was limited by a paucity of large-scale field data available in the literature. I endeavored to calibrate the eddy viscosity coefficient using the Jeon et al. (2018) flume study; however, HEC-RAS 2-D modeling of small scales flumes proved challenging due to the need for small mesh sizes and time steps to produce stable and accurate simulations. The eddy viscosity coefficient in this study was held at a constant value for all model simulations, while in reality this value likely increases with increasing contraction percentage and may change with discharge. Though this study held the eddy viscosity coefficient constant, general trends

observed in changes in spatial locations of increased relative V and τ were consistent with previous studies (e.g. Jeon et al., 2018) indicating that these results can provide useful insights to ISUDS effects on spatial patterns of V and τ.

Comparison of maximum relative changes in V to predictive relationships from previous studies and Chapter 3 using an area ratio predictor variable (*aaratio*) showed that the 2-D HEC-RAS predictions varied for a given *aaratio* but, generally fell within the range of relationships suggested by Seed (1997) and Yeo et al. (2005). The variability in 2-D HEC-RAS predictions from the regressions may be due in part to the lack of calibration of the eddy viscosity coefficients for increasing contraction percentages and discharges. Future studies are recommended to evaluate the effect of contraction percentage and discharge on the eddy viscosity coefficient and improve model accuracy. Such data would be particularly useful to practitioners modeling bridge abutments in 2-D HEC-RAS; however, such a study would require detailed field data or large-scale flume studies.

This study focused on rectangular channel geometries and vertical-wall ISUDS installed perpendicular to the bank. Many studies have been conducted on rectangular channels and some have evaluated changes in installation angle and structure shape (Melville, 1992; Yazdi *et al.*, 2010). However, studies on irregular and complex channel bathymetries are rare. Future research should evaluate the effects of compound channels, and other realistic channel bathymetries on flow fields in contracted regions.

4.1 Recommendations for Tool Development

A tool that integrates the 2-D spatial patterns in hydraulics revealed in this chapter with the predictive models for V and τ (Chapter 3) into a unified framework could provide valuable

insights into potential hydraulic and geomorphic effects of ISUDS before structure emplacement when more complex modeling is infeasible. Though the focus of this study was not on presenting this tool, an Excel-based management tool is being developed using spatial results from this study, mean predictive regressions developed in Chapter 3 and maximum tip velocity predictions from Yeo et al. (2005). The tool aims to combine results and recommendations from this study into a user-friendly format for ease of application (Appendix B) for a variety of users including state DOTs as they plan and design various ISUDS.

The tool predicts mean and relative changes in V and τ based on inputs of structure length, channel dimensions, discharge, Manning n, and bed slope. Absolute velocity and shear stress magnitudes are predicted based on estimates of V_i based on field or modeling data. Prediction of mean and maximum V and τ is important for anticipating and mitigating ISUDS effects on aquatic organism passage, entrainable grain sizes, and scour prone habitats. Previous research has developed equations to predict scour depths (eg. Pandey et al., 2018; Zhang & Nakagawa, 2008) and shear stresses around ISUDS (Molinas *et al.*, 1998); however, these typically require a form of Froude number and flow depth which may not be readily obtainable. Easily-applied models to predict changes in mean and maximum V and τ may be useful in certain situations to estimate potential scour impacts resulting from various ISUDS contraction percentages. The tool will also contain conservative recommendations on identification of channel locations at risk for increased V and τ based on results presented in this chapter.

Finally, the tool will contain a bank stability module focused on identifying locations susceptible to bank erosion. The described tool will largely serve as a risk assessment tool. Scour potential in response to changes in hydraulic conditions will be a function of substrate size and

type. Bank stability will be a function of bank angle, bank material and vegetative composition. To improve usability, the Excel-based tool will contain a set of Visual Basic for Applications macros to automate user tasks or calculations. The tool is anticipated to produce estimates of V and τ, identify largest grain sizes that may be entrained and help identify bank erosion risk potential in a qualitative sense: high risk, medium risk, low risk.

5.0 Conclusions

Two-dimensional hydraulic modeling results indicated that higher discharges and contraction percentages led to larger maximum values of V and τ thereby increasing the risk of potential bank erosion and bed scour. Maximum depth averaged V in the narrow and medium channel widths at a 10% contraction ranged from 1.1 - 1.3 times the V_i for all discharges. Maximum depth averaged V in the narrow and medium channel widths at a 50% contraction were higher relative to the 10% contraction and ranged from 1.7 - 2.2 times the V_i. Maximum depth averaged τ in the narrow and medium channel widths at a 10% contraction ranged from 1.2 - 1.6 times the τ_i for all discharges. Maximum depth averaged τ in the narrow and medium channel widths at a 50% contraction were higher relative to the 10% contraction and ranged from 2.4 - 4.6 times the τ_i.

Increasing discharge and contraction percentage led to an increase in streamwise length of channel impacted by V and τ at least 10% higher than the initial unobstructed channel condition. Longer structures and higher discharges therefore increase the area at higher risk for potential bed and bank erosion. Increasing channel contraction percentage pushed increased V and τ regions closer to the opposite bank. Results indicated contraction percentages over 30% may lead to increases in V and τ on the opposite bank regardless of channel size. Contractions above 30%

increased *V* on the opposite bank by 1.1 - 1.3 times the unobstructed channel condition for all channel sizes and modeled discharges. Relative changes in τ compared to unobstructed channel conditions were approximately 46% larger on average than relative changes in *V*. Findings from this study can be used with predictive relationships (Chapter 3) to develop straightforward and efficient tools that can be applied to ISUDS for planning, preliminary design, and decision making.

References

Brown, S., 1985. Design of Spur-Type Streambank Stabilization Structures. McLean, Virginia.

Brunner, G.W., 2016a. HEC-RAS River Analysis System User's Manual. Davis, California. https://www.hec.usace.army.mil/software/hec-ras/documentation/HEC-RAS 5.0 Users Manual.pdf.

Brunner, G.W., 2016b. HEC-RAS River Analysis System, 2D Modeling User's Manual Version 5.0. www.hec.usace.army.mil.

Lagasse, P.F., P.E. Clopper, J.E. Pagan-Ortiz, L.W. Zevenbergen, L. a. Arneson, J.D. Schall, and L.G. Girard, 2009. Bridge Scour and Stream Instability Countermeasures: Experience, Selection, and Design Guidance-Third Edition.

Melville, B.W., 1992. Local Scour at Bridge Abutments. Journal of Hydraulic Engineering 118:615–631.

Molinas, A., K. Kheireldin, and B. Wu, 1998. Shear Stress around Vertical Wall Abutments. Journal of Hydraulic Engineering 124:822–830.

Oullion, S. and D. Dartus, 1997. Three-Dimesnional Computation of Flow Around Groyne. Journal of Hydraulic Engineering 123:962–970.

Pandey, M., Z. Ahmad, and P.K. Sharma, 2018. Scour around Impermeable Spur Dikes: A Review. ISH Journal of Hydraulic Engineering 24:25–44.

Parker, G., P.R. Wilcock, C. Paola, W.E. Dietrich, and J. Pitlick, 2007. Physical Basis for Quasi-Universal Relations Describing Bankfull Hydraulic Geometry of Single-Thread Gravel Bed Rivers. Journal of Geophysical Research 112:F04005.

Rajaratnam, N. and B.A. Nwachukwu, 1983a. Erosion near Groyne-like Structures. Journal of Hydraulic Research 21:227–287.

Rajaratnam, N. and B.A. Nwachukwu, 1983b. Flow Near Groin-Like Structures. Journal of Hydraulic Engineering 109:463–480.

Seed, D.J., 1997. Guidelines on the Geometry of Groynes for River Training.

Yazdi, J., H. Sarkardeh, H.M. Azamathulla, and A.A. Ghani, 2010. 3D Simulation of Flow around a Single Spur Dike with Free-Surface Flow. International Journal of River Basin Management 8:55–62.

Yeo, H.-K., J.-G. Kang, and S.-J. Kim, 2005. An Experimental Study on Tip Velocity and Downstream Recirculation Zone of Single Groyne Conditions. KSCE Journal of Civil Engineering 9:29–38.

Zhang, H. and H. Nakagawa, 2008. Scour around Spur Dyke: Recent Advances and Future Researches. Annuals of Disas. Prev. Res. Inst., Kyoto Univ., Kyoto Univ:633–652.

Tables

Table 4.1. Summary of previous studies examining ISUDS effects on velocity and bed shear stress in river channels.

Characteristic	Shear Stress	Velocity	Study Examples
Length	Direct relationship	Direct relationship	Molinas et al., 1998 Yazdi et al., 2010
Permeability	Inverse relationship with shear and tip depth. Scour occurs at all openings in permeable ISUDS	Inverse relationship	Yeo et al., 2005 Ho et al., 2007 e.g., Zhang & Nakagawa, 2008
Installation Angle	Structures at 90° to flow have the highest shear stresses compared to structures orientated upstream or downstream	Structures at 90° in straight channels have the highest velocities	Yazdi et al., 2010 Melville, 1992

Table 4.2. Summary of 2-D model inputs and parameters used in the 42 HEC-RAS simulations.

Relative Size	Channel Width (ft)	Channel Depth (ft)	Slope	*Q* (cfs)	Mesh Size (ft)	Detailed Mesh at Jetty (ft)	Length of Detailed Mesh Up and Downstream
Narrow	60.4	2.86	0.0059	10, 100, & 300	30 x 30	12 x 12	100 ft
Medium	114.03	13.07	0.0018	100, 1000, 3000	10 x 10	4 x 4	100 ft
Wide	519.17	19.43	0.0018	333, 3333, 33333	6 x 6	2.4 x 2.4	100 ft

Figures

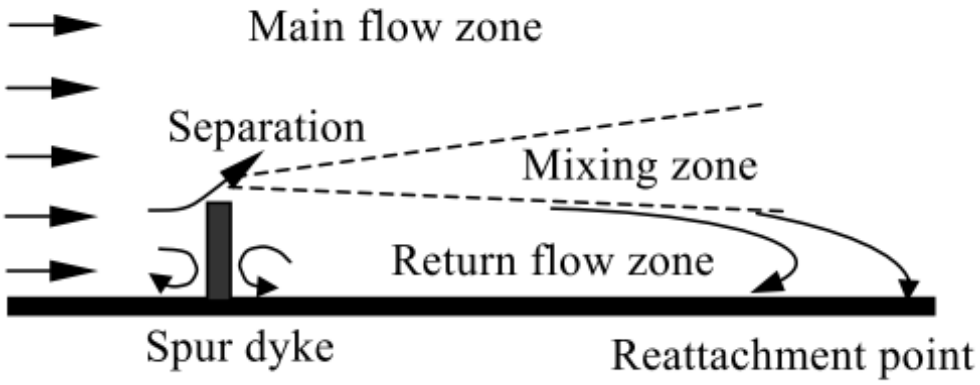

Figure 4.1. Main flow zones near an ISUDS as represented by Zhang et al. (2008).

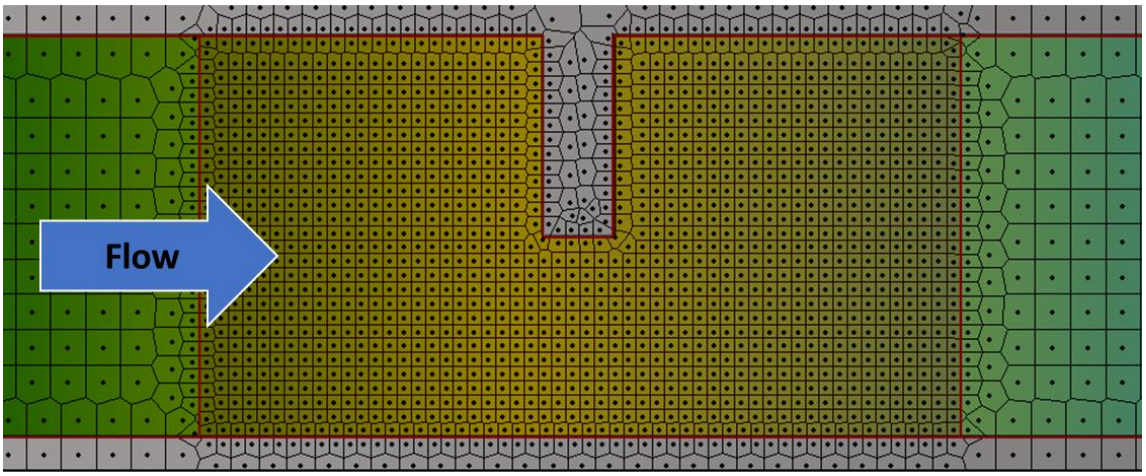

Figure 4.2. Representative mesh used in the 2-D HEC-RAS simulations (medium channel width and a 50% contraction) with increased resolution in the vicinity of the structure.

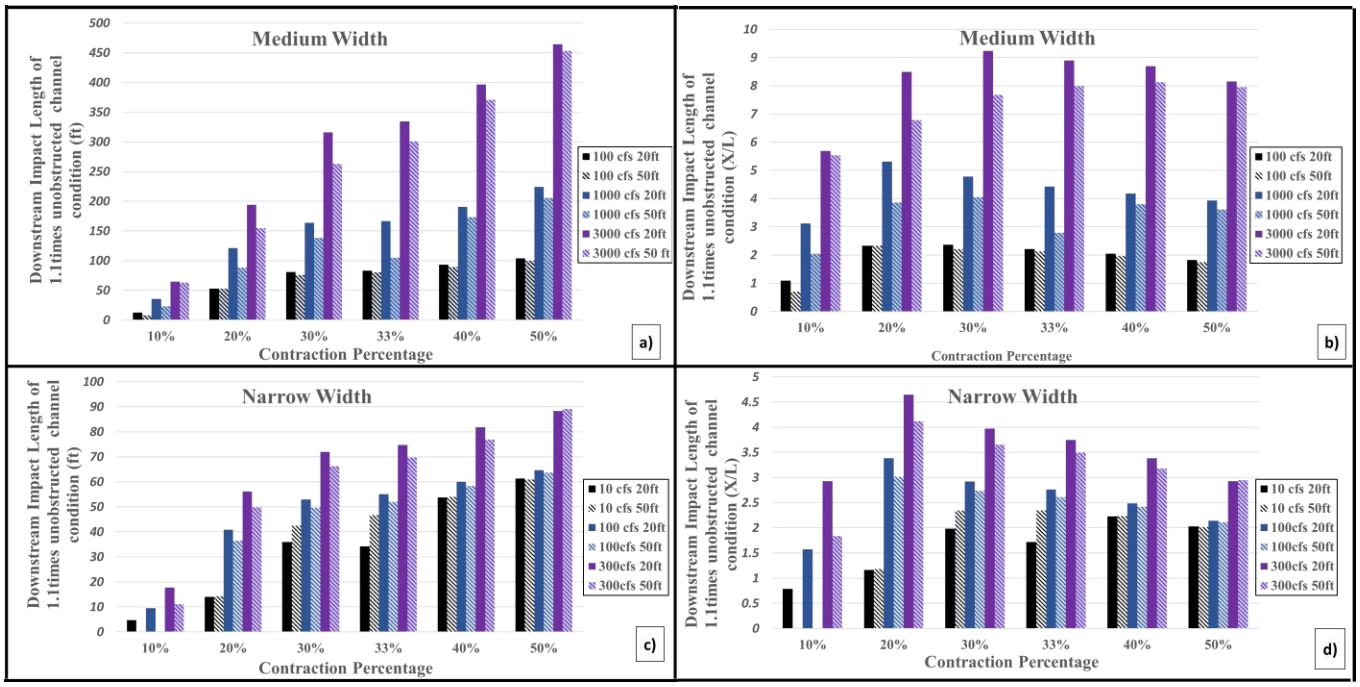

Figure 4.3. Downstream length of area with >10% increase in unobstructed channel velocity for a range of discharges and contraction percentages for medium and narrow width channels represented as a distance (a,b) and as a ratio of structure length (c,d).

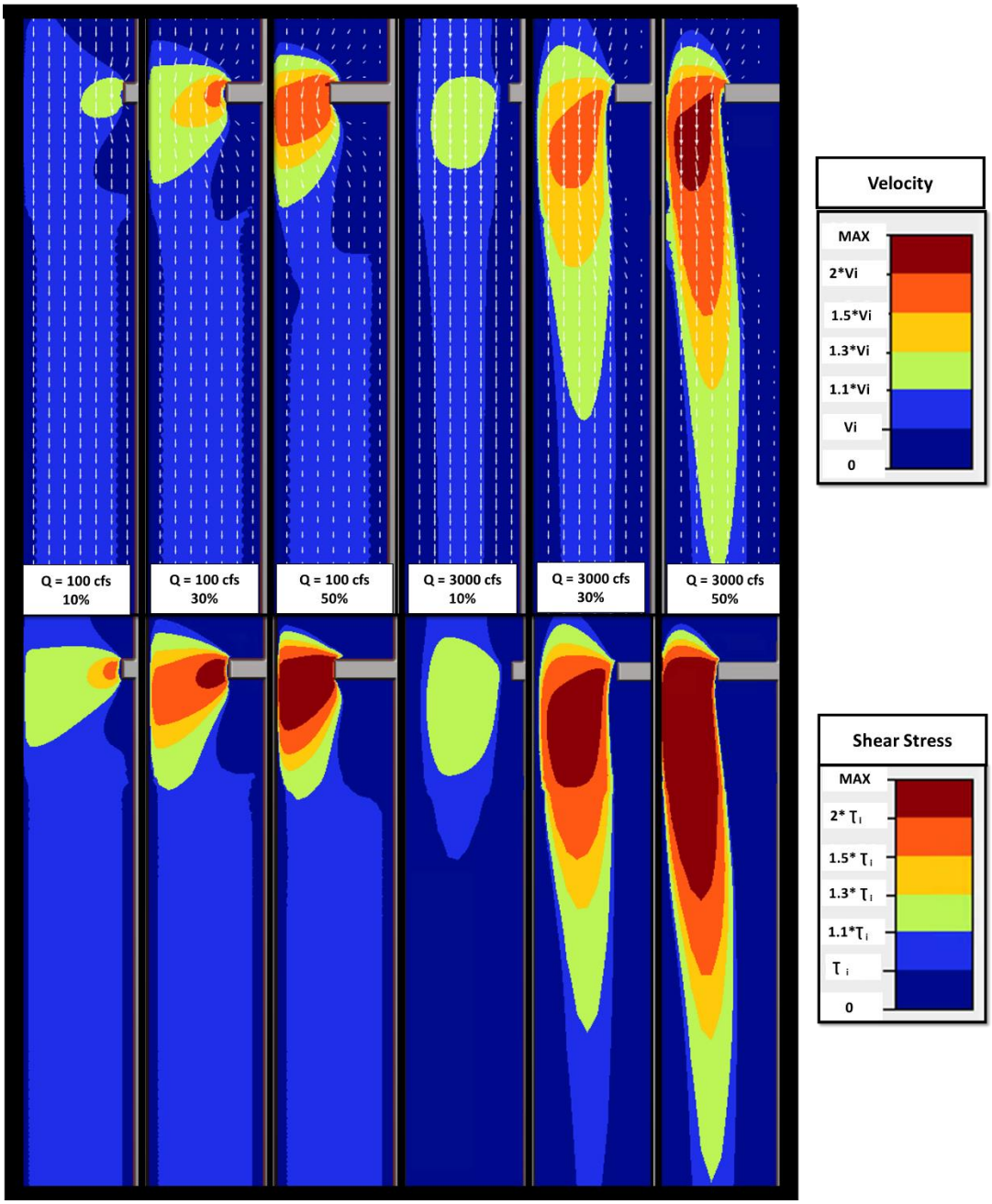

Figure 4.4. Relative shear stress and velocity regions for low and high discharge in the medium sized channel for three contraction percentages. An increase in discharge leads to longer impacted regions downstream and higher maximum values for all contraction percentages.

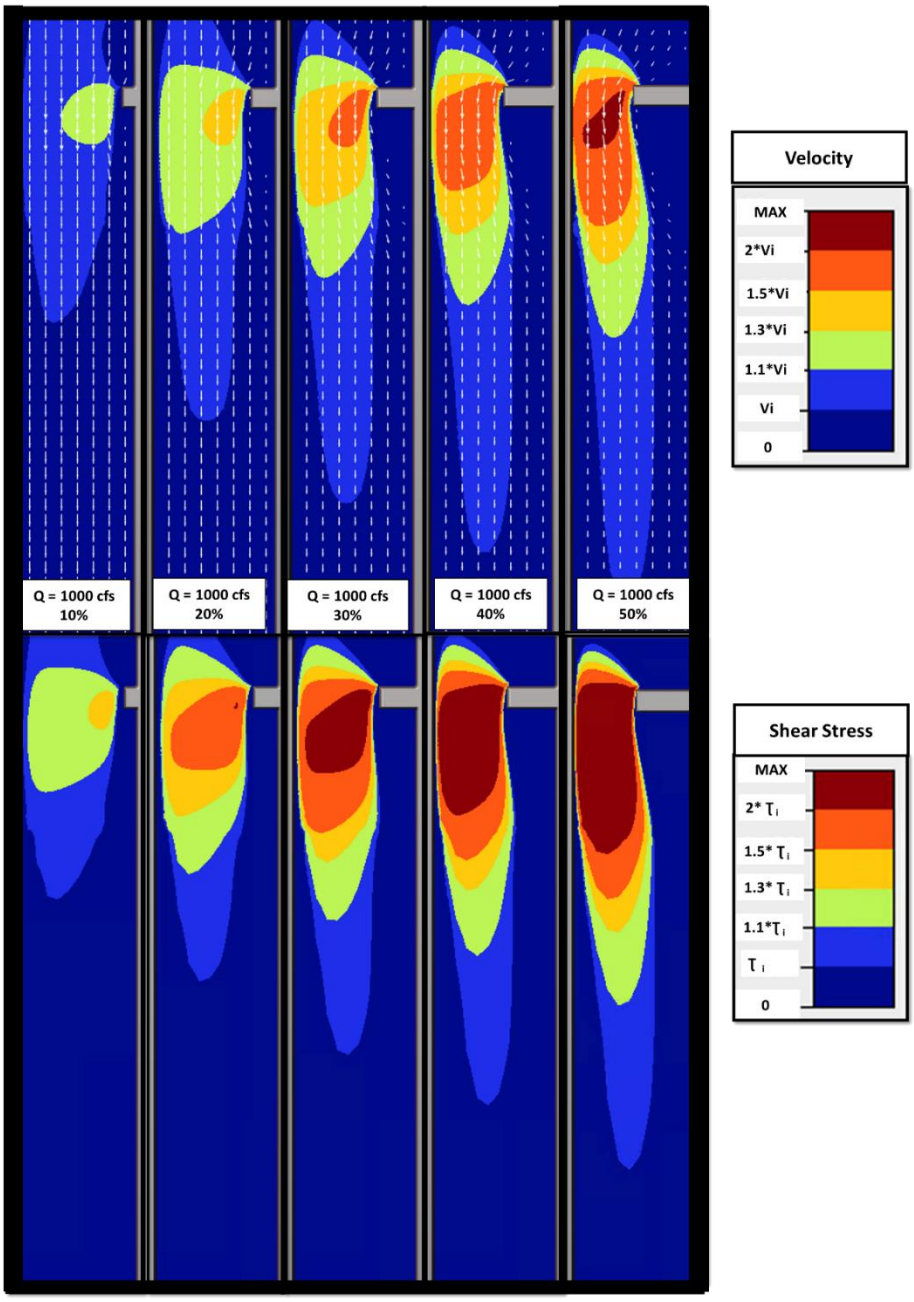

Figure 4.5. Relative shear stress and velocity regions for a range of contraction percentages in the medium channel width. An increase in contraction percentage leads to longer impacted regions downstream and higher maximum values.

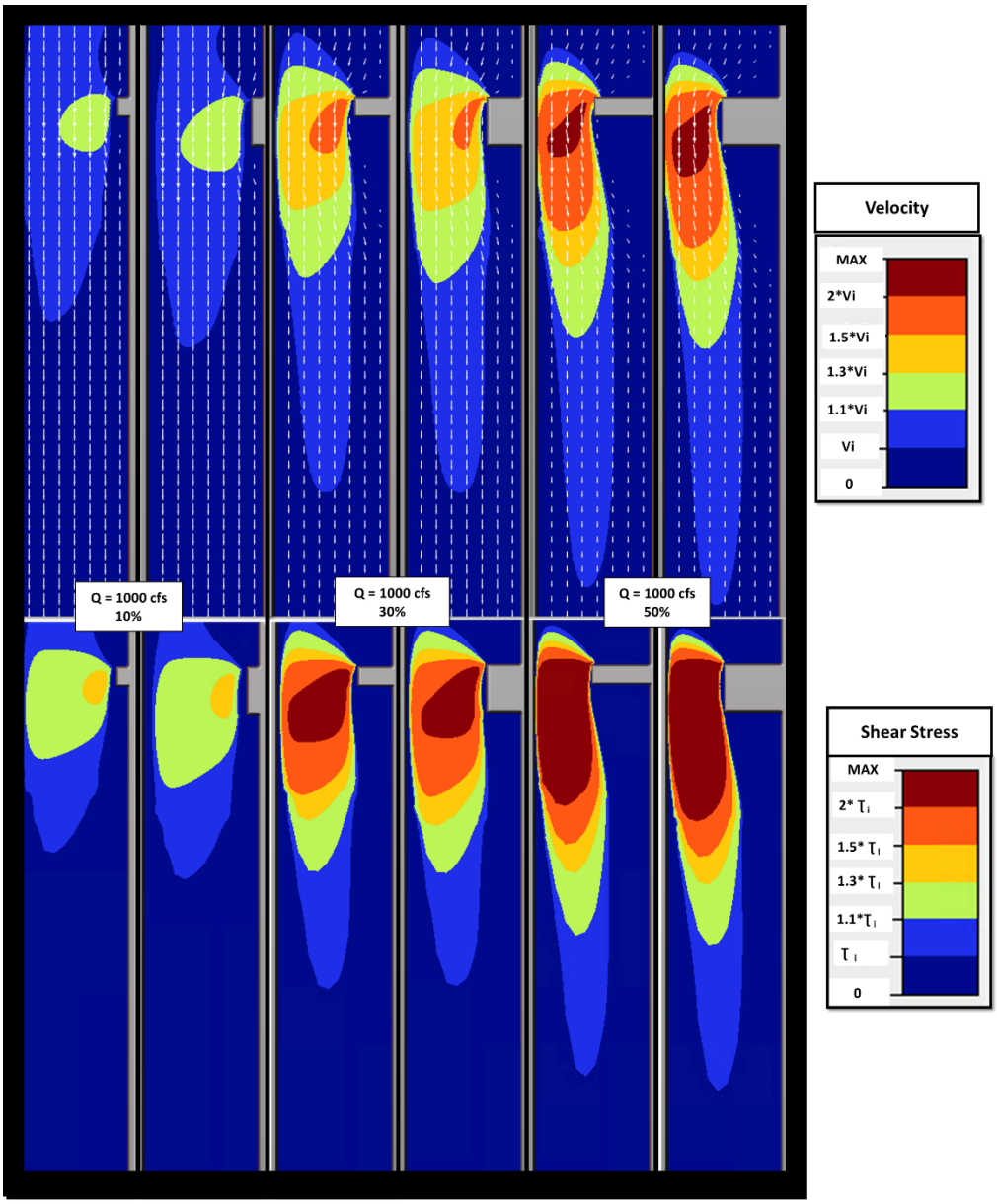

Figure 4.6. Relative shear stress and velocity regions for two different structure widths (20ft and 50ft) at a range of contraction percentages for the medium channel width. An increase in structure width leads to longer downstream regions with amplified velocities and shear stresses.

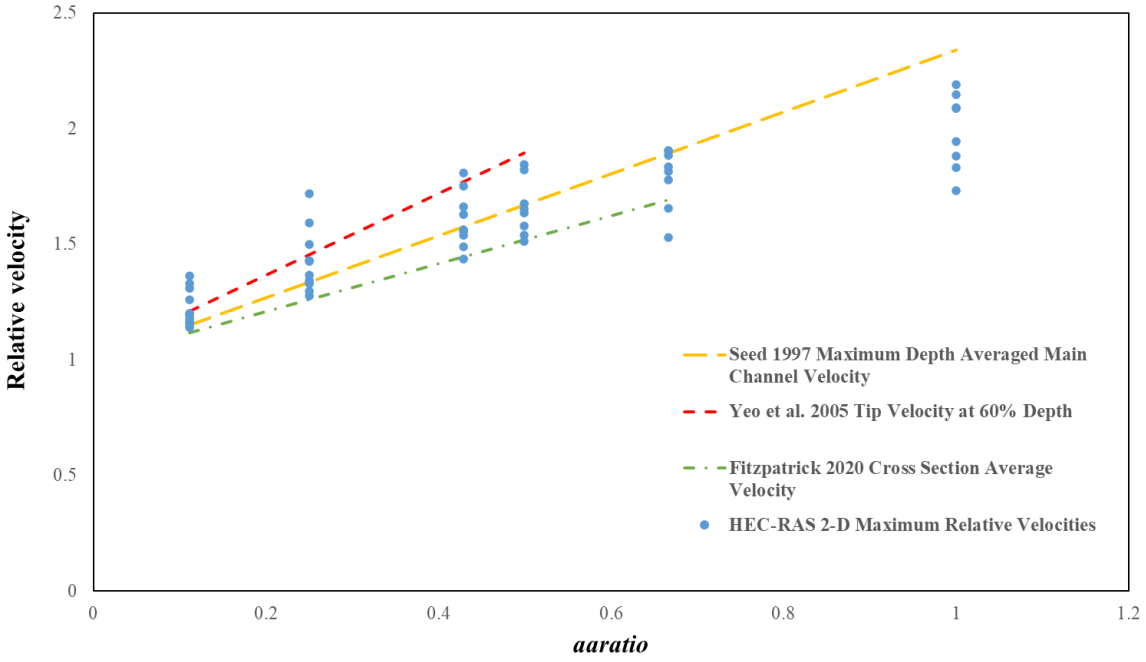

Figure 4.7. HEC-RAS 2-D maximum velocities for medium and narrow channel widths compared to three predictive models of relative changes in velocity due to emplaced ISUDS.

CHAPTER 5

CONCLUSIONS

A wide range of human activities in river environments requires emplacement of in-stream unsubmerged deflection structures (ISUDS) including groynes, spur dikes, abutments, and riprap construction platforms. Understanding the potential hydraulic and geomorphic impacts of these structures is essential for limiting unintended consequences of emplacement of ISUDS. Abrupt flow contractions at structures can lead to increased bed scour and bank erosion with consequent effects on channel stability and habitat. Quantitative predictions of changes in velocity and shear stress due to these structures and identification of regions at high risk for bank and bed erosion can help inform preliminary structure design, environmental management, and regulatory decision making. In this study, I performed 50,000+ 1-D HEC-RAS simulations to develop parsimonious regression models to quantify changes in velocity and shear stress in regions contracted by ISUDS (Objectives 1, 2, and 3). The regression models were compared to collected field measurements (Objective 4) and previous experimental studies. Additionally, I conducted 42 2-D HEC-RAS simulations to examine spatial distributions of velocity and shear stress near ISUDS, concentrating on near-bank regions and locations of velocity and shear stress maxima (Objective 5).

Practical relationships to predict mean changes in velocity and shear stress due to emplacement of ISUDS were developed based on 1-D modeling results to inform preliminary structure design, environmental management, and regulatory decisions. Changes in velocity and shear stress estimated with HEC-RAS for a wide range of conditions were found to be well

represented by easily applied regression models based on a channel contraction area ratio for contraction percentages $\leq$ 50% and Froude numbers < 0.8. The new regression relationships for relative velocity were reasonably supported by results from a field study and previously conducted flume studies. Two-dimensional hydraulic modeling results indicated that higher discharges and contraction percentages led to larger velocity and shear stress maxima in contracted regions, as well as longer downstream distances where velocities and shear stresses were $\geq$ 110% of unobstructed channel conditions. Maximum depth averaged relative changes in velocity and shear stress in the narrow and medium channel widths, at a 50% contraction, were higher relative to the 10% contraction and ranged from 1.7 - 2.2 times the initial velocity and 2.4 - 4.6 times the initial shear stress for a given discharge. When contraction percentages reached 30%, flows were constricted enough to lead to increases of at least 1.1 times the initial velocity and 1.5 times the initial shear stress on the opposite bank for all channel widths. Results from this study are being used to develop an Excel-based tool that combines the predictive regression models and the results of the 2-D analysis of spatial patterns of increased velocity and shear stress resulting from ISUDS, which can be easily applied by practitioners for planning, design, and permitting when more complex modeling is infeasible (Objective 6).

This work adds to the body of previous research on ISUDS by developing physically-based, generalized models for predicting effects on mean velocity and shear stress in a wide range of river settings and structure contractions. Most previous studies have focused on using a narrow range of experimental conditions and/or 2-D and 3-D numerical models to develop predictive relationships based on inputs that are often unavailable in practice. Further, previous studies typically have not evaluated changes in the extent of impacted regions due to changes in

hydraulics and structure or channel size. This study addressed the need for parsimonious models that can be readily applied in diverse river settings.

Synthesis of results from the predictive regression models and 2-D model simulated spatial distributions of increased velocity and shear stress resulting from ISUDS provided valuable information on potential hydraulic and geomorphic effects. In addition to meeting all the proposed objectives, this study highlighted the potential application of existing studies and findings from the current study to temporary structures such as in-stream riprap platforms used in constructing transportation infrastructure. Recognizing the connection between semi-permanent, commonly studied structures and temporary riprap construction platforms is essential to future development of design standards for DOTs implementing riprap platforms for bridge construction and maintenance. This work can be applied to a large array of structures including both temporary and semi-permanent in-stream unsubmerged structures and advances the current set of tools available for preliminary structure design and environmental management decisions.

APPENDIX A

HYDRAULIC MODELING AND STATISTICAL ANALYSIS

Description

This appendix serves as supplemental material to Chapter 3 for hydraulic modeling and regression statistical analysis.

Tables

Table A1. Comparison of 1-D HEC-RAS model results to flume studies.

Flume Study	Q (ft/s)	Contr. %	% Error Upstream Vel.	% Error Vel. at Contracted *xs*	% Error Upstream WSE
Jeon et al. 2018 C1	0.982	33.33%	1.45%	-5.17%	0%
Jeon et al. 2018 C2	1.86	33.33%	-1.10%	-5.96%	4.76%
Duan et al. 2009 Flat bed	2.05	32.89%	-2.39%	16.58%	NA

Table A2. Selected relative velocity regression models.

Dependent Variable	Model	RMSE	$adjR^2$ for linear Models
1 Variable *aaratio*	Linear model	0.027	0.991
	Power function nonparametric	0.074	NA
2 Variables *aaratio and Fr*	Linear model: *aaratio and Fr*	0.021	0.995
	Power function: *aaratio and Fr*	0.070	NA
	Linear: *aaratio* and *Fr*_hydraulic geometry	0.022	0.994
	Linear: *aaratio* and *Fr*_darcy	0.022	0.994
	Linear: *aaratio* and *Fr*_ND	0.023	0.994
All Independent Variables	Linear: Inclusion of all 8 independent variables	0.015	0.997

Table A3. Selected relative shear stress regression models.

Dependent Variable	Model	RMSE	$adjR^2$ for linear Models
1 Variable *aaratio*	Linear model	0.146	0.975
	Power function nonparametric	0.228	NA
	Quadratic	0.117	NA
2 Variables *aaratio and Fr*	Linear Model	0.104	0.988

Figures

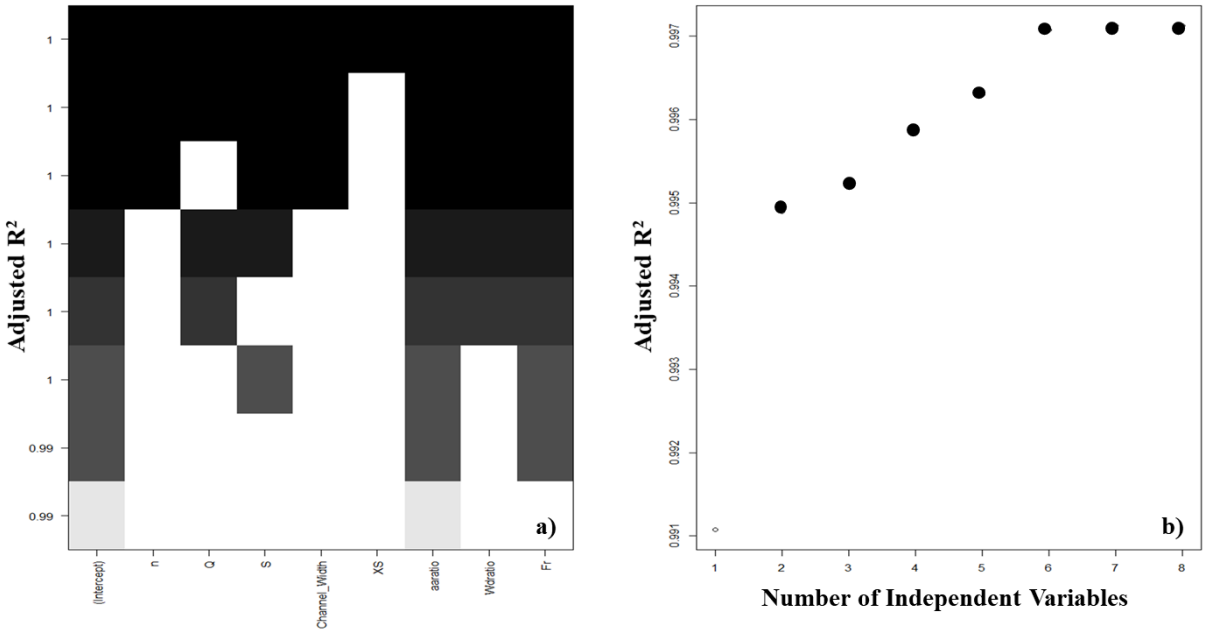

Figure A1. Results from linear regression analysis using best subsets. Figure A1(a) depicts the results from the best subsets analysis preformed in R using the 'Leaps' package showing the independent variables used for the best linear model for a given number of predictor variables based on $adjR^2$. Figure A1(b) shows that increasing the number of variables in a linear regression slightly improves the adjR^2, but all $adjR^2$ values are above 0.99.

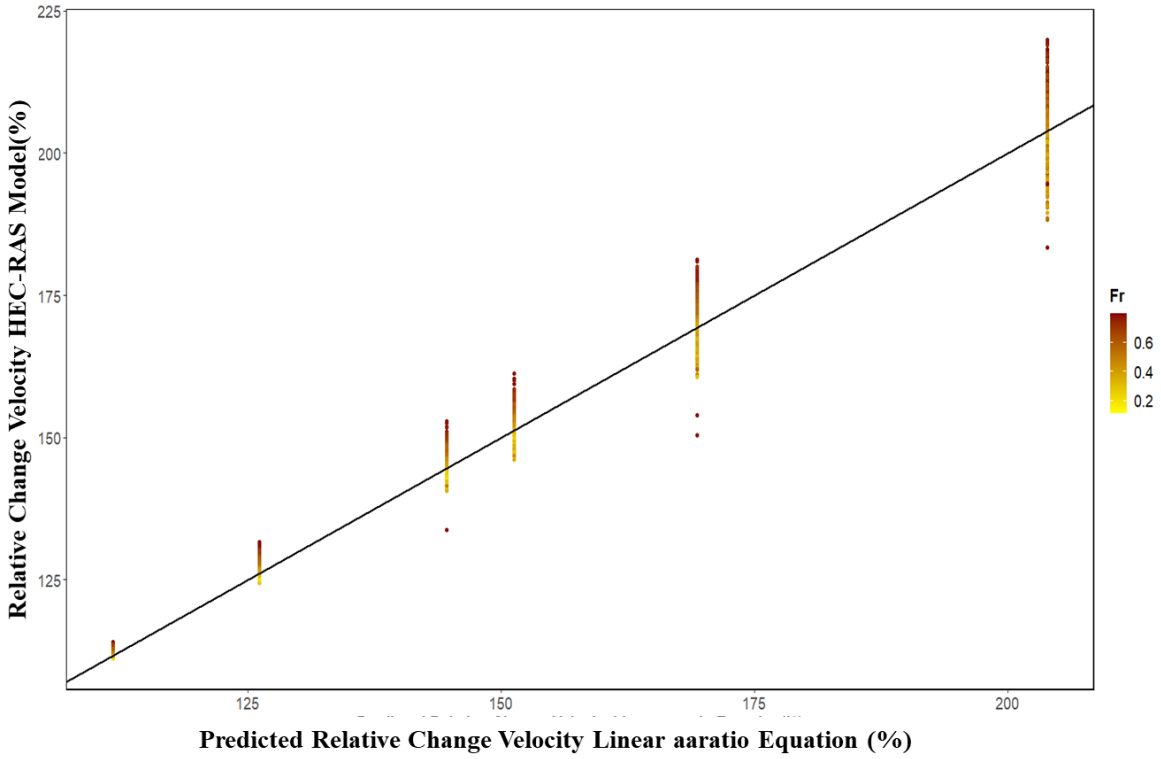

Figure A2. Predicted relative changes in velocity using the linear *aaratio* regression versus the HEC-RAS model relative changes in velocity. The linear *aaratio* model generally underpredicts for larger Froude numbers and overpredicts for smaller Froude numbers.

APPENDIX B

COMPARISON OF REGRESSION MODEL PREDICTIONS TO HYDRAULICS OF COMPLEX CHANNELS

Description

This appendix serves as supplemental material to Chapters 3 and 4 providing additional insight into potential errors associated with assuming rectangular channel geometries to develop *aaratios* when utilizing developed regressions for actual channel bathymetries.

Additional Analysis

Three existing actual channel bathymetry 1-D HEC-RAS models were used to determine absolute velocity and shear stress for six channel contraction percentages: 10%, 20%, 30%, 33%, 40% and 50%. Actual channel bathymetry 1-D HEC-RAS models were provided by the Georgia Department of Transportation for the Flint River, Chattooga River and Walnut Creek (Figure B1). The absolute values of velocity and shear stress for the actual channel bathymetries were compared to developed regressions in Chapter 3 with associated *aaratios* calculated assuming rectangular channel shape. This analysis was conducted because practitioners may utilize the developed equations for non-rectangular channels and calculate *aaratios* assuming rectangular channel conditions as described in Chapter 3 if bathymetry data is unknown.

Percent errors in predicted absolute velocity using the power regression developed in Chapter 3 generally underpredicted mean absolute velocity for actual channel bathymetries

ranging from underpredicting value by 9% - 35% (Table B1). Percent errors in predicted mean absolute shear stress utilizing the developed quadratic equation and estimating water depth utilizing the Manning equation assuming rectangular channel shape were variable. Predictions ranged between overpredicting shear stress by 59% to under predicting shear stress by 46% (Table B2). This analysis focused on a worst-case scenario, where channel bathymetry and initial velocity or depth at the discharge of interest was unknown.

Using the developed equations for relative changes with actual *aaratios* determined using channel bathymetry data is expected to increase prediction accuracy for non-rectangular channel bathymetries. Initial values can be obtained through field measurements, hydraulic modeling or estimated using the appropriate equations adjusted for channel shape. If measurements for initial velocity and *aaratio* are accurate then predictions for absolute velocities should fall near the original estimated range of errors for the rectangular channel geometries presented in Chapter 3. The tool described in Chapter 4 uses a hierarchal approach and calculates absolute velocity and shear stress based on the best available data starting with calculating the *aaratio* using channel bathymetry then moving towards estimating *aaratio* assuming a rectangular channel condition (Figure B2). If measured or modeled initial values are given, these values are used for predicting absolute velocity and shear stress using the relative regressions instead of using estimated initial values or in the case of velocity, the developed power function. Figure 1B outlines the hierarchal method used for tool development.

Tables

Table B1. Percent error between actual channel bathymetry absolute velocities and absolute velocities predicted using developed power regression with assumed rectangular *aaratios.*

Percent Contraction	Rectangular *aaratio*	Chattooga Percent Error	Flint Percent Error	Walnut Percent Error
10%	0.11	-13%	-23%	-20%
20%	0.25	-10%	-26%	-15%
30%	0.43	-9%	-28%	-10%
33%	0.50	-9%	-29%	-9%
40%	0.67	-11%	-32%	-9%
50%	1.00	-16%	-35%	-13%

Table B2. Percent error between actual channel bathymetry absolute shear stress and absolute shear stress predicted using developed quadratic regression with assumed rectangular *aaratios.*

Percent Contraction	Rectangular *aaratio*	Chattooga Percent Error	Flint Percent Error	Walnut Percent Error
10%	0.11	0%	-20%	25%
20%	0.25	6%	-15%	20%
30%	0.43	7%	-25%	59%
33%	0.50	6%	-32%	40%
40%	0.67	-1%	-38%	46%
50%	1.00	-18%	-46%	27%

Figures

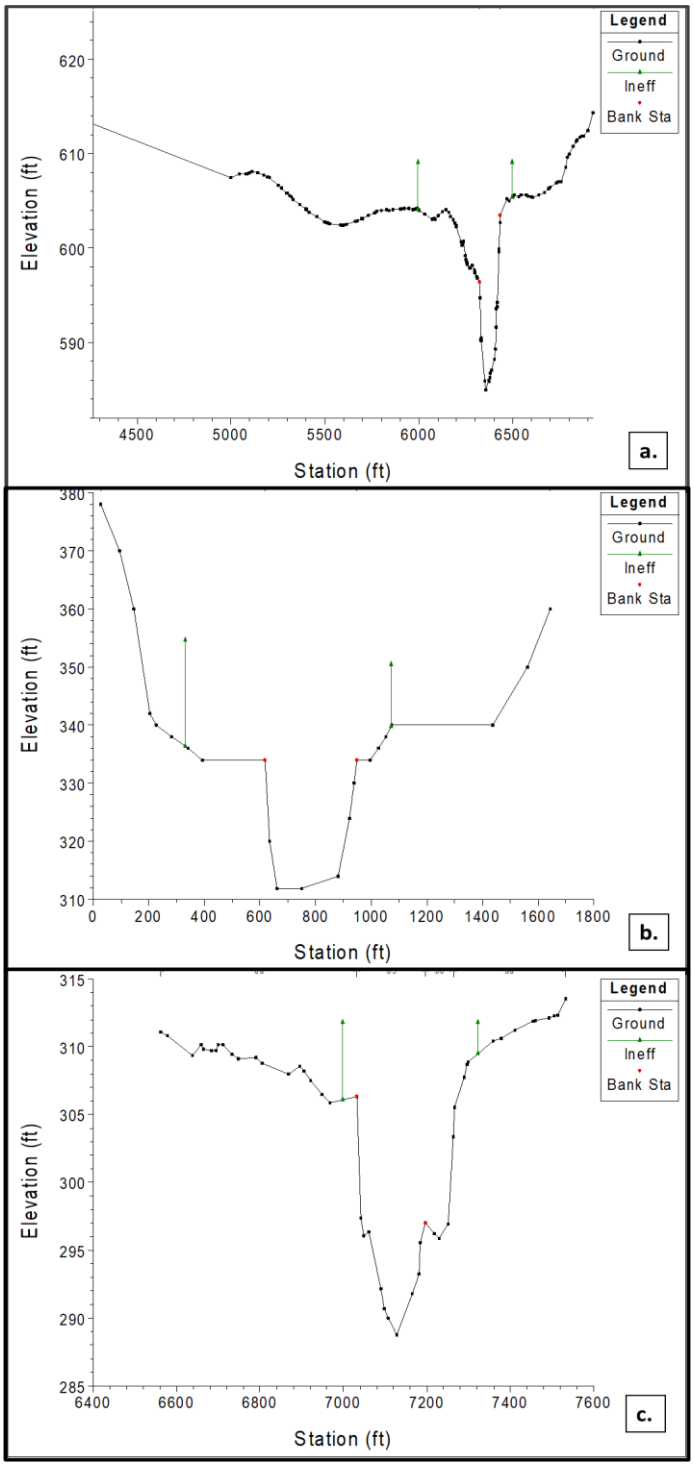

Figure B1. One-dimensional HEC-RAS cross sections for the Chattooga River (a), the Flint River (b) and Walnut Creek (c).

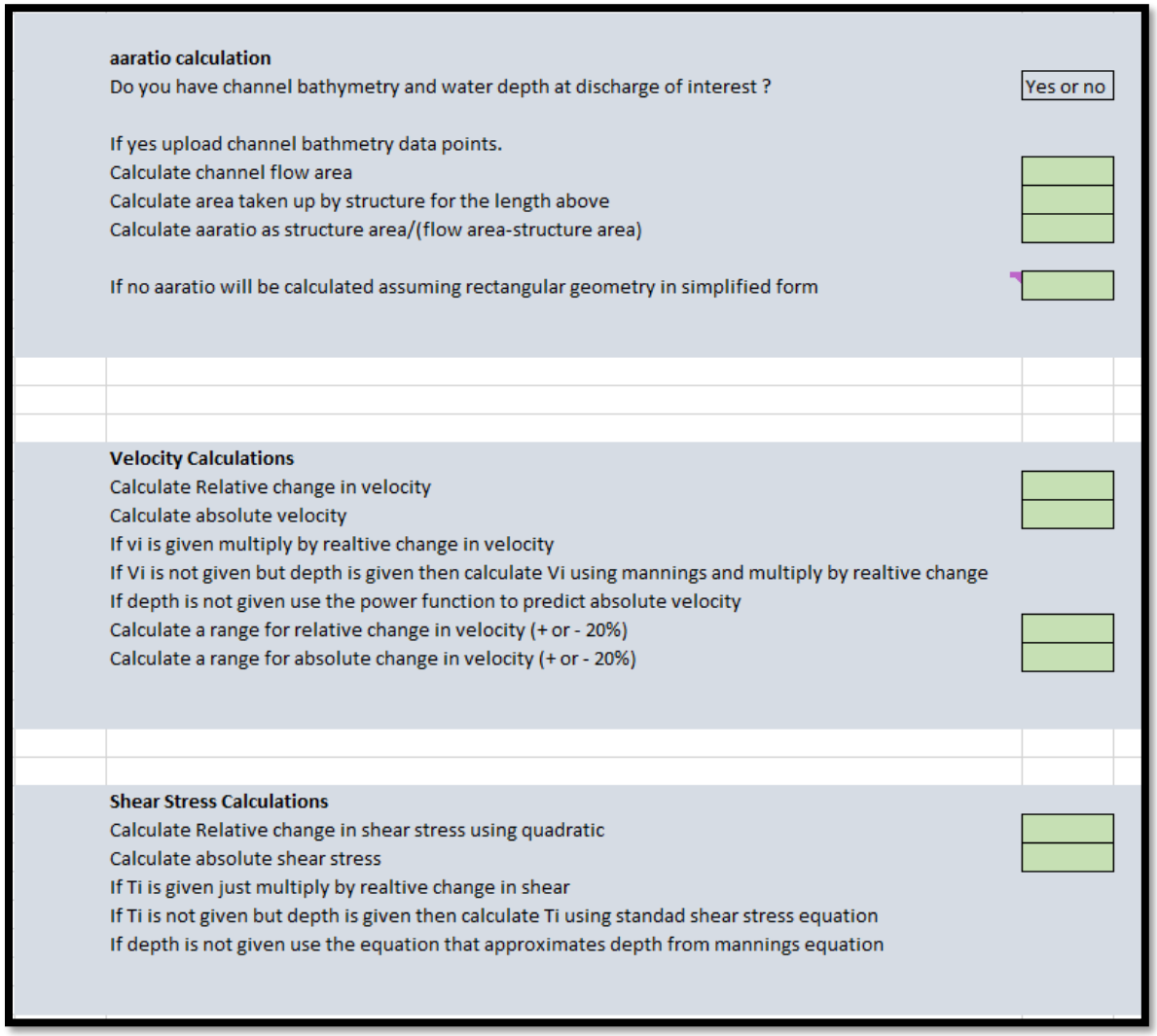

Figure B2. Outline of the hierarchal method used for tool development.

APPENDIX C

SELECTED DOT SURVEY RESULTS

Description

This appendix provides additional information about the Qualtrics Survey sent to representatives at all 50 state Departments of Transportation (DOT). Representatives were selected to include a bridge engineer, a hydraulics engineer, and an environmental representative. The survey resulted in 74 responses from 26 states and 46 fully completed surveys. Survey results were used to supplement information provided by the Georgia Department of Transportation (GDOT) to gain insight about temporary riprap construction platform implementation across the United States. Most respondents responded to the survey as individuals, however seven responses were submitted as groups. One state could respond with multiple surveys if multiple individuals chose to respond. Survey respondents were asked if they were familiar with structure design, structure permitting or construction and provided questions relevant to their knowledge.

Survey Results

Question 1

What **name or names** does your state Department of Transportation commonly call the temporary in-stream access structure used for bridge construction shown in the previous photo? Select all that apply.

Figure C1. Photo shown in survey. Photo curtesy of GDOT.

Response 1

Responses to Question 1 (Figure C2) indicated that there are numerous names for the structure shown in the provided photo (Figure C1). Information obtained from GDOT is not shown in Figure C2, as information from GDOT was obtained from in person meetings. However, GDOT refers to the structure shown in the provided photo as a riprap jetty. The multiple names for these structures may make it challenging to compile information regarding structure design and implementation. For the remainder of this appendix the structure will be referred to as a temporary riprap construction platform.

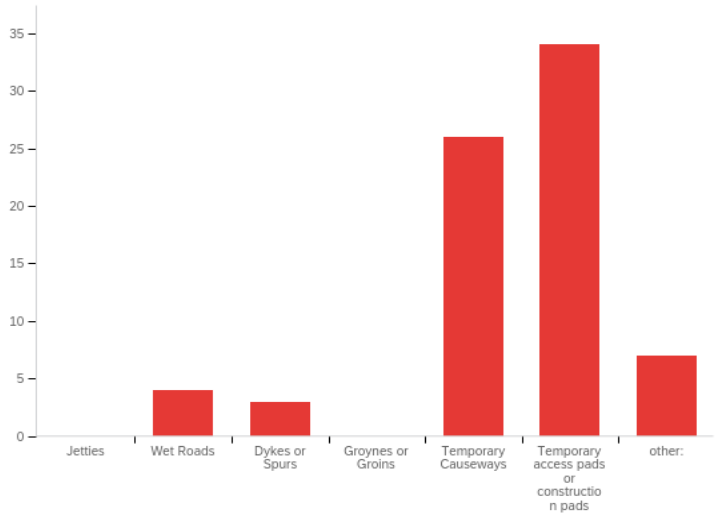

Figure C2. Response to Question 1 about the name of temporary access construction structures used for bridge construction based on the provided photo.

Question 2

How often are the temporary access structures of interest used by your state DOT during bridge construction projects?

Response 2

Responses to Question 2 (Figure C3) indicated that the frequency of use of temporary riprap construction platforms varies between DOTs. Implementation of these structures is highly site and project dependent.

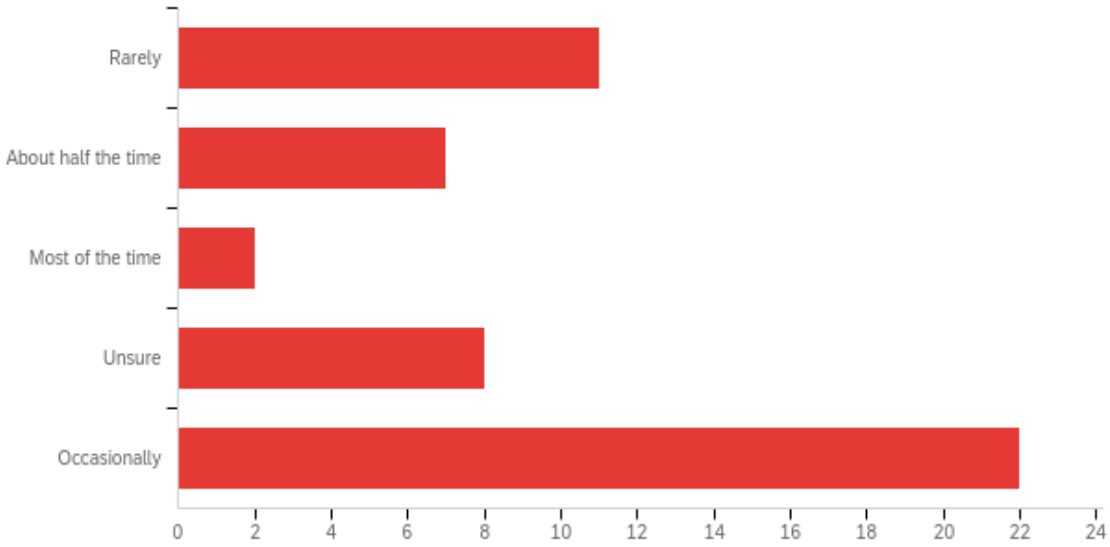

Figure C3. Response to Question 2 about the frequency of use of temporary riprap construction platforms.

Question 3

Does your state DOT have design guidelines or a design manual that provides guidelines on the design or implementation of temporary bridge construction access structures?

Response 3

Responses to Question 3 (Figure C4) indicated that more respondents were unaware of design manuals or guidelines for implementation of temporary riprap construction platforms then respondents that were aware of design guidelines. This suggests there may be a need for improved design guidelines or manuals for these structures.

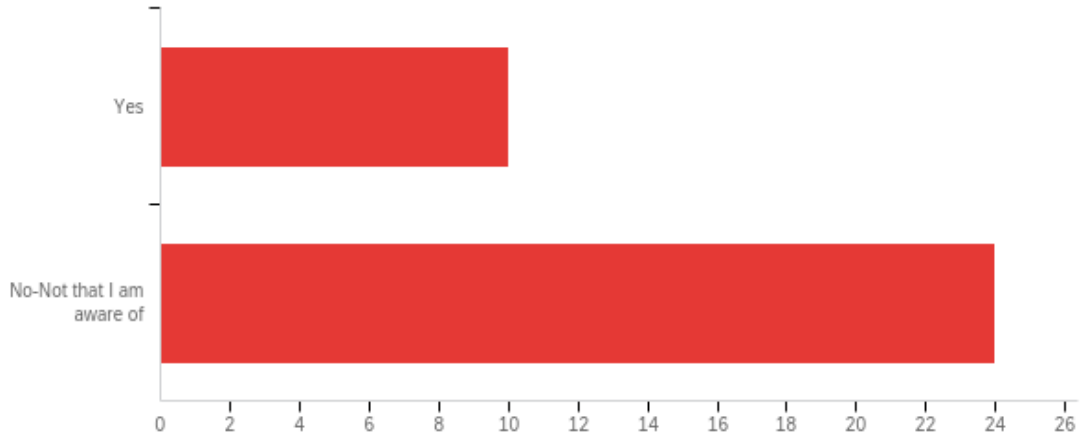

Figure C4. Response to Question 3 about availability of design guidelines and manuals for temporary riprap construction platforms.

Question 4

Based on your experience please estimate the maximum and minimum percent of a channel width that could be blocked by these temporary structures. You can SKIP this question if you would not like to provide an estimate. (Include the case where 2 temporary structures could be in the channel at the same time from either side of the channel.)

Response 4

Responses to Question 4 (Figure C5) indicated that channel contraction percentages for temporary riprap construction platforms range between 10% - 70% with the most common maximum contraction being 50%.

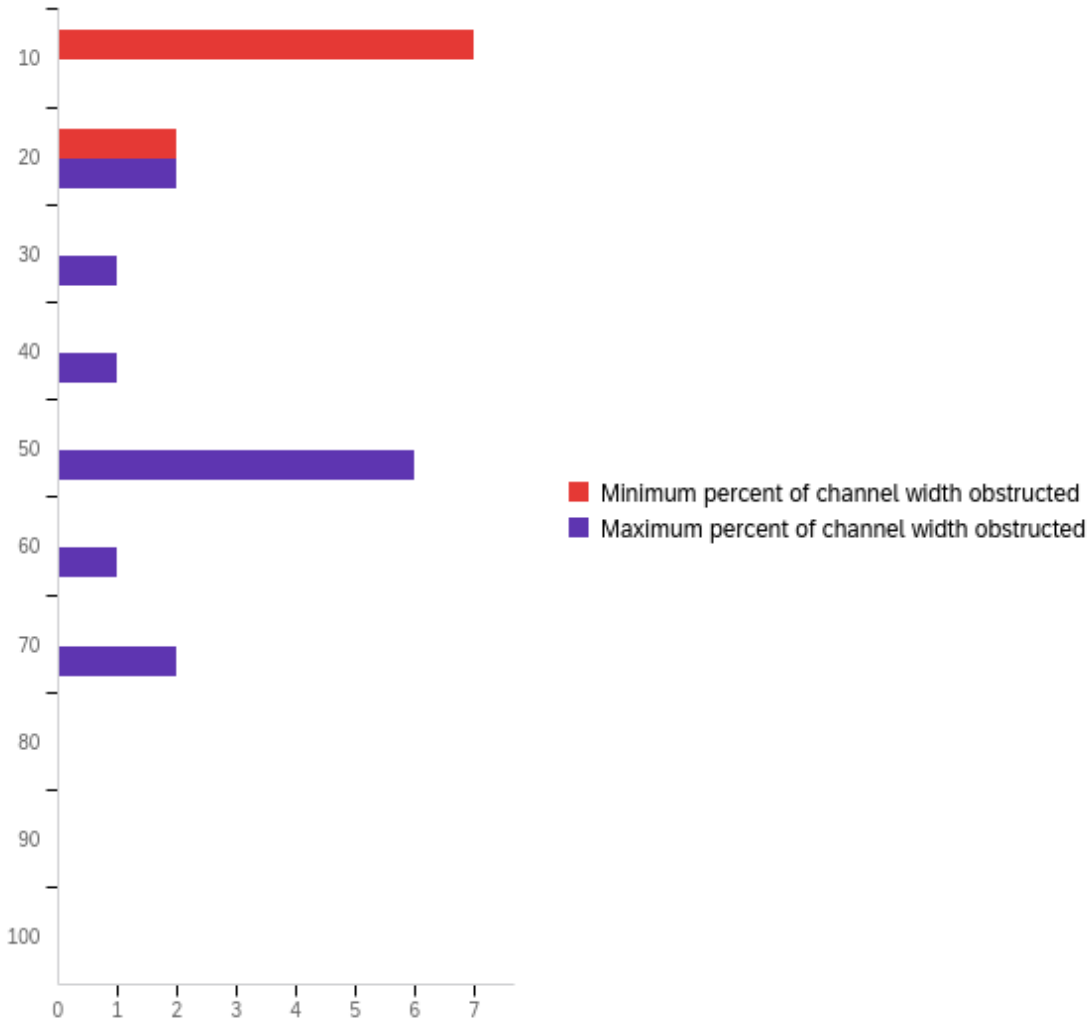

Figure C5. Response to Question 4 about the range of channel contraction percentages caused by temporary riprap construction platforms.

Question 5

Based on your experience please estimate the maximum and minimum temporary access structures width in FEET (top width NOT the length the structure protrudes into the stream). You can SKIP this question if you would not like to provide an estimate.

Response 5

Responses to Question 5 indicated that the top width of temporary riprap construction platforms ranges between 10ft - 250ft. The most common maximum listed was 20ft which is large enough for most construction vehicles to drive on.

- Minimum =10ft
- Maximum= 250ft
- Most common max=20ft

Question 6

How often are the temporary construction structures overtopped/flooded during the bridge construction period?

Response 6

Responses to Question 6 (Figure C6) indicated that installed structures usually do not overtop. Respondents indicated in related questions that determining the height to install temporary riprap construction platforms is dependent on site conditions and potential risk. Some DOTs base the height of the installed structure based on the average water depth, where others base it on a specified height above a given flood event.

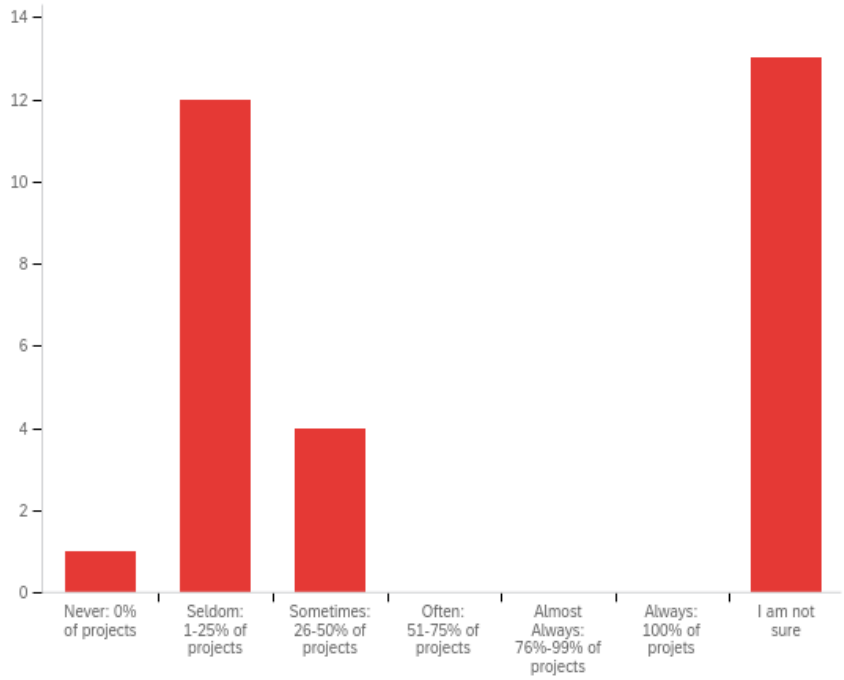

Figure C6. Response to Question 6 about the frequency that temporary riprap construction platforms overtop while installed in river channels for bridge construction.

Question 7

On a scale of 1 to 5 how satisfied is your state DOT with the time it currently takes to respond to environmental permitting questions related to hydraulic and environmental effects of temporary bridge construction access features? 1=Inefficient/ Room for improvement 5=Very Efficient/Doesn't need improvement

Response 7

Responses to Question 7 (Figure C7) indicated that the majority of respondents believed the time it takes their state DOTs to respond to permitting agency questions related to hydraulic and

environmental effects of temporary bridge construction access features to be average (score of 3). Only two respondents believed there was no room for improvement.

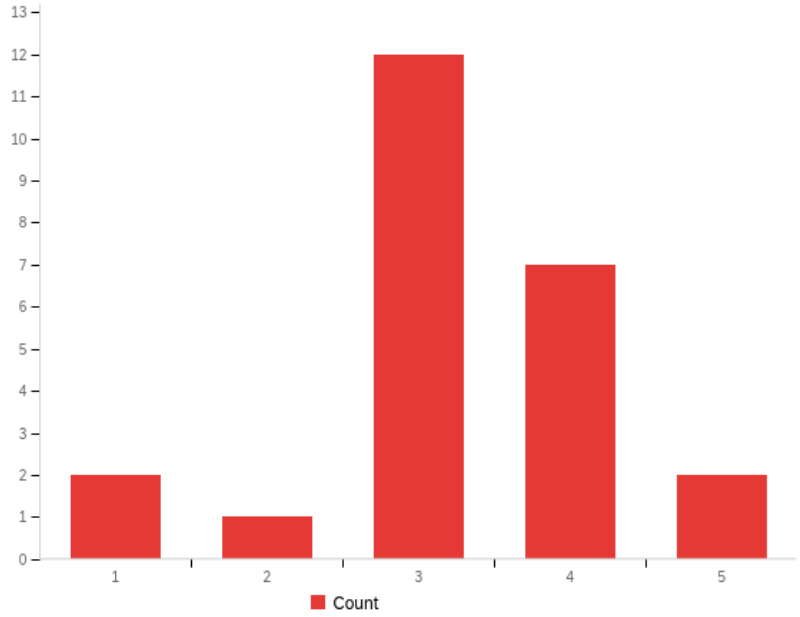

Figure C7. Response to Question 7 where respondents ranked on a scale of 1 to 5 how satisfied they were with their state DOTs time to respond to environmental permitting questions related to hydraulic and environmental effects of temporary bridge construction access features. 1=Inefficient/ Room for improvement 5=Very Efficient/Doesn't need improvement.

Question 8

How effective are your current state DOT responses at addressing all environmental permitting questions about temporary in-stream structures used for bridge construction?

Response 8

Responses to Question 8 (Figure C8) indicated that the majority of respondents found their state DOTs to be moderately effective at addressing all environmental permitting agency questions about temporary bridge construction access features.

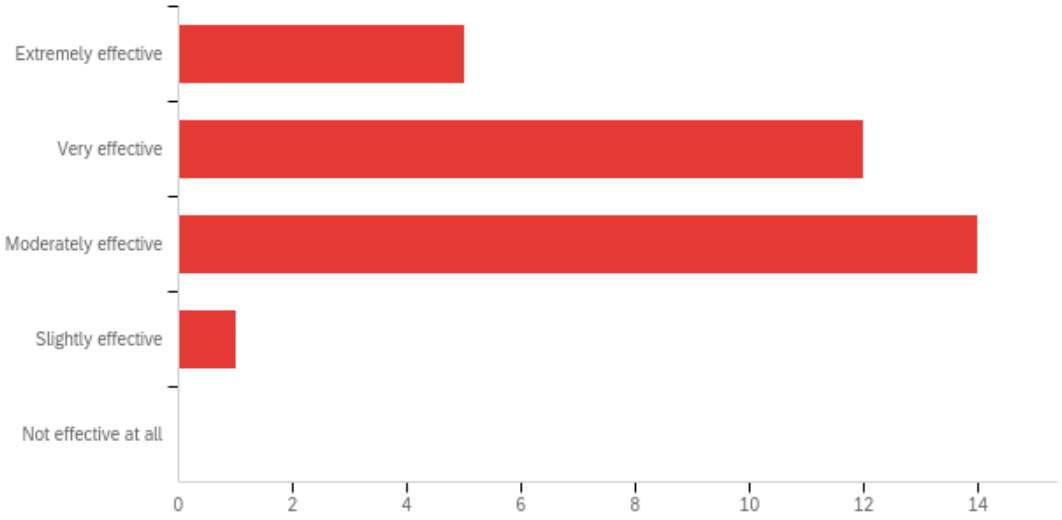

Figure C8. Response to Question 8 about the effectiveness of state DOTs in addressing all environmental permitting questions about temporary in-stream structures used for bridge construction.

Question 9

Does your State DOT have a specific protocol, tool, or guidelines for responding to permitting agency concerns about the temporary structures used for bridge construction?

Response 9

Responses to Question 9 (Figure C9) indicated most respondents have a specific protocol, tool or guidelines for responding to permitting agency concerns about temporary riprap construction

platforms. However, seven respondents indicated they did not have specific methods to respond to permitting agencies suggesting some DOTs may still need assistance developing tools and guidelines.

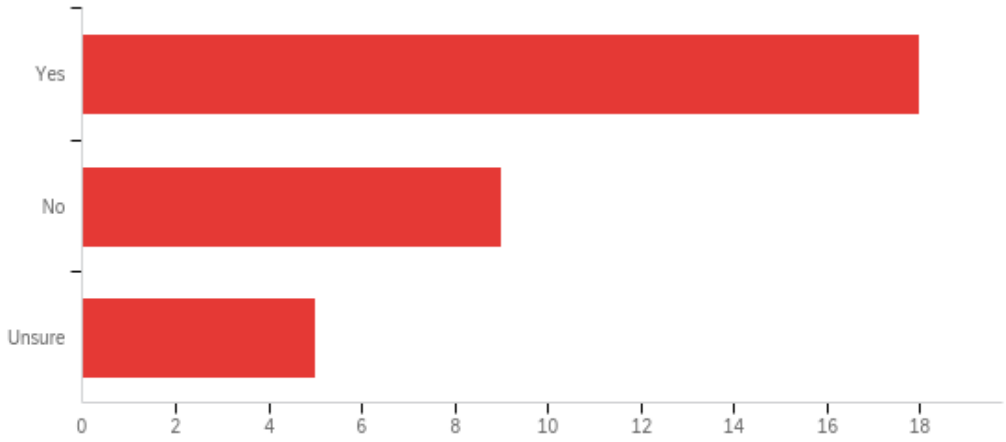

Figure C9. Response to Question 9 about the availability of a specific protocol, tool, or guidelines for responding to permitting agency concerns about temporary in-stream structures used for bridge construction.

Question 10

Do you think there is room for improvement on how your State DOT responds to environmental permitting agency concerns about temporary in-stream structures?

Response 10

Responses to Question 10 (Figure C10) indicated that the majority of respondents believe there is room for improvement on how their state DOTs respond to environmental permitting agency concerns about temporary riprap construction platforms.

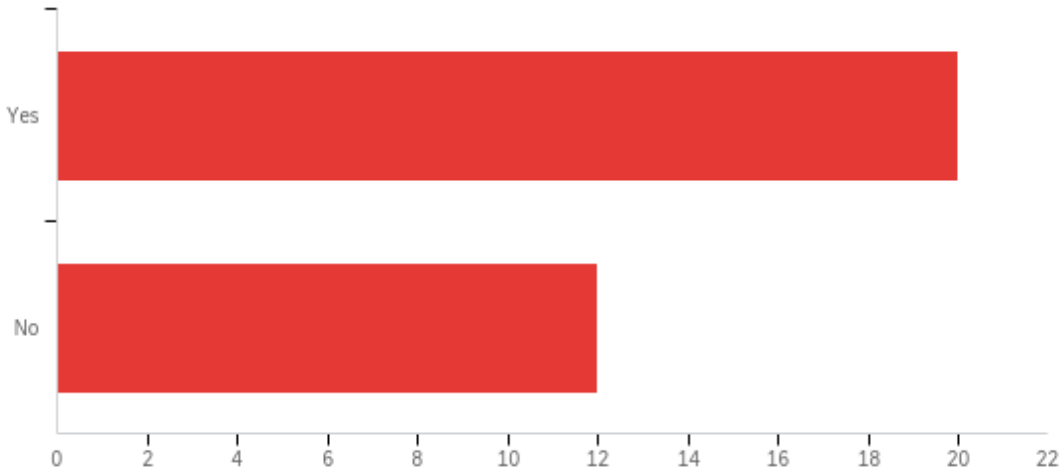

Figure C10. Response to Question 10 about the respondent's opinion on room for improvement on how their state DOTs respond to environmental permitting agency concerns about temporary riprap construction platforms.

Question 11

How do you think your State DOT could improve on answering environmental permitting concerns? Select ALL that apply.

*This question was only asked to respondents that believed there was room for improvement in Question 10.

Response 11

Respondents to Question 11 most commonly selected that the development of a standard tool to estimate potential impacts due to temporary riprap construction platforms would help their state DOT improve on answering environmental permitting agency concerns (Figure C11). Results from this thesis are being used to develop such a tool to fill this need.

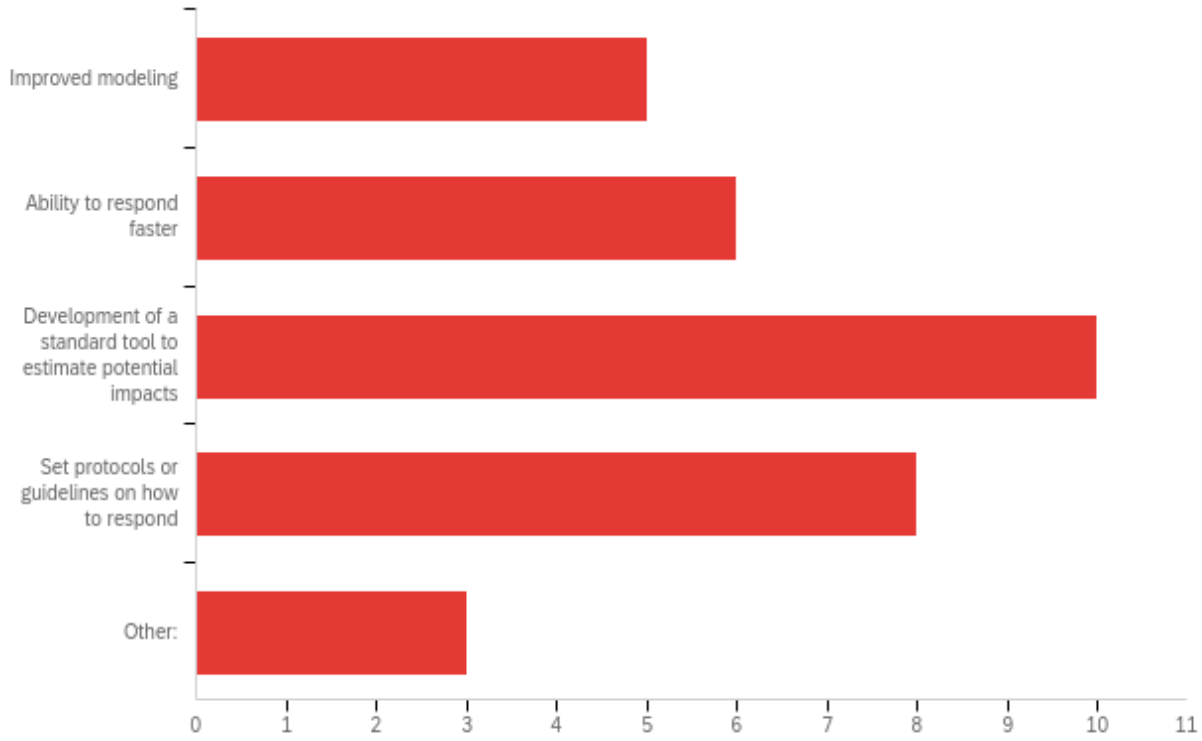

Figure C11. Response to Question 11 about the respondent's opinion on how to improve upon their state DOTs ability to respond to environmental permitting agency concerns about temporary riprap construction platforms.

Question 12

What do you think are the main concerns of the permitting agencies regarding environmental impacts from temporary-in stream bridge construction access structures? Drag and drop the issues into the box you think best describes the level of importance/concern.

Response 12

Responses to Question 12 suggested shear changes and maximum scour depth are not typically main concerns of environmental permitting agencies when implementing temporary riprap construction platforms for bridge construction (Figure C12). Shear changes (bed shear stress)

was listed most commonly as sometimes a concern. Velocity changes, bank erosion, endangered species, general habitat quality and quantity and water quality were all selected as most commonly being a main concern.

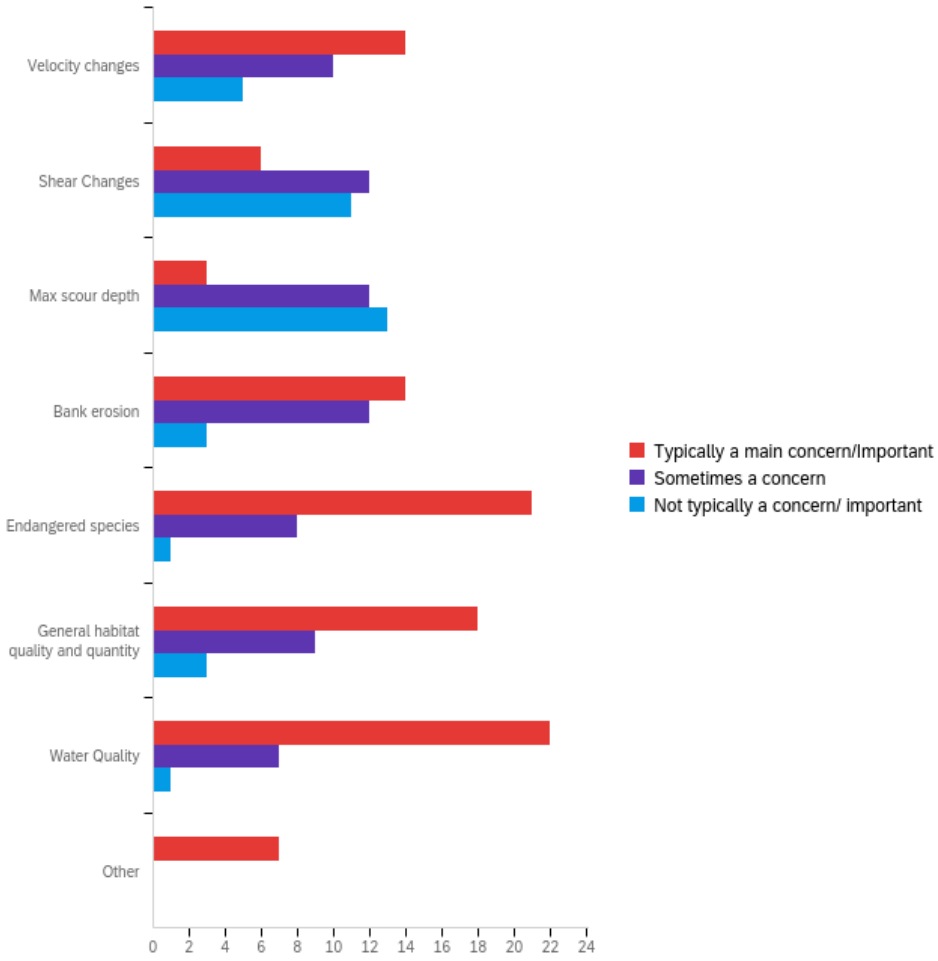

Figure C12. Response to Question 12 about the respondent's opinion on the main concerns of permitting agencies regarding environmental impacts from temporary in-stream bridge construction access structures.